NASA Technical Memorandum 78790

Effect of Canard Vertical Location, Size, and Deflection on Canard-Wing Interference at Subsonic Speeds

Blair B. Gloss, Edward J. Ray,
and Karen E. Washburn

DECEMBER 1978

NASA

NASA Technical Memorandum 78790

Effect of Canard Vertical Location, Size, and Deflection on Canard-Wing Interference at Subsonic Speeds

Blair B. Gloss, Edward J. Ray,
and Karen E. Washburn
Langley Research Center
Hampton, Virginia

National Aeronautics
and Space Administration

**Scientific and Technical
Information Office**

1978

SUMMARY

A generalized close-coupled canard-wing configuration was tested in the Langley high-speed 7- by 10-foot tunnel at Mach numbers of 0.40, 0.70, and 0.85 over an angle-of-attack range from -4° to 24°. Studies were made to determine the effects of canard vertical location, size, and deflection and wing leading-edge sweep on the longitudinal characteristics of the basic configuration. The two wings tested had thin symmetrical circular-arc airfoil sections with characteristically sharp leading edges swept at 60° and 44°. Two balances which allow separation of the canard-forebody contribution from the total forces and moments were used in this study. The data in this report supplement several earlier publications by the National Aeronautics and Space Administration.

INTRODUCTION

The studies presented in references 1 to 14 indicate that close-coupled canard-wing configurations can provide substantial improvements in fighter maneuverability. In particular, these studies have indicated the effects of canard size, vertical location, and deflection and wing leading-edge sweep on canard-wing interference at subsonic, transonic, and supersonic speeds (refs. 4, 8, and 9); the effects of canard planform, vertical location, and wing leading-edge sweep on canard-wing interference for high angles of attack at subsonic speeds (refs. 10 and 11); the effects of canard location on the wing buffet characteristics (ref. 12); trim characteristics of a canard-wing configuration with a variable camber wing (ref. 13); and a detailed pressure distribution study on a canard-wing configuration at transonic speeds (ref. 14). The present investigation was made to provide a systematic data base on the effects of canard size, deflection, and vertical location for a close-coupled configuration with intermediate and high wing sweep. These tests were made in the Langley high-speed 7- by 10-foot tunnel at Mach numbers of 0.40, 0.70, and 0.85 at angles of attack from approximately -4° to 24° with canard deflections from 0° to 10°. These data supplement references 8, 9, and 11.

SYMBOLS

The International System of Units (SI), with U.S. Customary Units presented in parentheses, is used for the physical quantities in this paper. Measurements and calculations were made in U.S. Customary Units. The longitudinal data presented in this report are referred to the stability axis system. The moment reference point was taken to be at fuselage station 63.71 cm (25.08 in.) for both balances.

A aspect ratio, b^2/S_W

b wing span, 50.8 cm (20.0 in.)

C_D drag coefficient (main balance), $\frac{\text{Drag}}{qS_W}$

C_L lift coefficient (main balance), $\frac{\text{Lift}}{qS_W}$

$C_{L,c}$ lift coefficient obtained from canard balance, $\frac{\text{Canard balance lift}}{qS_W}$

C_m pitching-moment coefficient (main balance), $\frac{\text{Pitching moment}}{qS_W\bar{c}}$

$C_{m,c}$ pitching-moment coefficient obtained from canard balance, $\frac{\text{Canard pitching moment}}{qS_W\bar{c}}$

$\bar{c}$ wing mean geometric chord, 23.31 cm (9.18 in.)

L/D lift-drag ratio (main balance)

M free-stream Mach number

q free-stream dynamic pressure, Pa (lb/ft^2)

S_c exposed canard areas, cm^2 (in^2) (165.16 cm^2 (25.60 in^2) for canard I; 230.06 cm^2 (35.66 in^2) for canard II; 288.73 cm^2 (44.75 in^2) for canard III)

S_W reference area of wing with leading and trailing edges extended to plane of symmetry, 1032.7 cm^2 (160.0 in^2)

z vertical distance from wing chord plane to canard chord plane, positive up, cm (in.)

α angle of attack, deg

δ canard deflection angle, positive when trailing edge down, deg

Λ_c canard leading-edge sweep angle, deg

Λ_W wing leading-edge sweep angle, deg

MODEL DESCRIPTION

A three-view drawing of the general research model is presented in figure 1. This model was designed so that various wing and canard planforms could be attached to the common fuselage to vary their positional relationship. Figure 2 presents a photograph of the model with the large canard and 60° swept wing. Table I presents the pertinent geometric parameters associated with this model.

Two different untwisted wing planforms were used (wing I with $\Lambda_W = 60^\circ$ and wing II with $\Lambda_W = 44^\circ$); however, both wings had the same area, mean geometric chord, symmetrical circular-arc airfoil sections, and maximum thickness which varied linearly from 6 percent of the chord at the root to 4 percent of the chord at the tip. The two wings were located longitudinally so that the distance was the same for each configuration between quarter-chord points of the mean geometric chords of a given canard and wing.

Canard I had a leading-edge sweep angle of 51.7° and an exposed area S_c of 16.0 percent of the wing reference area S_W. Canards II and III had the same leading-edge sweep and exposed areas of 22.3 and 28.0 percent, respectively, of the wing reference area. Each canard was tested in the chord plane of the wing ($z/\bar{c} = 0.0$ ("mid" canard)) and in a position 18.5 percent of the wing geometric chord above the wing chord plane ($z/\bar{c} = 0.185$ ("high" canard)). Body fairings were used to fair the canard mounting brackets into the fuselage for the high canard ($z/\bar{c} = 0.185$), and these were left on the fuselage for the mid canard ($z/\bar{c} = 0.0$). The canard was untwisted and had symmetrical circular-arc airfoil sections. The thickness varied linearly from 6 percent of the chord at the root to 4 percent at the tip.

APPARATUS, TESTS, AND CORRECTIONS

The present investigation was conducted in the Langley high-speed 7- by 10-foot tunnel (ref. 15). The forces and moments developed by the model were measured by means of two internally mounted six-component strain-gage balances. One balance was housed within the forward segment of the fuselage and was rigidly attached to the rearward fuselage segment. A small unsealed gap was maintained between fuselage segments to prevent fouling. This balance (hereafter called the canard balance) measured the loads on the canard and on the forward segment of the fuselage (shaded area in fig. 1). The second balance (hereafter called the main balance) was housed in the rearward segment of the fuselage and measured the total model loads.

Tests were made at Mach numbers of 0.40, 0.70, and 0.85 while the angle of attack was varied in 2° increments from approximately -4° to 24° at a sideslip angle of 0°. The Reynolds number for each Mach number is shown in the following table:

Reynolds number, per meter	Mach number
8.383×10^6	0.40
11.739	.70
12.113	.85

All tests were made with the boundary-layer transition fixed on the model by means of narrow strips of carborundum grit as outlined in reference 16. Past experience has shown that blockage and jet boundary corrections are very small for this size model when tested in the slotted-wall test section of the Langley high-speed 7- by 10-foot wind tunnel; thus, blockage and jet boundary corrections are neglected for this study. The angle of attack of the model has been corrected for sting and balance deflections caused by aerodynamic loads. All measurements were corrected to a condition of free-stream static pressure on the base of the model. However, drag measurements were not corrected at the forebody base because of the small amount of clearance at the model location.

PRESENTATION OF DATA

These data provide part of a systematic data base on the effect of canard size, vertical location, and deflection and also supplement the conclusions of references 8, 9, and 11. The data are presented without analysis. To aid in using the data, the results are presented as follows:

Langley Research Center
National Aeronautics and Space Administration
Hampton, VA 23665

October 13, 1978

REFERENCES

1. Behrbohm, Hermann: Basic Low Speed Aerodynamics of the Short-Coupled Canard Configuration of Small Aspect Ratio. SAAB TN 60, Saab Aircraft Co. (Linköping, Sweden), July 1965.

2. Lacey, David W.; and Chorney, Stephen J.: Subsonic Aerodynamic Characteristics of Close-Coupled Canards With Varying Area and Position Relative to a 50° Swept Wing. Tech. Note AL-199, Naval Ship Res. & Develop. Center, Mar. 1971. (Available from DDC as AD 882 702L.)

3. McKinney, Linwood W.; and Dollyhigh, Samuel M.: Some Trim Drag Considerations for Maneuvering Aircraft. J. Aircr., vol. 8, no. 8, Aug. 1971, pp. 623-629.

4. Dollyhigh, Samuel M.: Static Longitudinal Aerodynamic Characteristics of Close-Coupled Wing-Canard Configurations at Mach Numbers From 1.60 to 2.86. NASA TN D-6597, 1971.

5. Ottensoser, Jonah: Wind Tunnel Data on the Transonic Aerodynamic Characteristics of Close-Coupled Canards With Varying Planform, Position and Deflection Relative to a 50° Swept Wing. Test Rep. AL-88, Naval Ship Res. & Develop. Center, May 1972.

6. Krouse, John R.: Effects of Canard Planform on the Subsonic Aerodynamic Characteristics of a 25° and a 50° Swept-Wing Research Aircraft Model. Evaluation Rep. AL-91, Naval Ship Res. & Develop. Center, May 1972.

7. Lacey, David W.: Transonic Characteristics of Close-Coupled Canard and Horizontal Tail Installed on a 50 Degree Sweep Research Aircraft Model. Evaluation Rep. AL-81, Naval Ship Res. & Develop. Center, Aug. 1972.

8. Gloss, Blair B.; and McKinney, Linwood W.: Canard-Wing Lift Interference Related to Maneuvering Aircraft at Subsonic Speeds. NASA TM X-2897, 1973.

9. Gloss, Blair B.: Effect of Canard Location and Size on Canard-Wing Interference and Aerodynamic-Center Shift Related to Maneuvering Aircraft at Transonic Speeds. NASA TN D-7505, 1974.

10. Gloss, Blair B.: The Effect of Canard Leading-Edge Sweep and Dihedral Angle on the Longitudinal and Lateral Aerodynamic Characteristics of a Close-Coupled Canard-Wing Configuration. NASA TN D-7814, 1974.

11. Gloss, Blair B.: Effect of Wing Planform and Canard Location and Geometry on the Longitudinal Aerodynamic Characteristics of a Close-Coupled Canard Wing Model at Subsonic Speeds. NASA TN D-7910, 1975.

12. Gloss, Blair B.; Henderson, William P.; and Huffman, Jarrett K.: Effect of Canard Position and Wing Leading-Edge Flap Deflection on Wing Buffet at Transonic Speeds. NASA TM X-72681, 1975.

13. Gloss, Blair B.: Effect of Camber on the Trimmed Lift Capability of a Close-Coupled Canard-Wing Configuration. NASA TM-78686, 1978.

14. Gloss, Blair B.; and Washburn, Karen E.: A Study of Canard-Wing Interference Using Experimental Pressure Data at Transonic Speeds. NASA TP-1355, 1978.

15. Schaefer, William T., Jr.: Characteristics of Major Active Wind Tunnels at the Langley Research Center. NASA TM X-1130, 1965.

16. Braslow, Albert L.; Hicks, Raymond M.; and Harris, Roy V., Jr.: Use of Grit-Type Boundary-Layer-Transition Trips on Wind-Tunnel Models. NASA TN D-3579, 1967.

TABLE I.- GEOMETRIC CHARACTERISTICS

Body:	
Length, cm (in.)	96.52 (38.00)
Wing (wings I and II are the same except when specified):	
A (b^2/S_w)	2.5
b, cm (in.)	50.80 (20.00)
Λ_w for -	
Wing I, deg	60
Wing II, deg	44
$\bar{c}$, cm (in.)	23.31 (9.18)
Airfoil section	Circular arc
S_w (area extended to plane of symmetry), cm^2 (in^2)	1032.2 (160.00)
Root chord, cm (in.)	29.80 (11.73)
Tip chord, cm (in.)	6.77 (2.67)
Maximum thickness at -	
Root, percent chord	6
Tip, percent chord	4

	Canard I	Canard II	Canard III
Canard:			
Λ_c, deg	51.7	51.7	51.7
Airfoil section	Circular arc	Circular arc	Circular arc
S_c, cm^2 (in^2)	165.16 (25.60)	230.06 (35.66)	288.73 (44.75)
b, cm (in.)	27.94 (11.00)	31.65 (12.46)	34.49 (13.58)
Root chord, cm (in.)	13.54 (5.33)	15.95 (6.28)	17.92 (7.05)
Tip chord, cm (in.)	2.71 (1.07)	3.18 (1.25)	3.59 (1.41)
Maximum thickness at -			
Root, percent chord	6	6	6
Tip, percent chord	4	4	4
$\bar{c}$	3.67	4.33	4.86

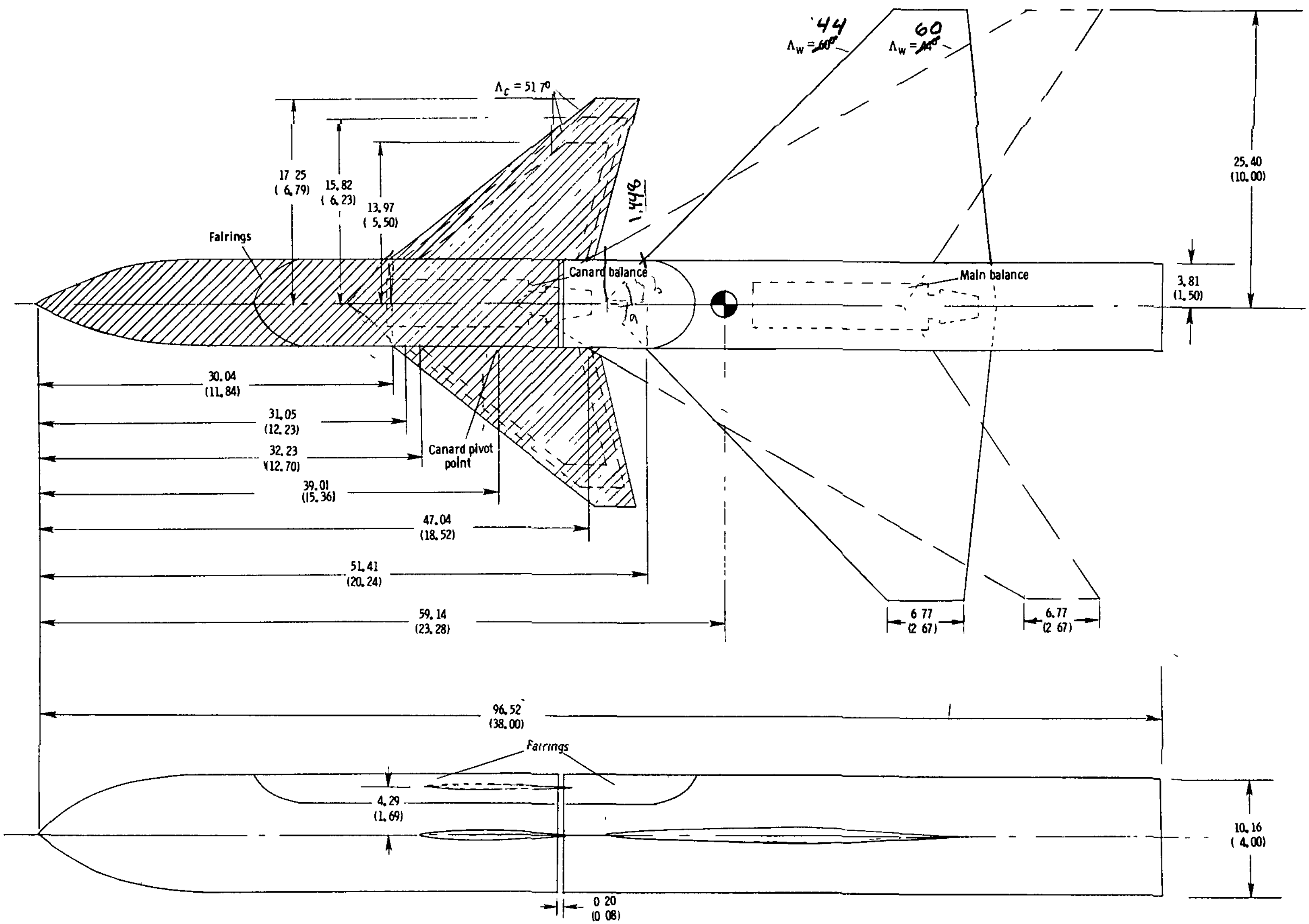

Figure 1.- Sketch of general research model. All dimensions are in centimeters (inches).

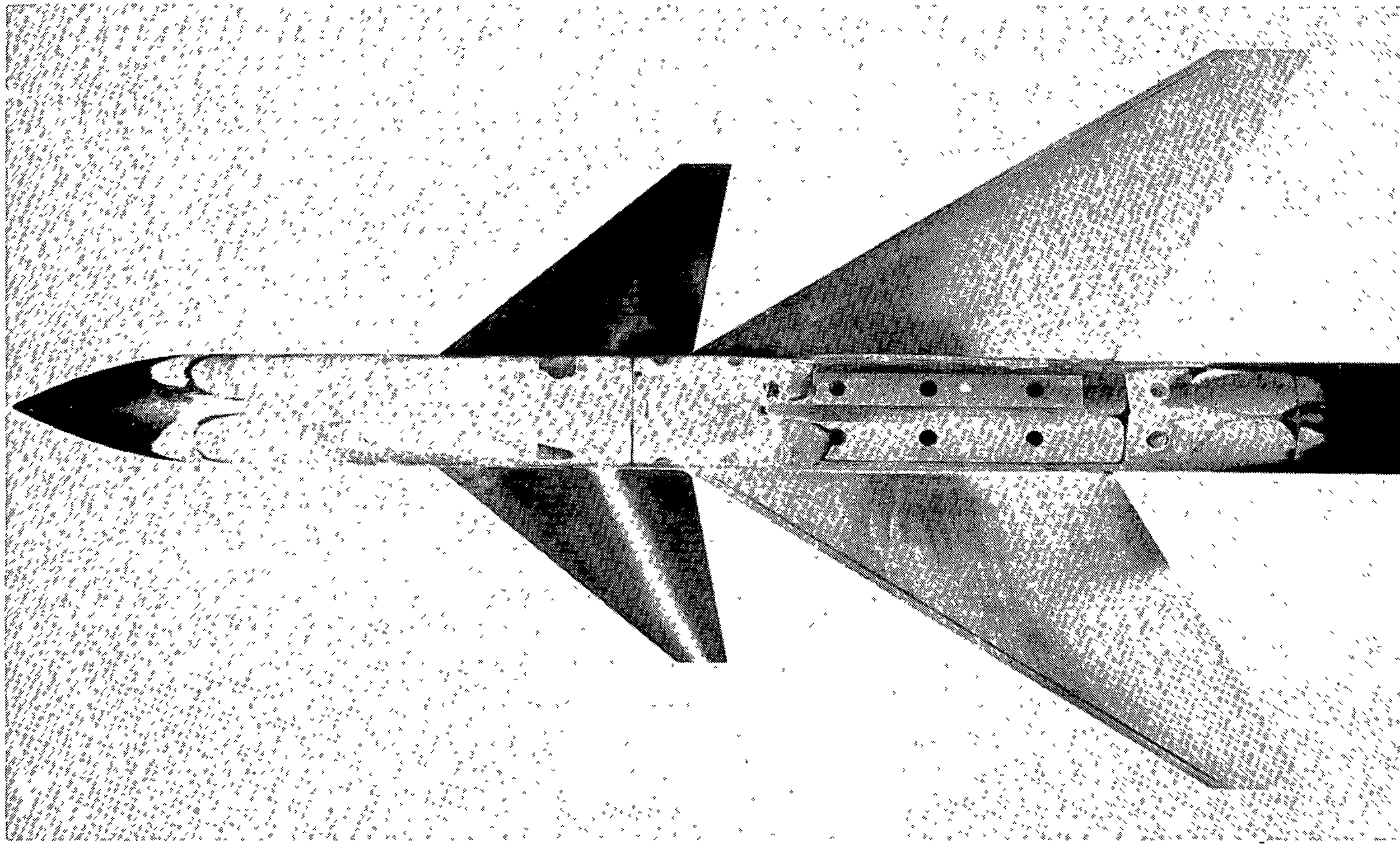

L-73-1637

Figure 2.- Typical configuration of model.

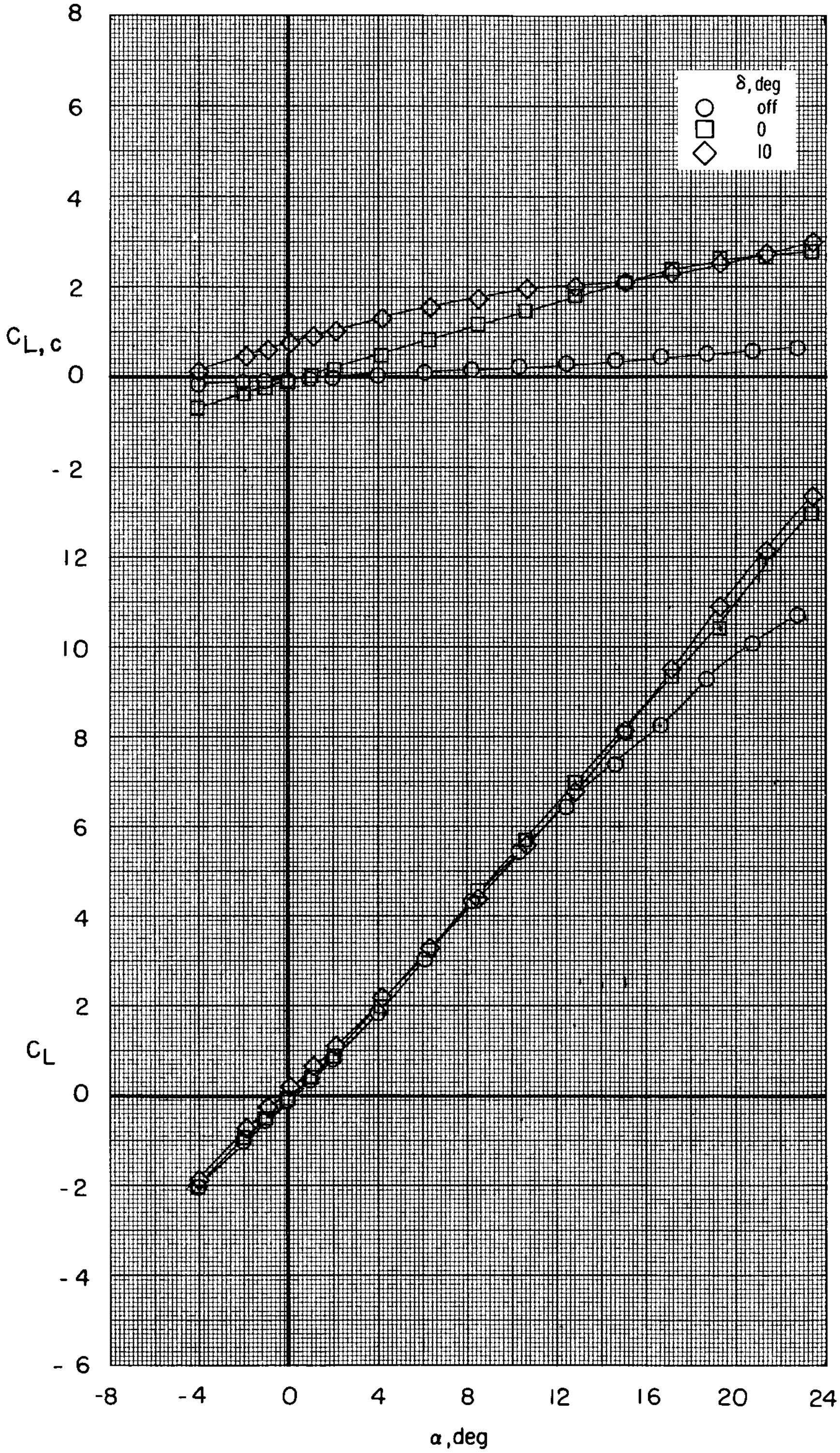

(a) M = 0.40.

Figure 3.- Effect of canard I (S_c/S_w = 0.16) deflection on longitudinal characteristics of wing I (Λ_w = 60°) for $z/\bar{c}$ = 0.0.

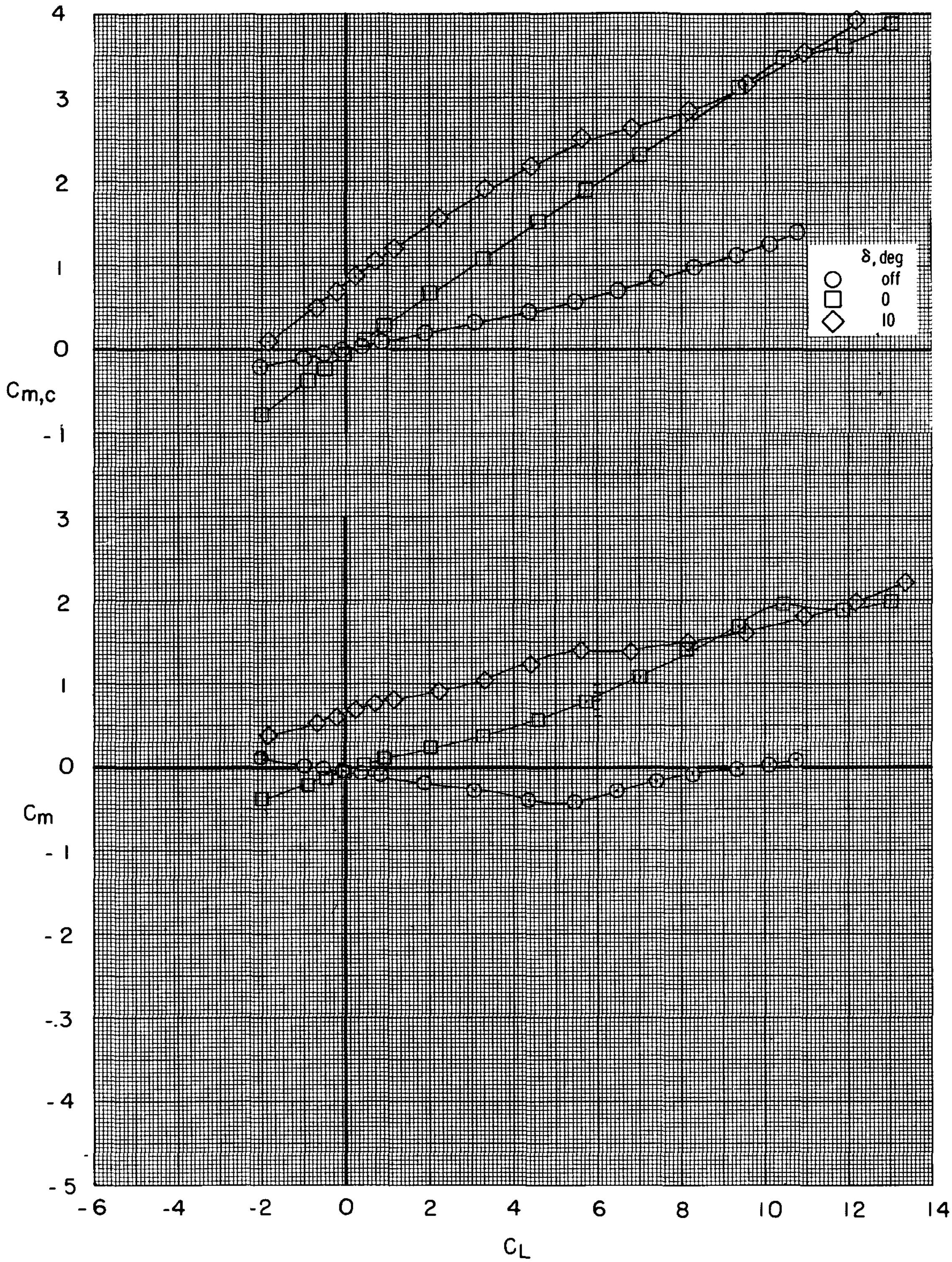

(a) Continued.

Figure 3.- Continued.

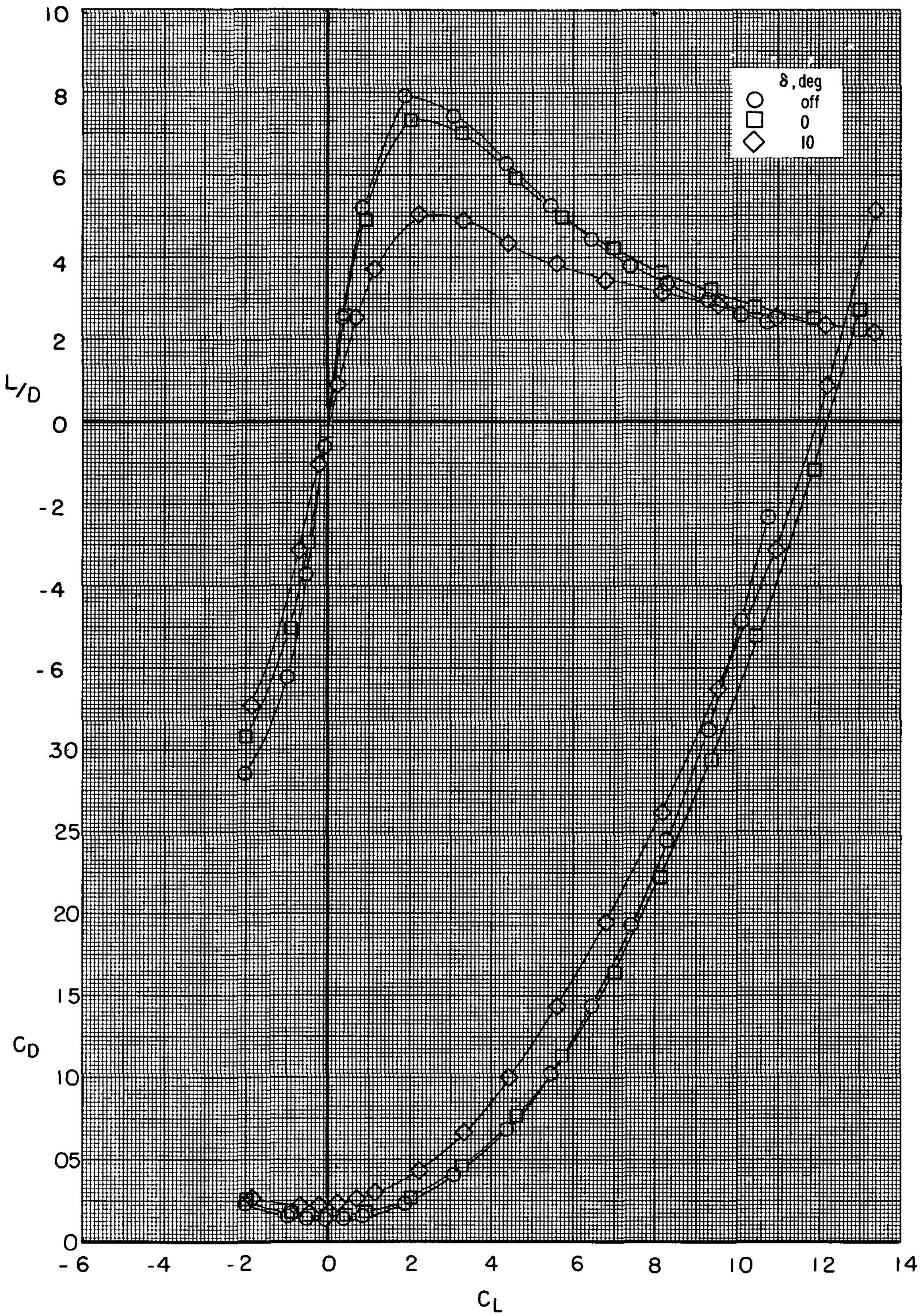

(a) Concluded.

Figure 3.- Continued.

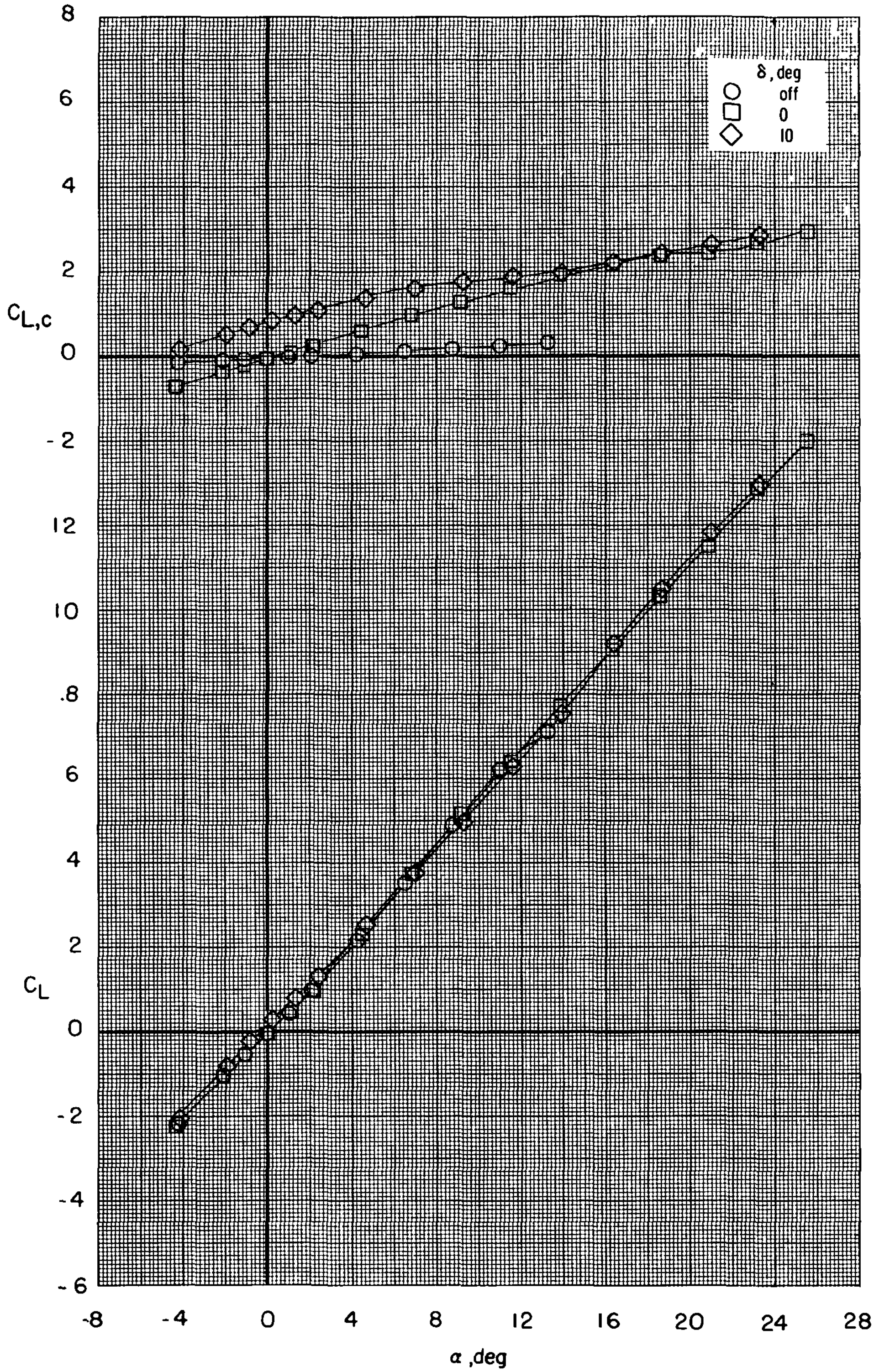

(b) M = 0.70.

Figure 3.- Continued.

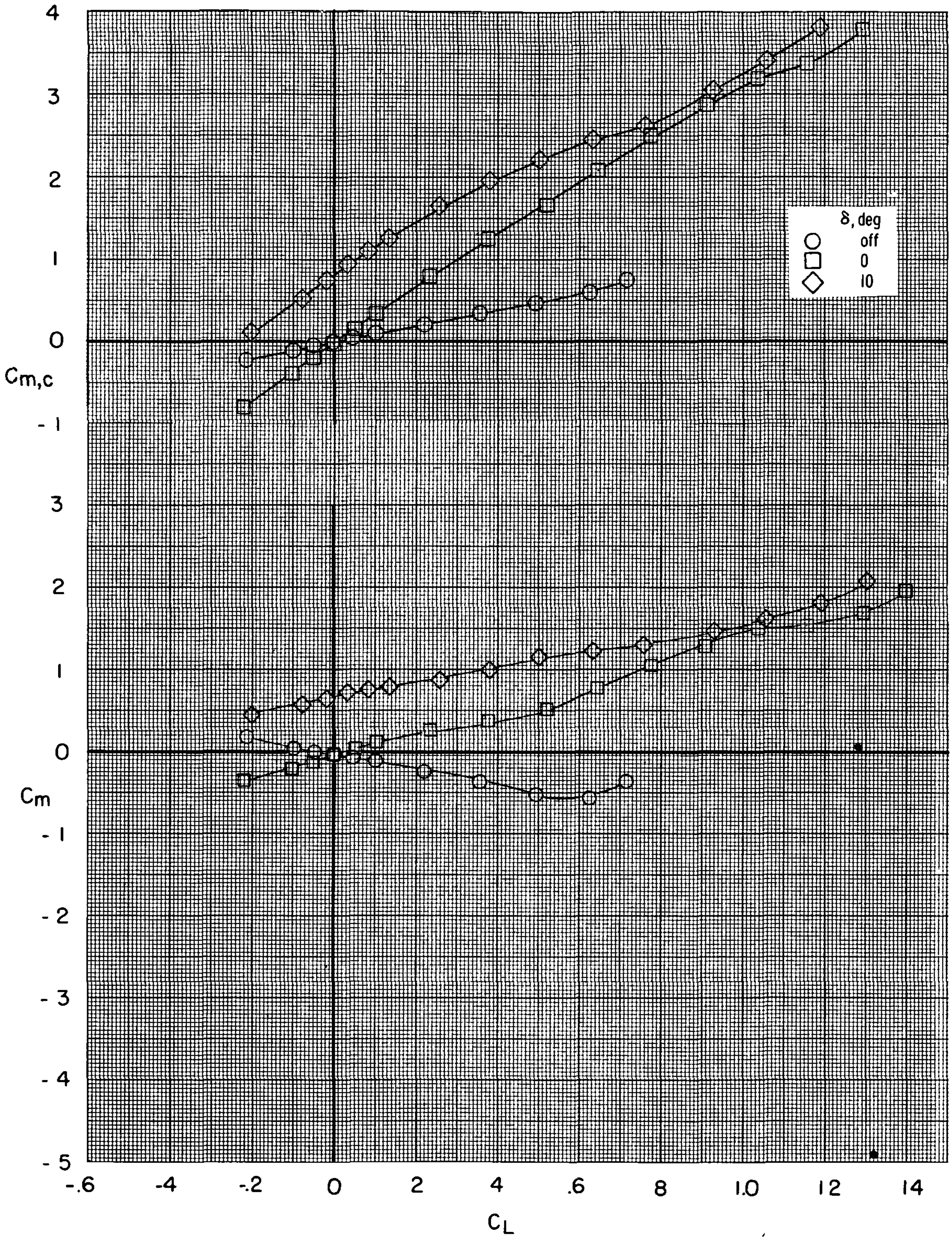

(b) Continued.

Figure 3.- Continued.

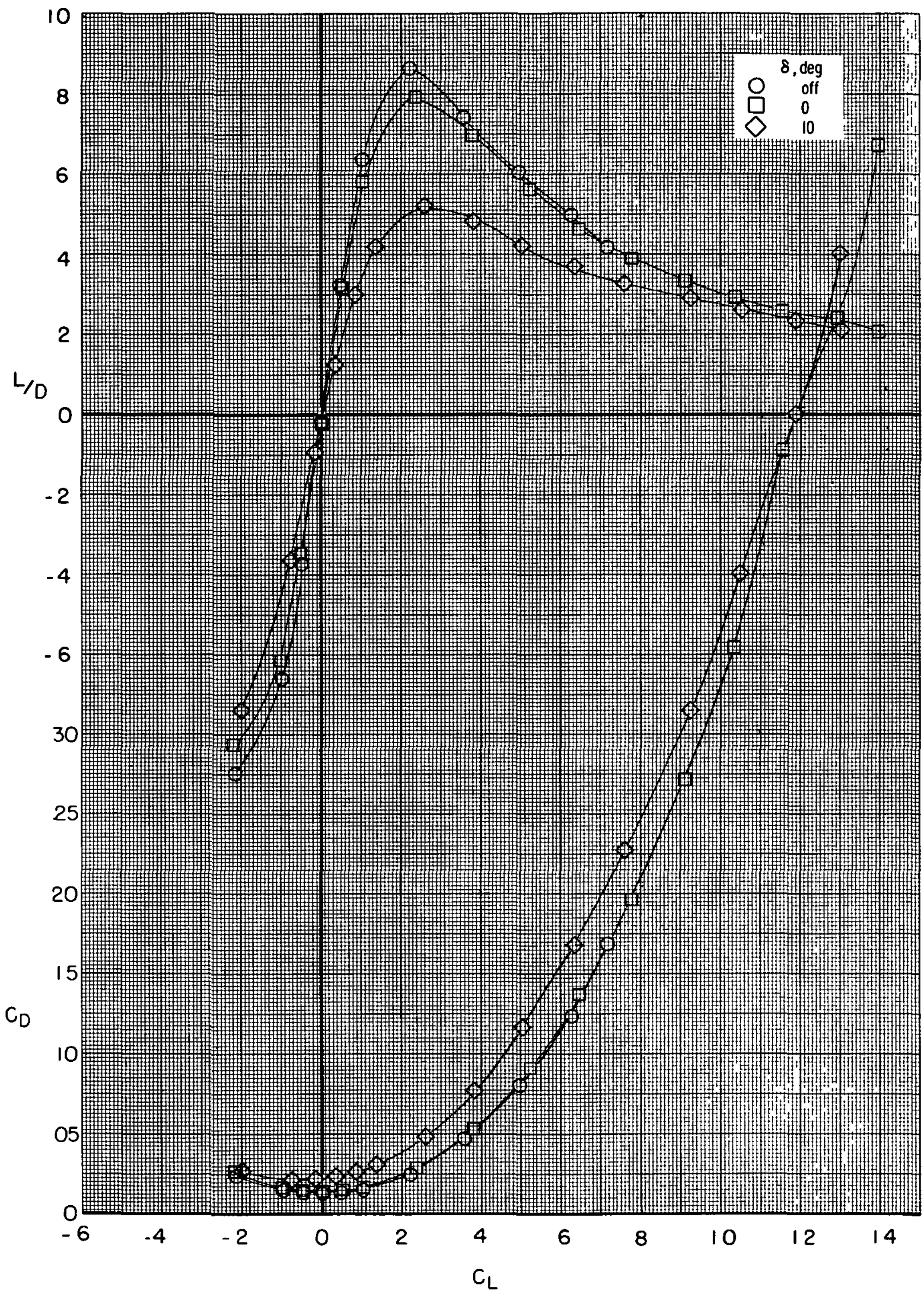

(b) Concluded.

Figure 3.- Continued.

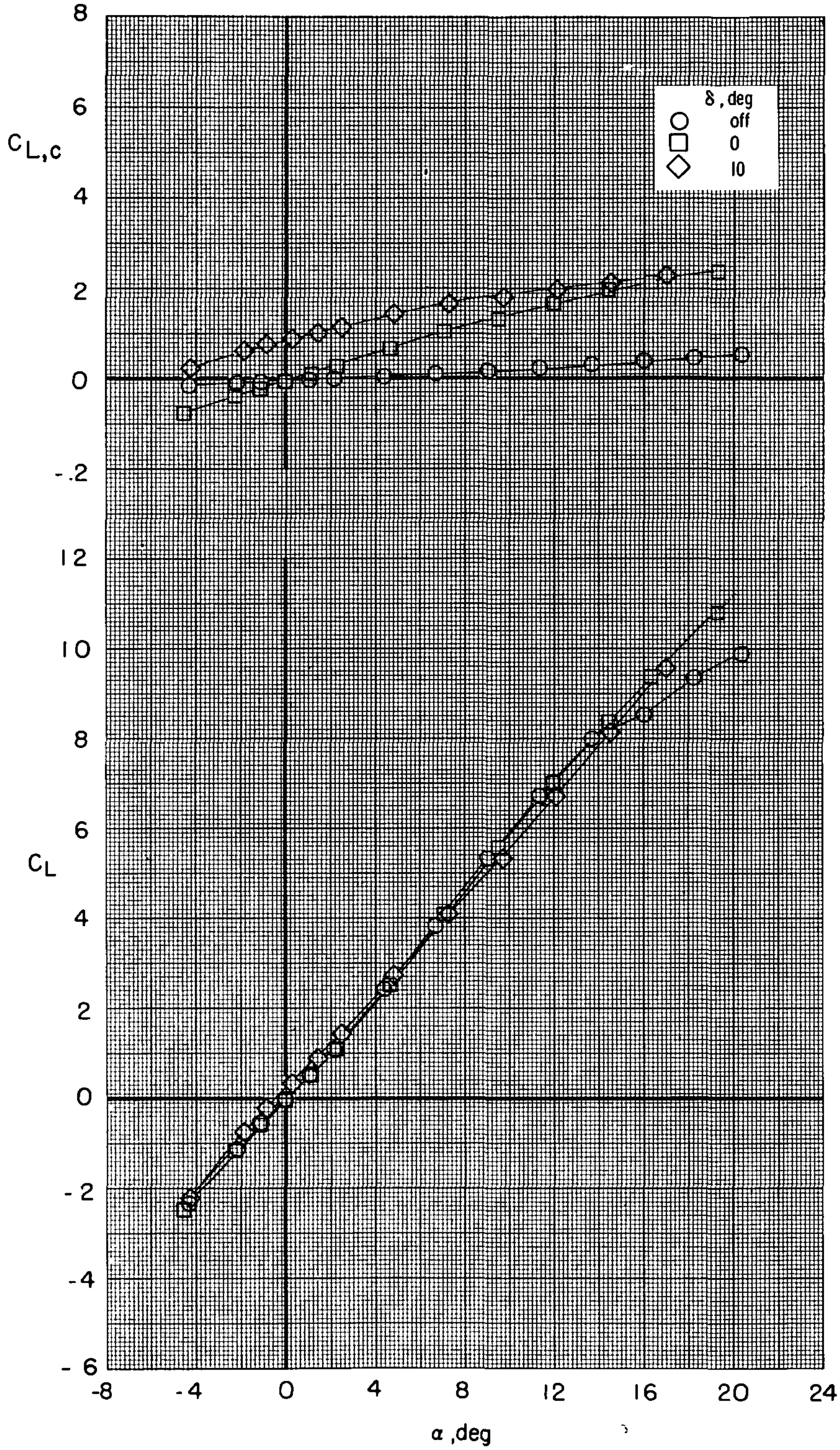

(c) M = 0.85.

Figure 3.- Continued.

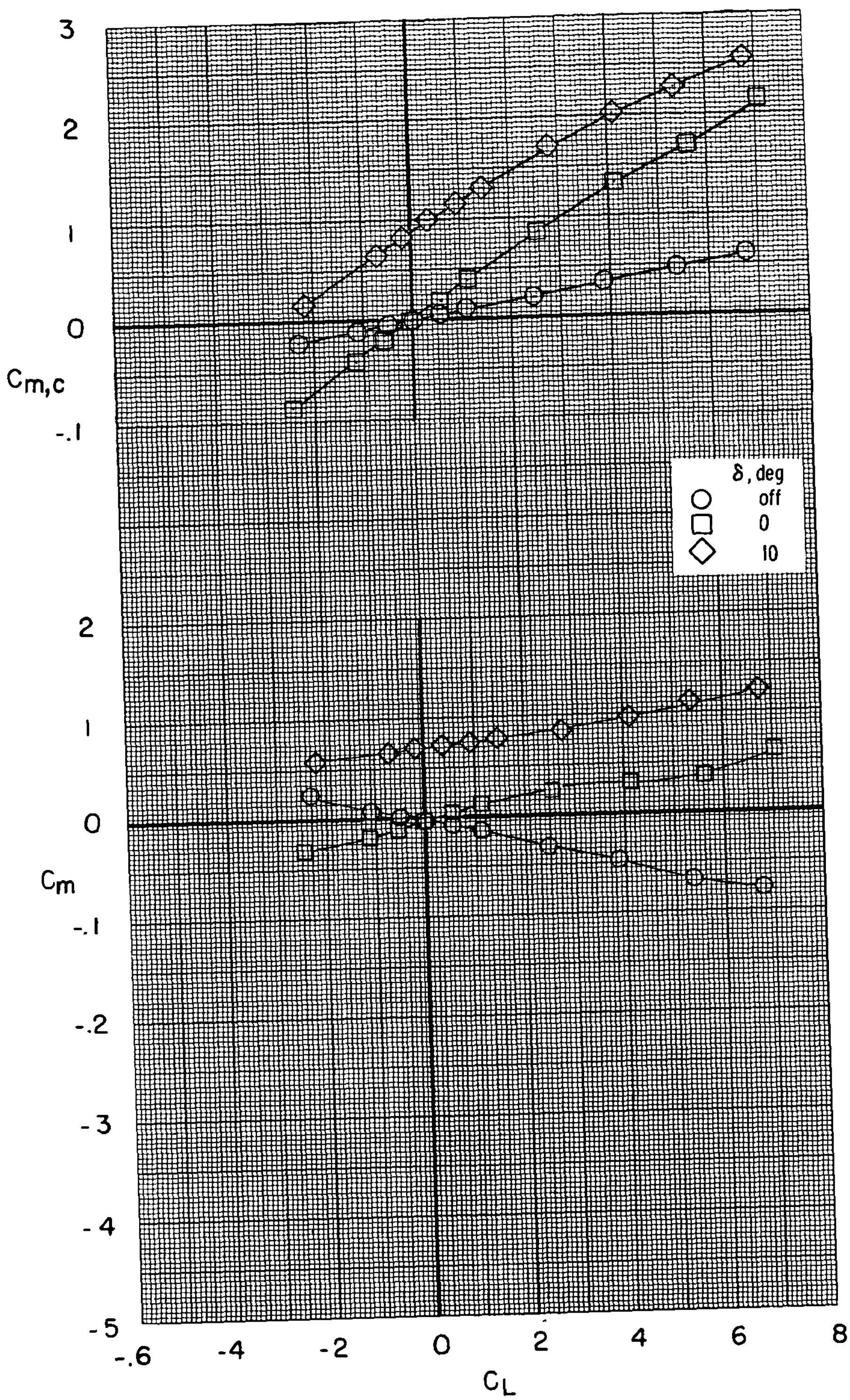

(c) Continued.

Figure 3.- Continued.

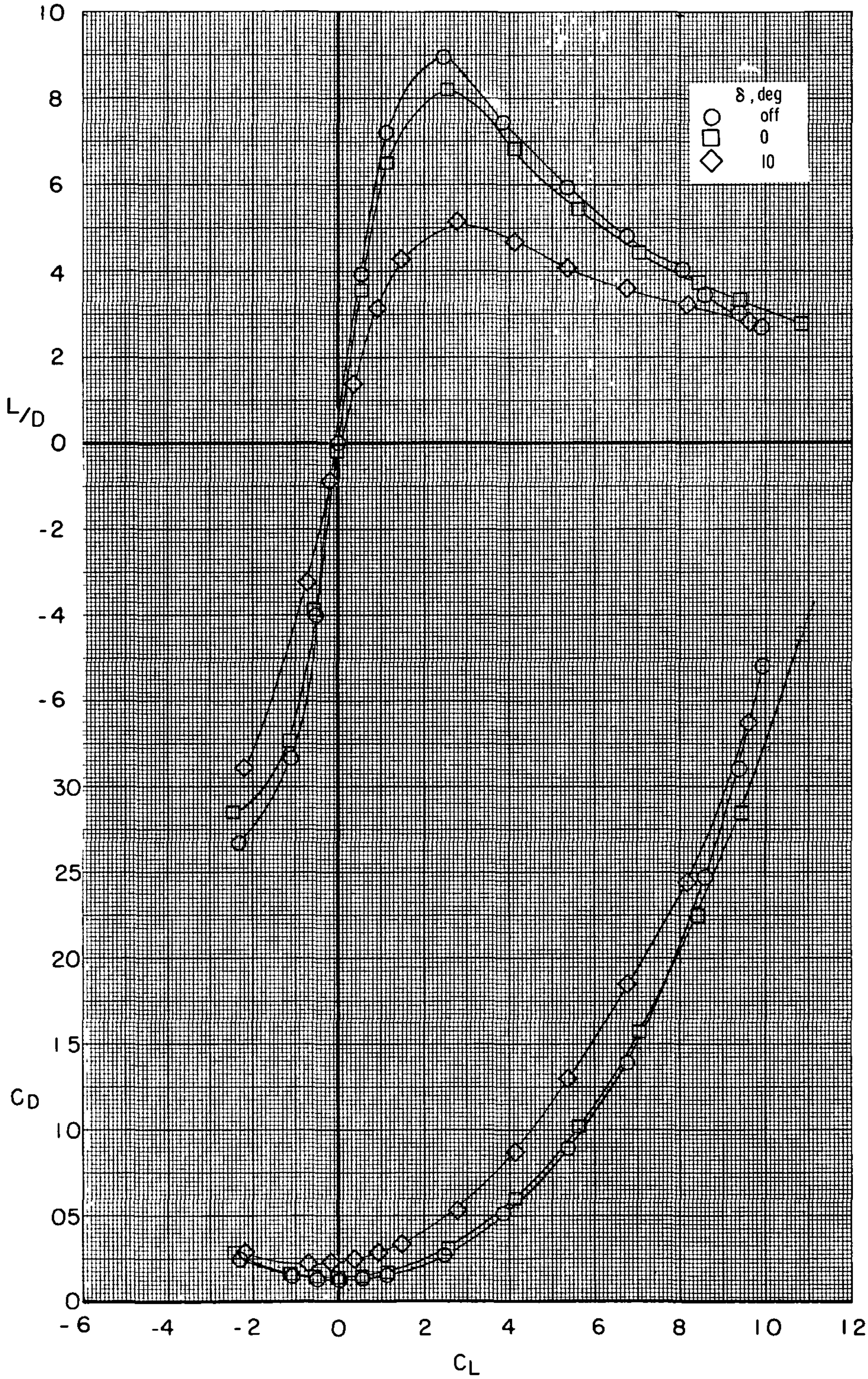

(c) Concluded.

Figure 3.- Concluded.

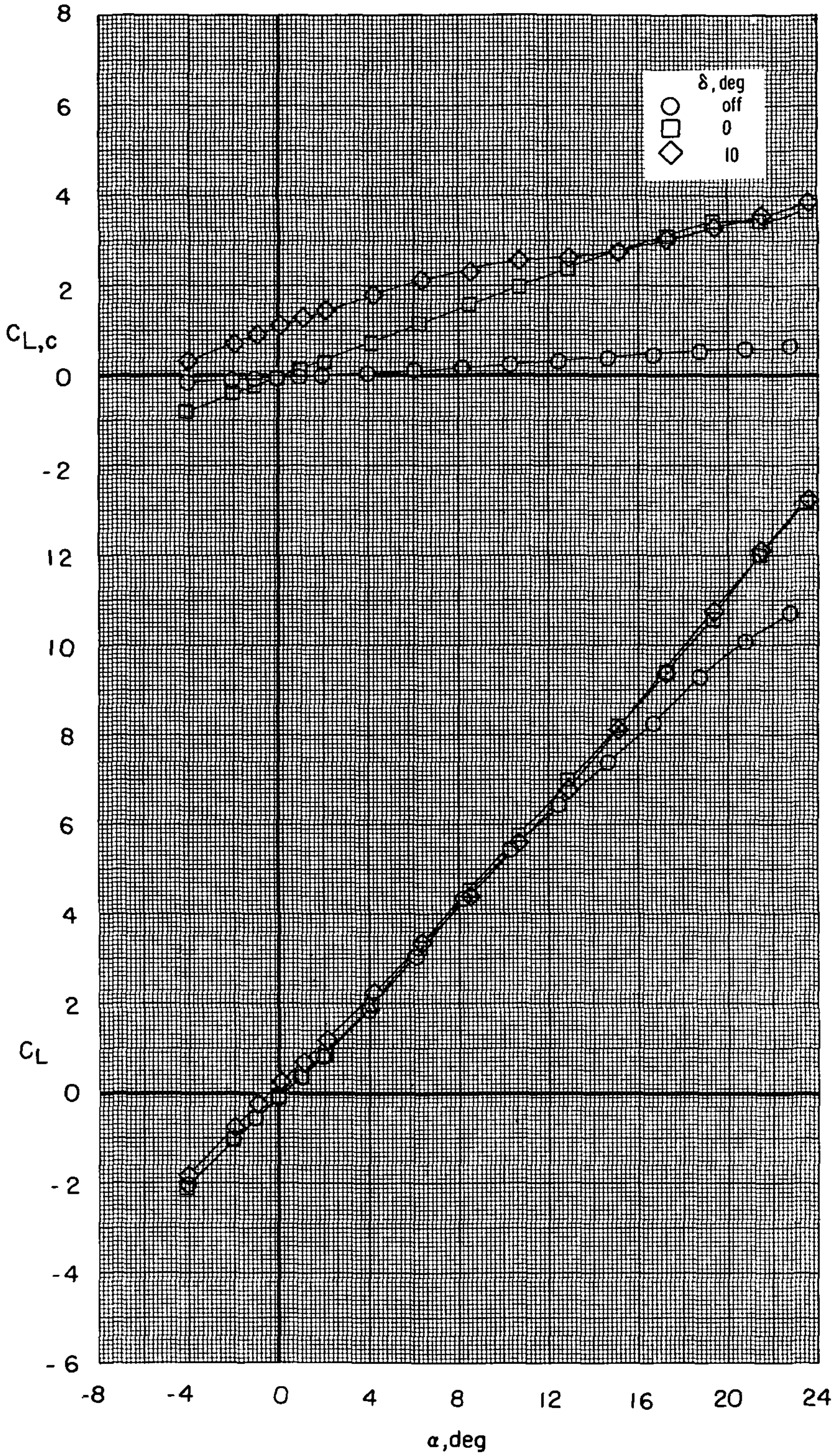

(a) M = 0.40.

Figure 4.- Effect of canard II (S_c/S_W = 0.22) deflection on longitudinal characteristics of wing I (Λ_W = 60°), $z/\bar{c}$ = 0.0.

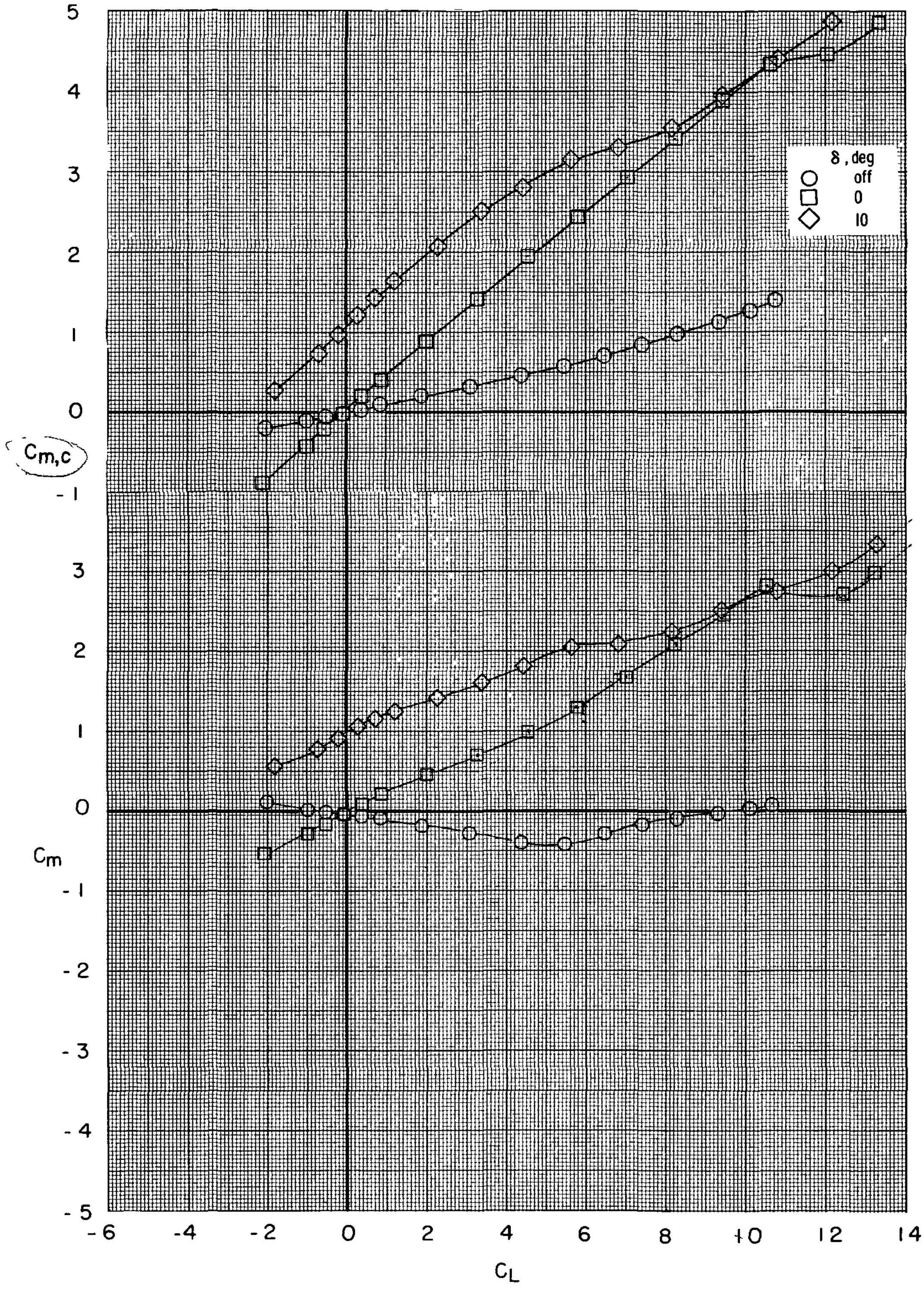

(a) Continued.

Figure 4.- Continued.

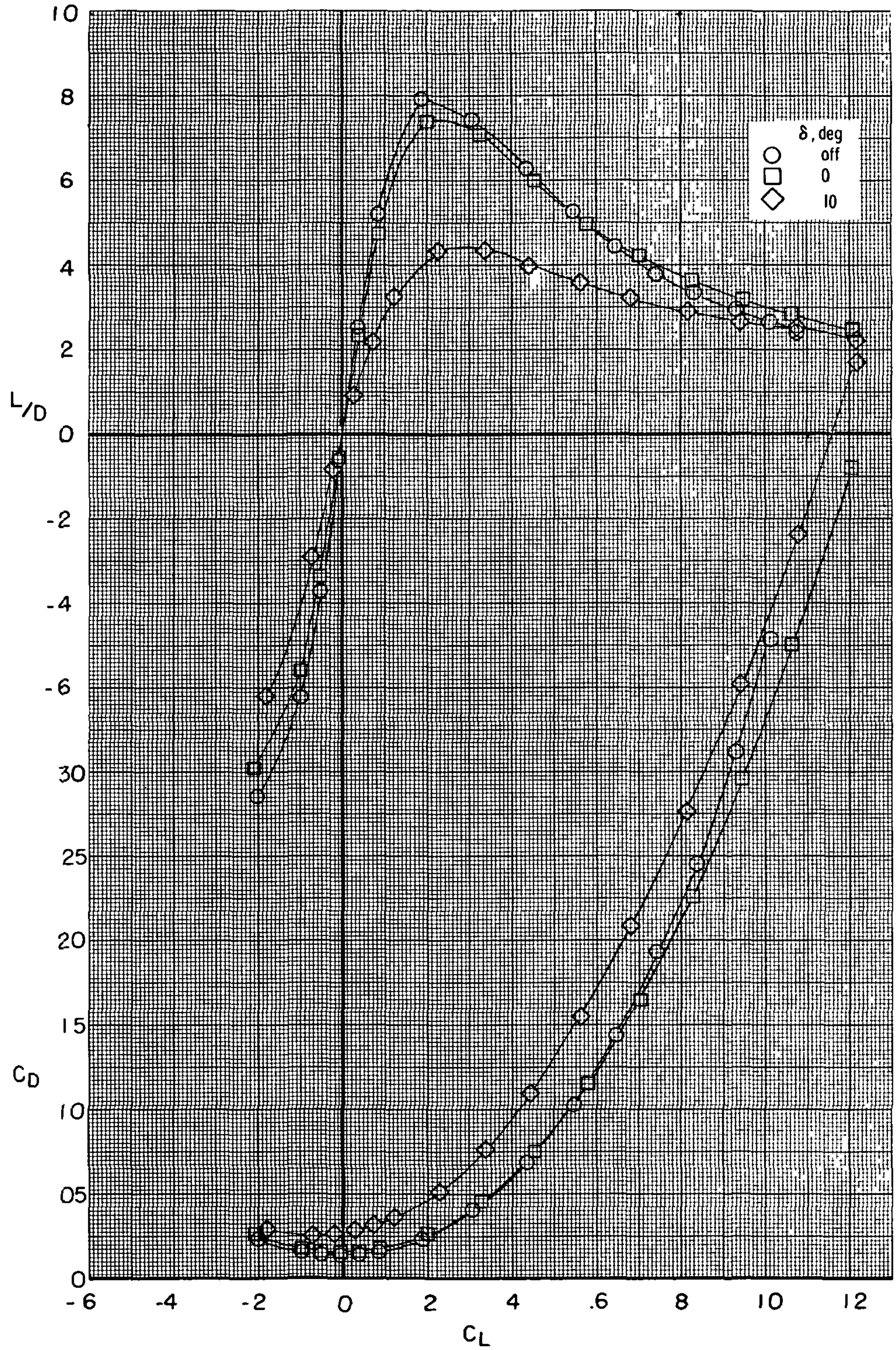

(a) Concluded.

Figure 4.- Continued.

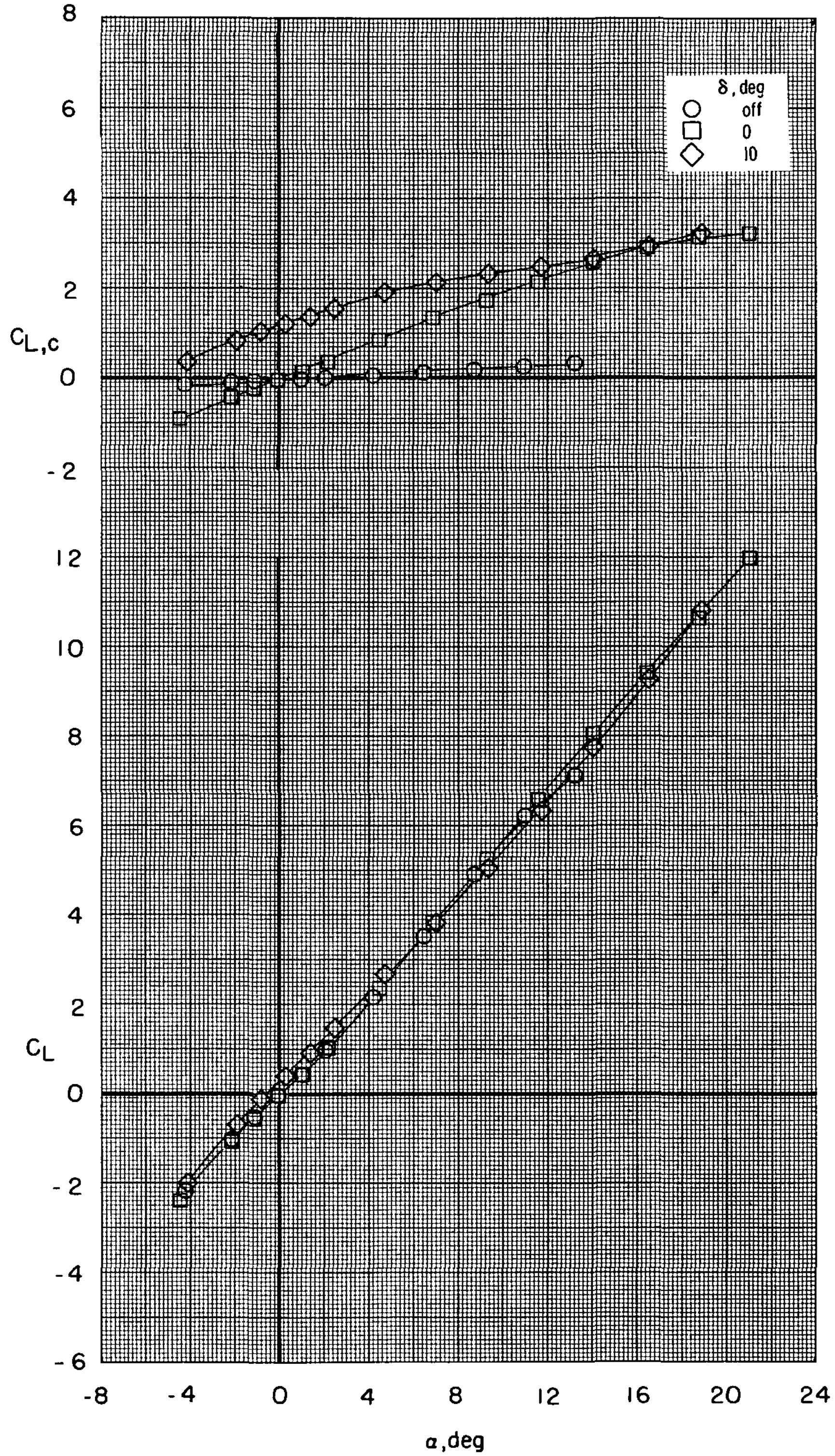

(b) M = 0.70.

Figure 4.- Continued.

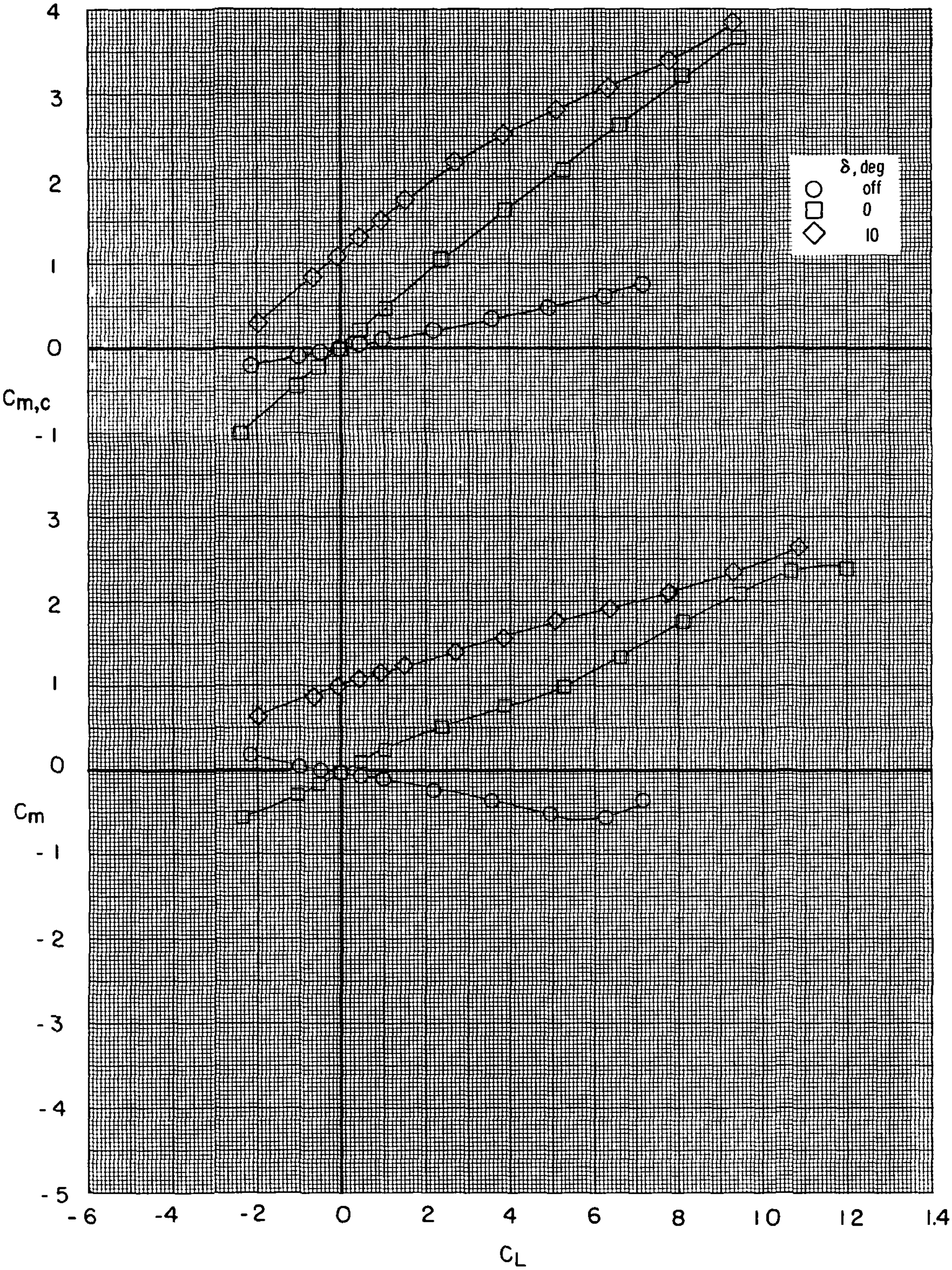

(b) Continued.

Figure 4.- Continued.

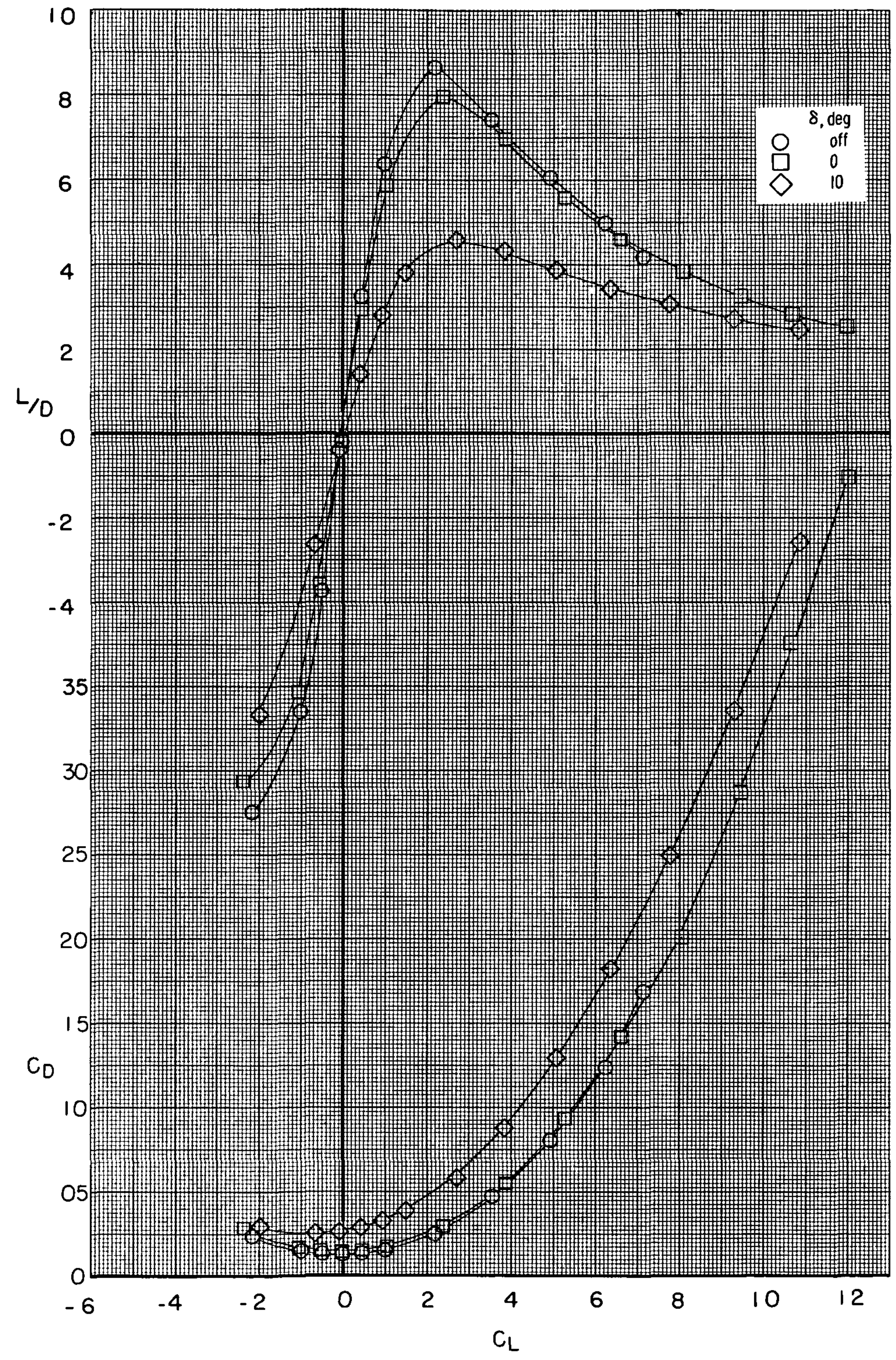

(b) Concluded.

Figure 4.- Continued.

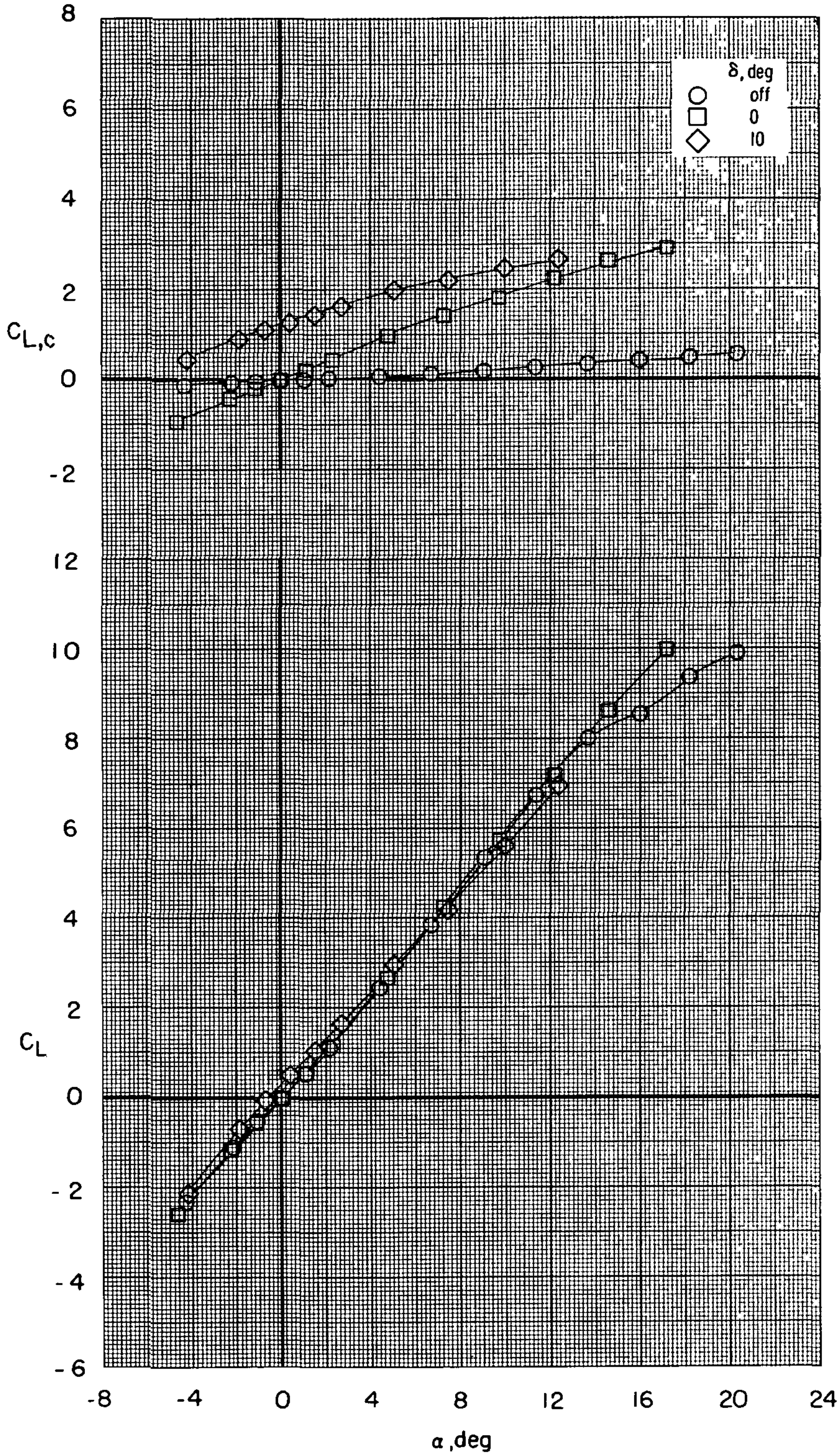

(c) M = 0.85.

Figure 4.- Continued.

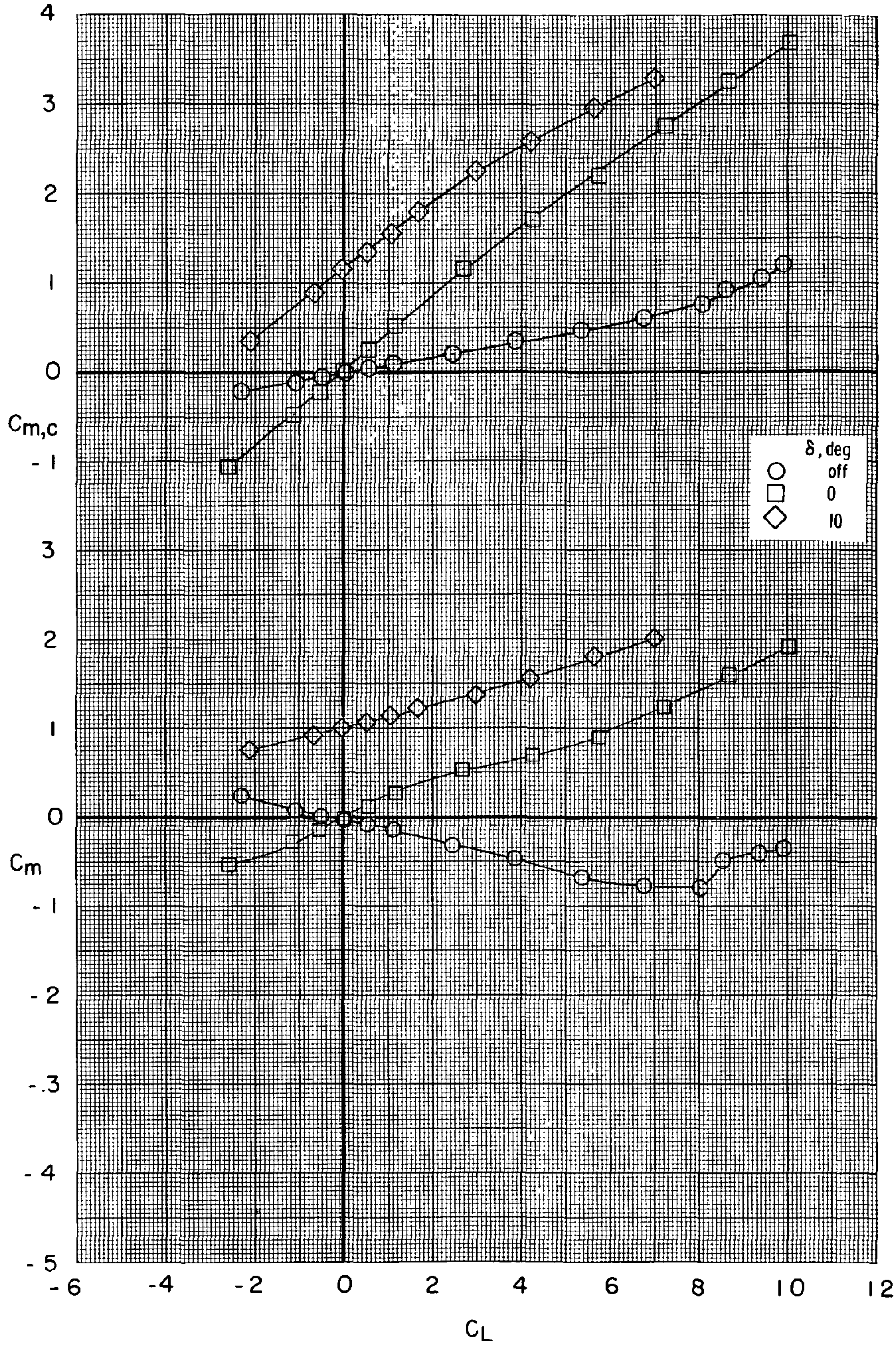

(c) Continued.

Figure 4.- Continued.

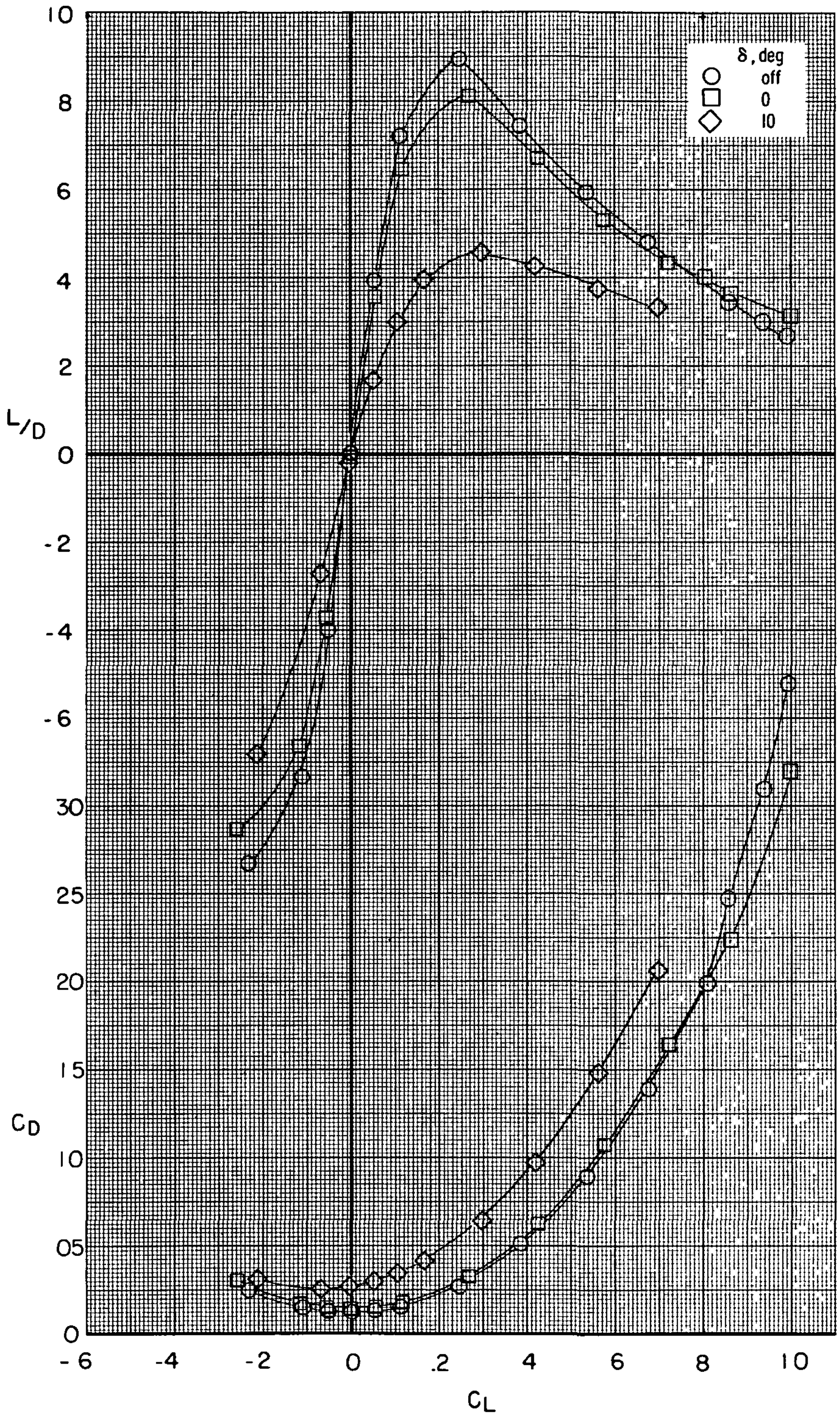

(c) Concluded.

Figure 4.- Concluded.

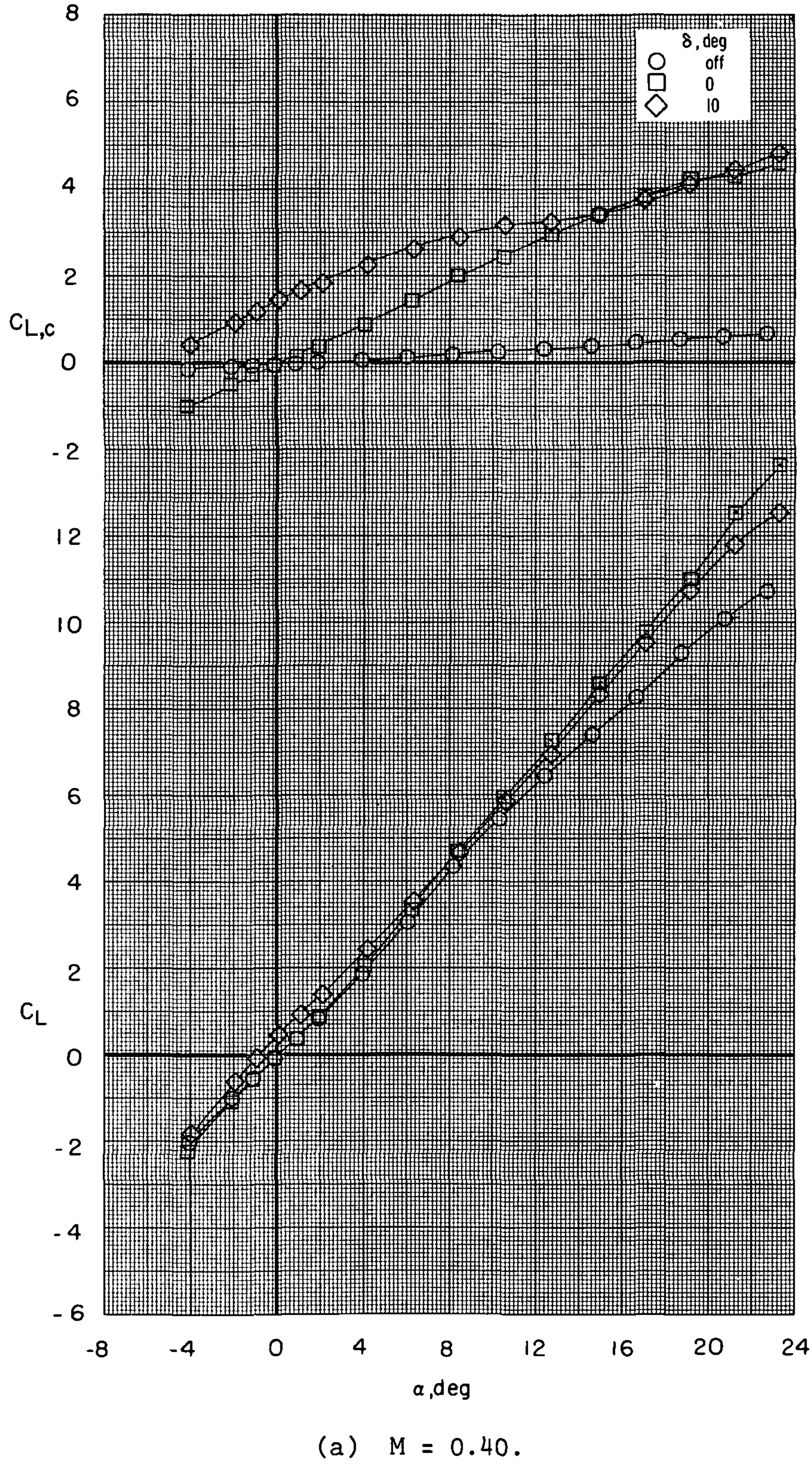

(a) M = 0.40.

Figure 5.- Effect of canard III (S_c/S_w = 0.28) deflection on longitudinal characteristics of wing I (Λ_w = 60°) for $z/\bar{c}$ = 0.0.

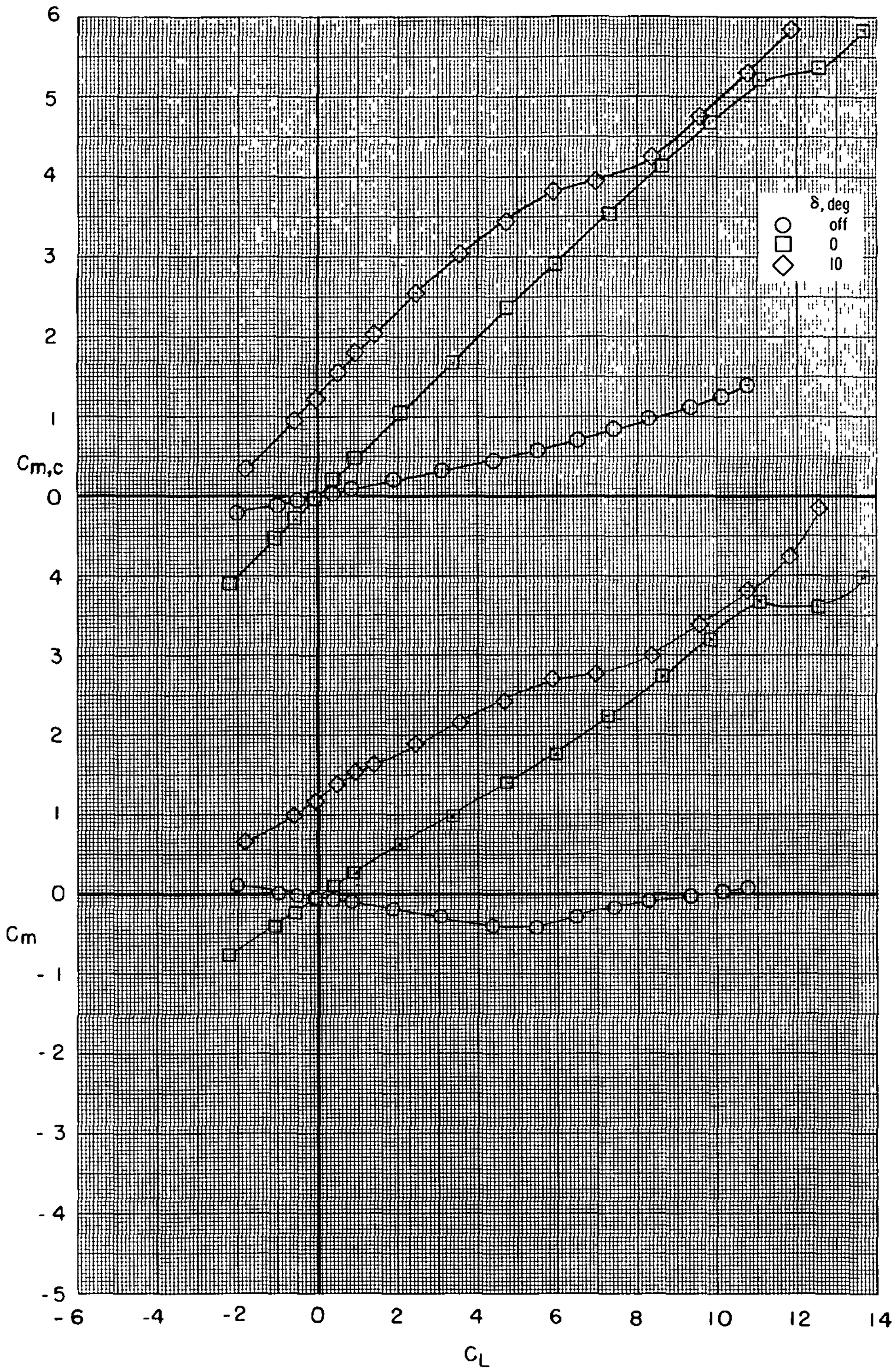

(a) Continued.

Figure 5.- Continued.

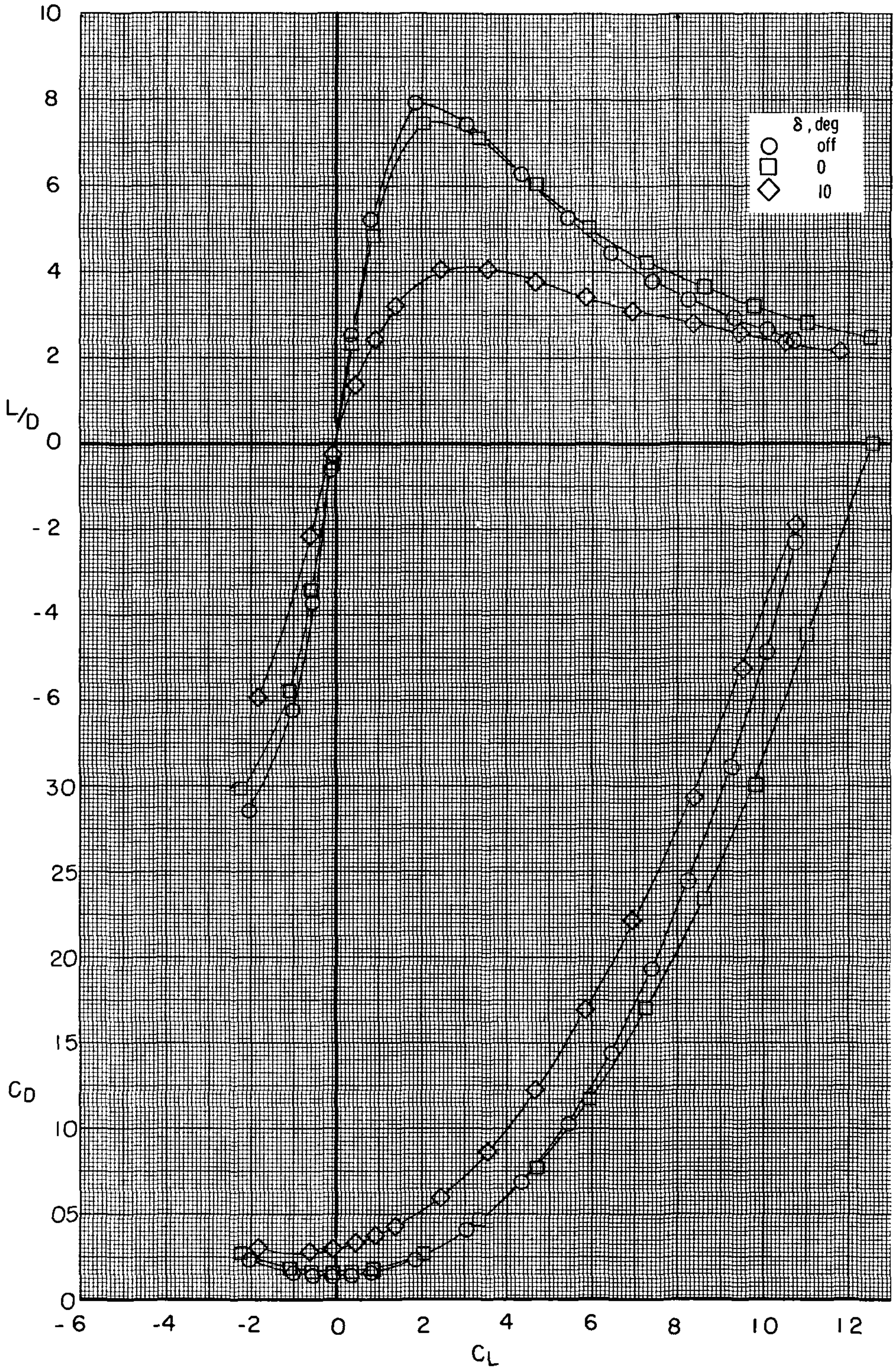

(a) Concluded.

Figure 5.- Continued.

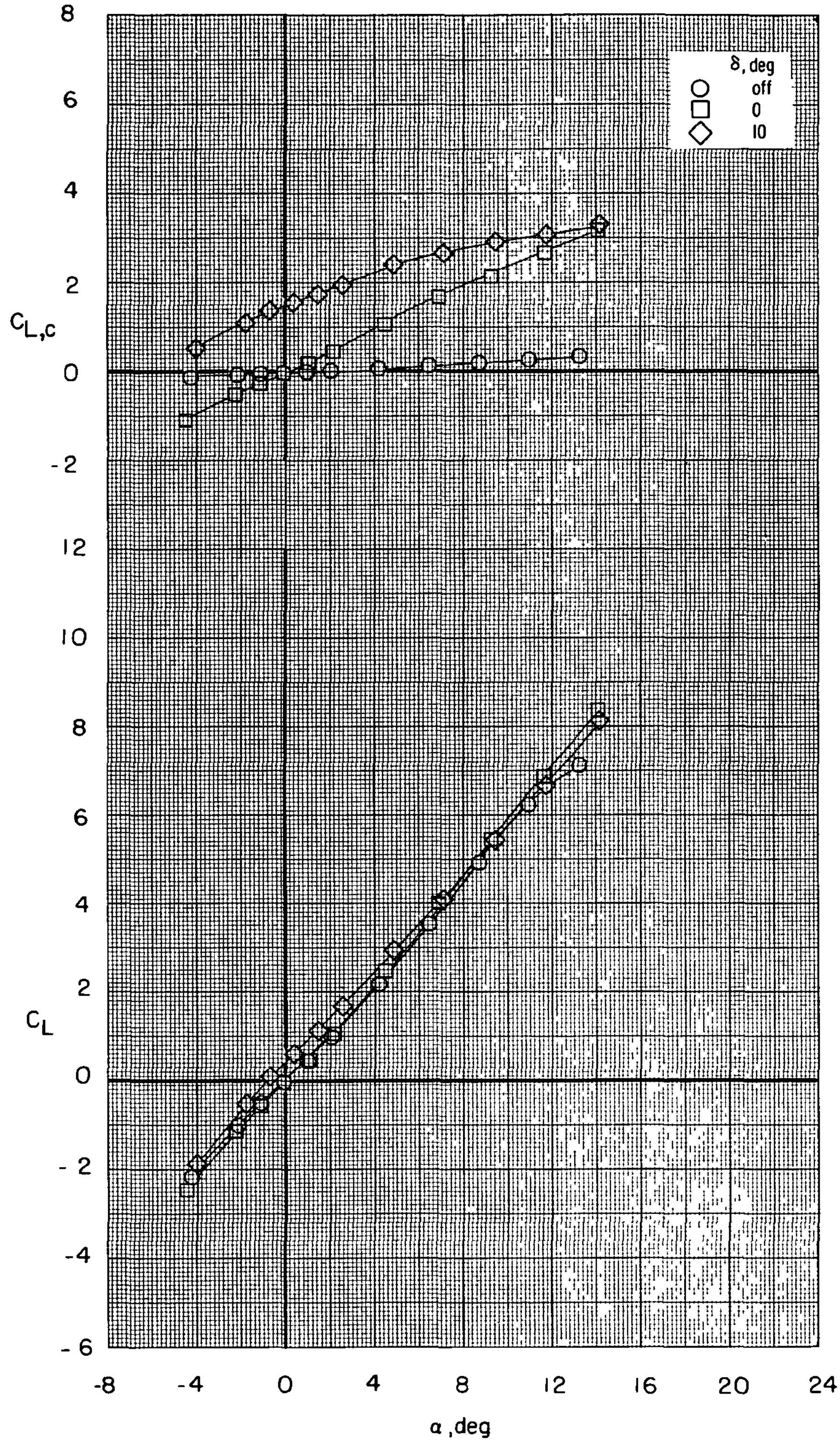

(b) M = 0.70.

Figure 5.- Continued.

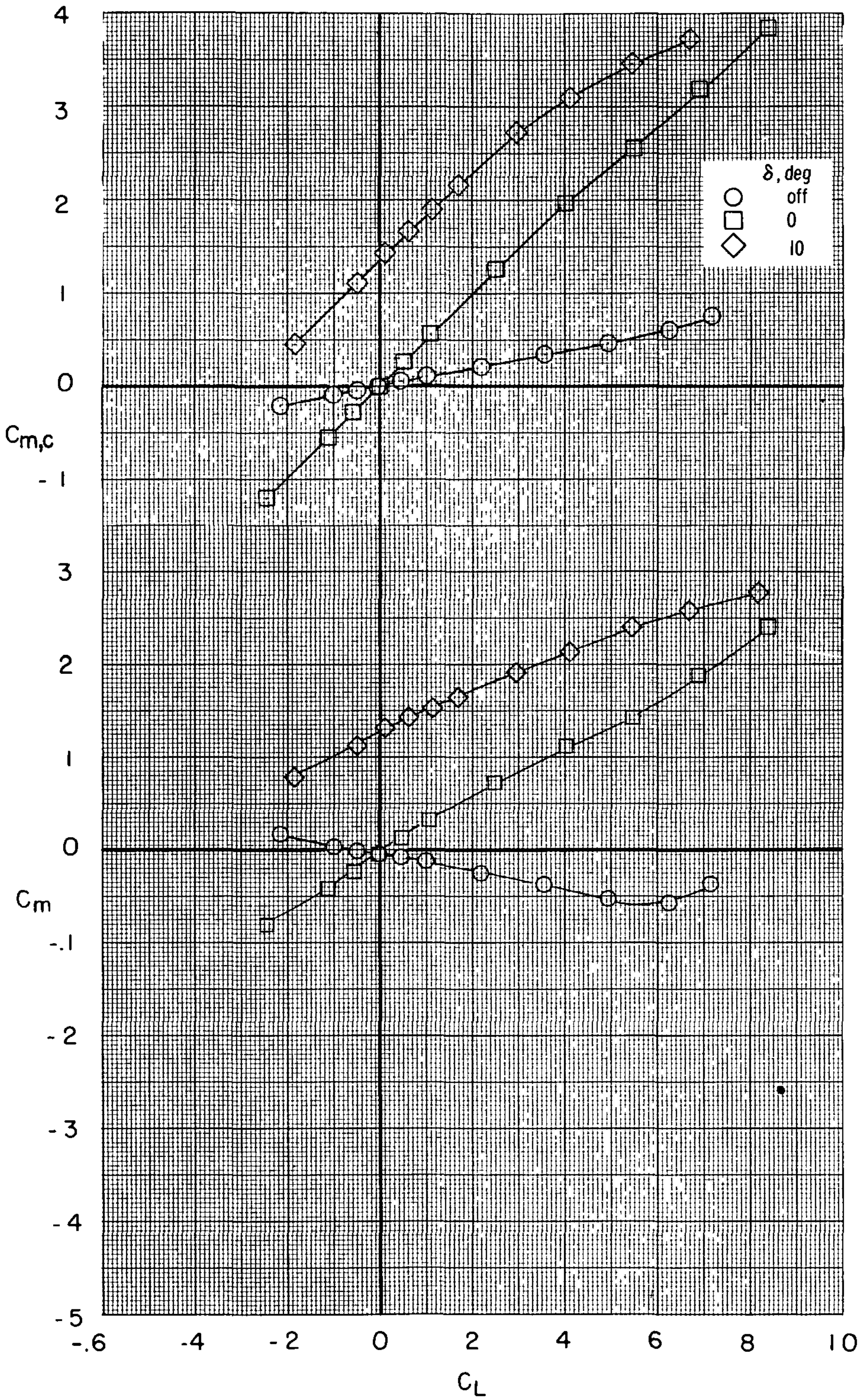

(b) Continued.

Figure 5.- Continued.

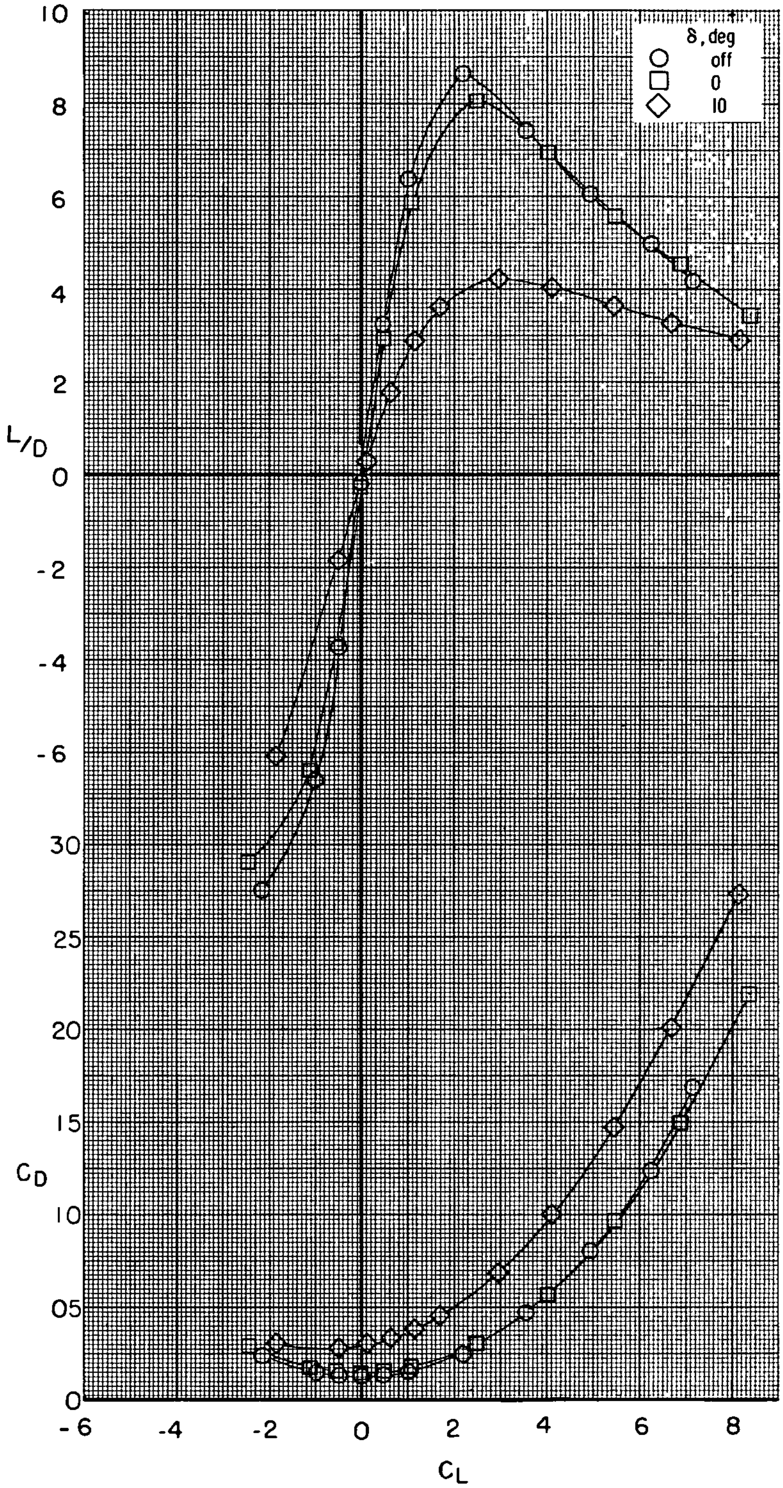

(b) Concluded.

Figure 5.- Continued.

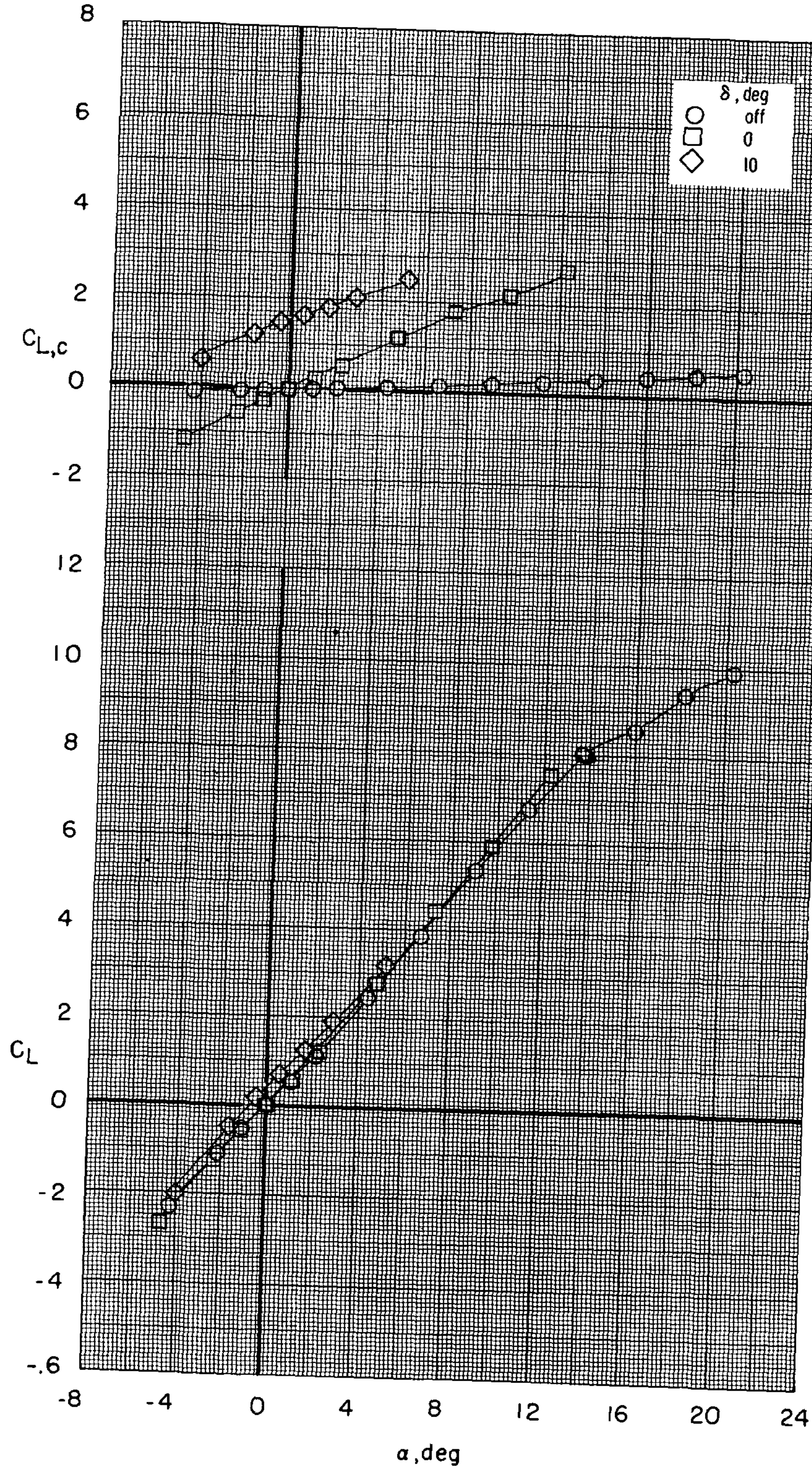

(c) M = 0.85.

Figure 5.- Continued.

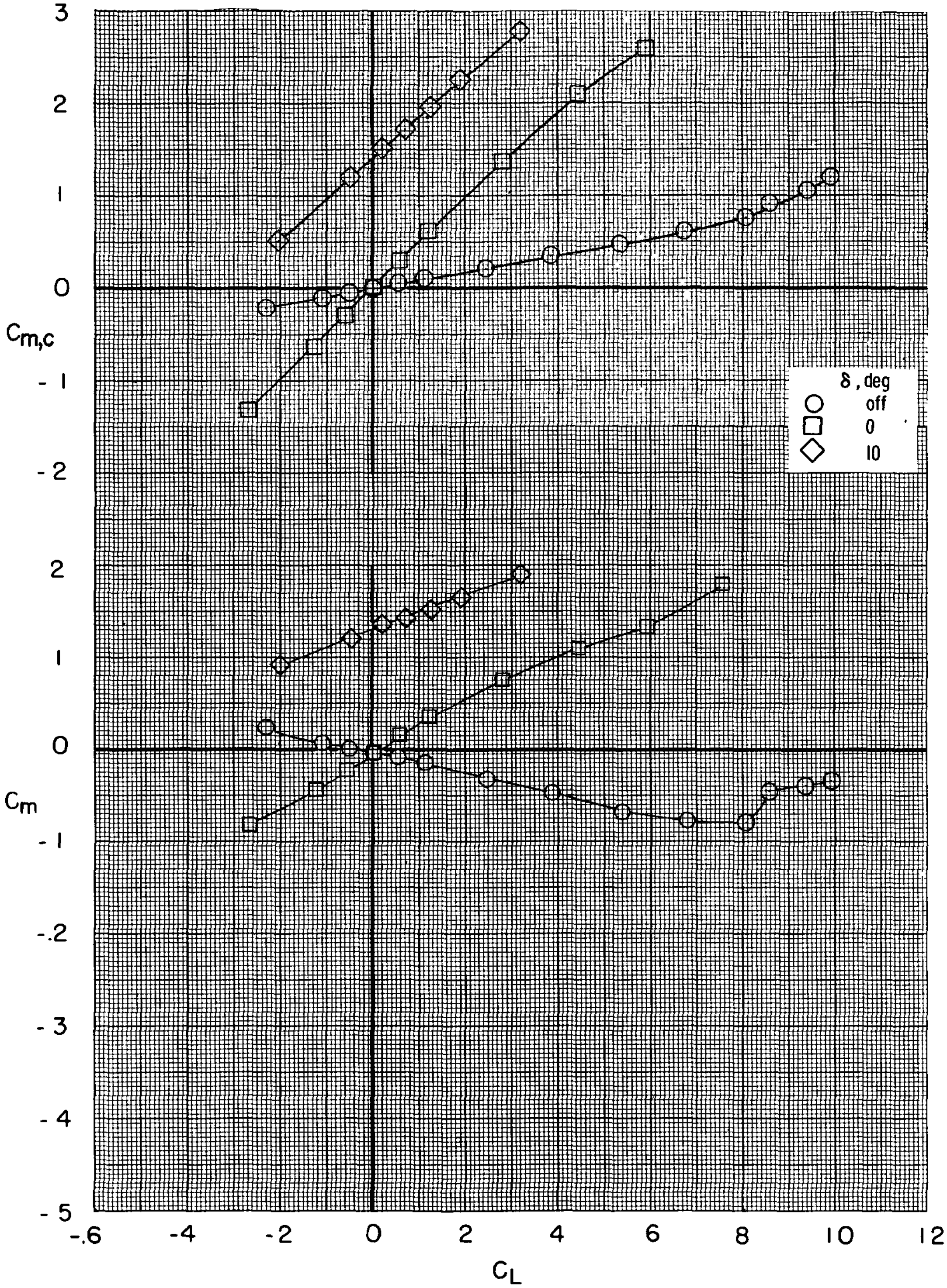

(c) Continued.

Figure 5.- Continued.

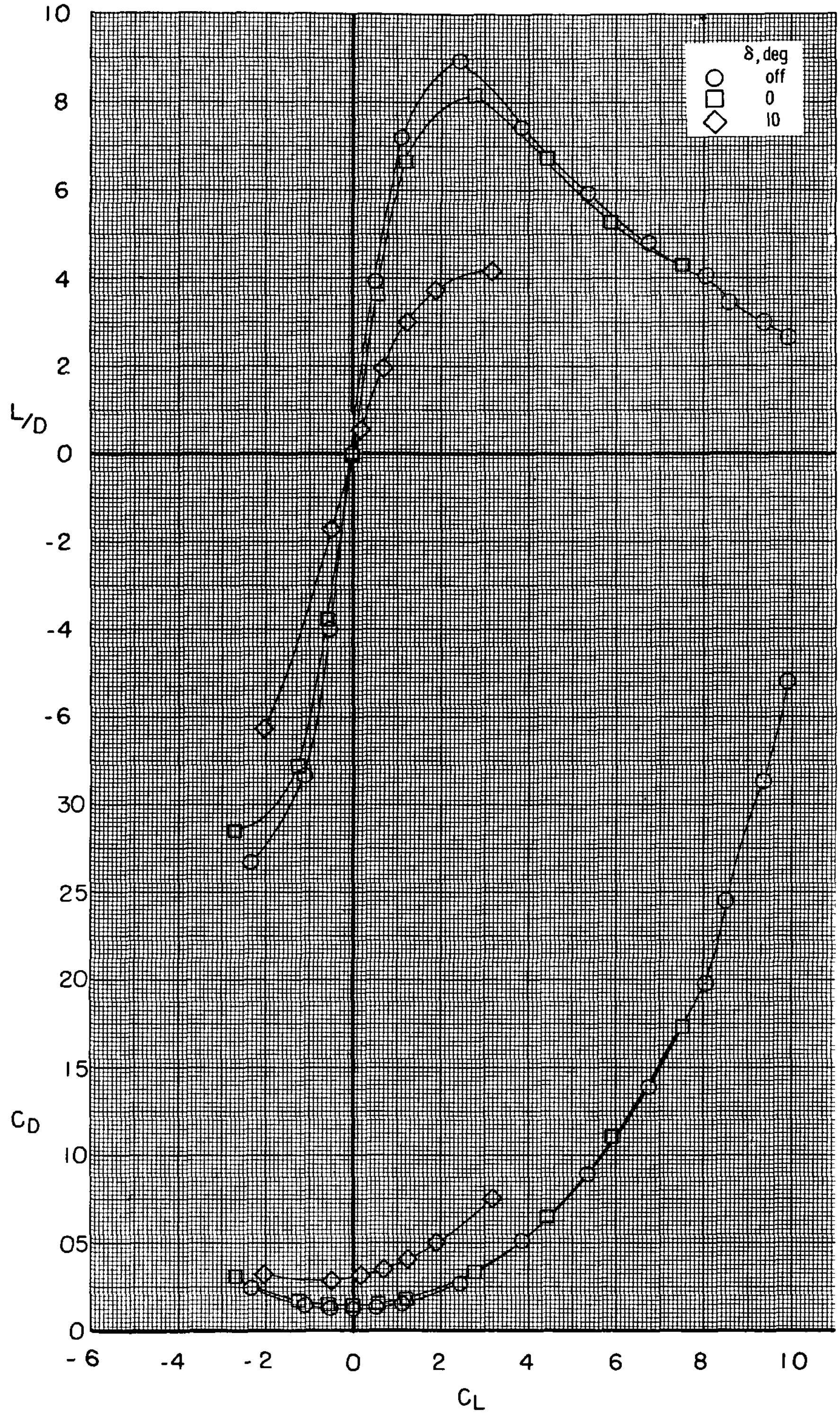

(c) Concluded.

Figure 5.- Concluded.

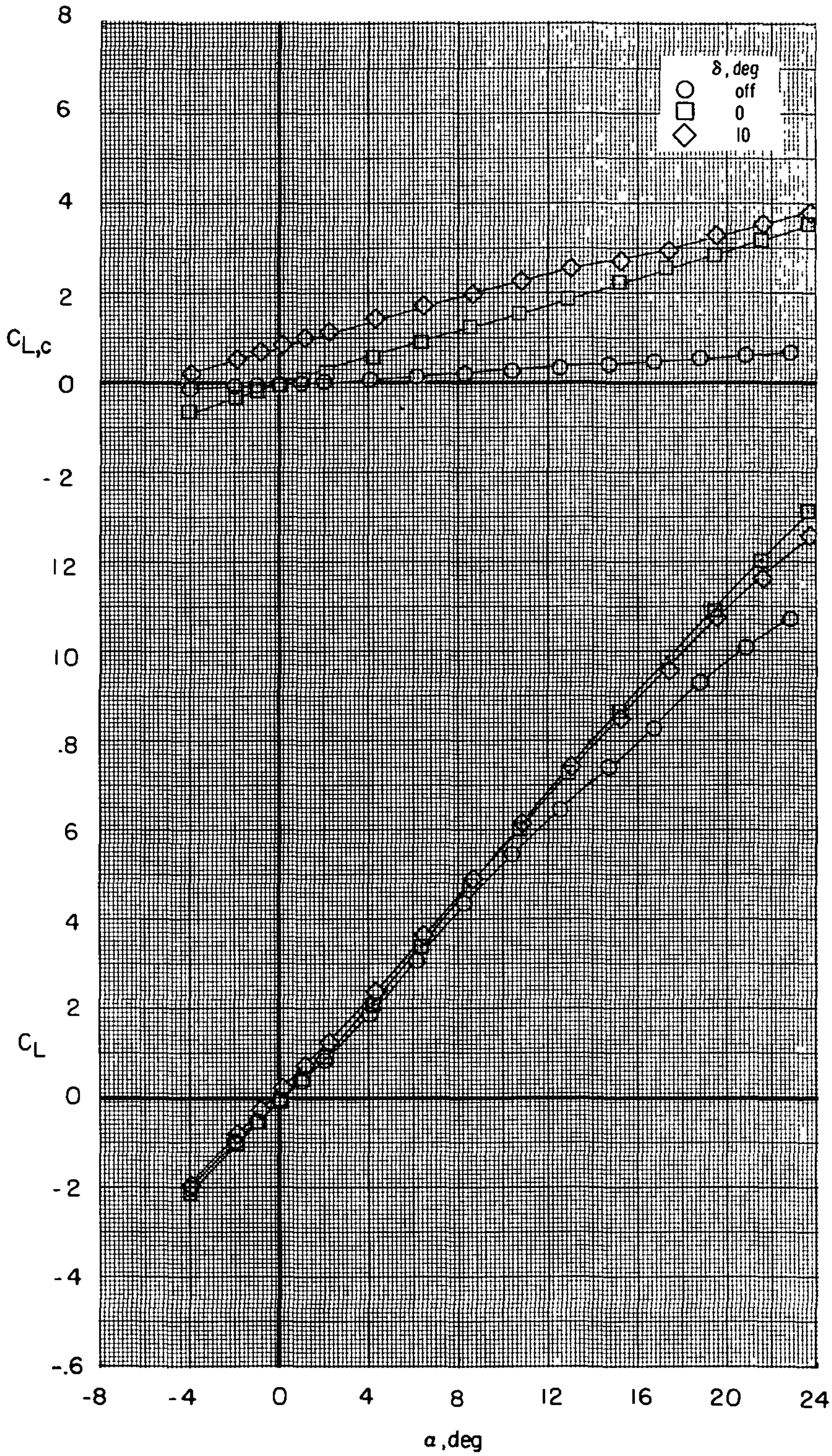

(a) M = 0.40.

Figure 6.- Effect of canard I ($S_c/S_W = 0.16$) deflection on longitudinal characteristics of wing I ($\Lambda_W = 60^o$) for $z/\bar{c} = 0.185$.

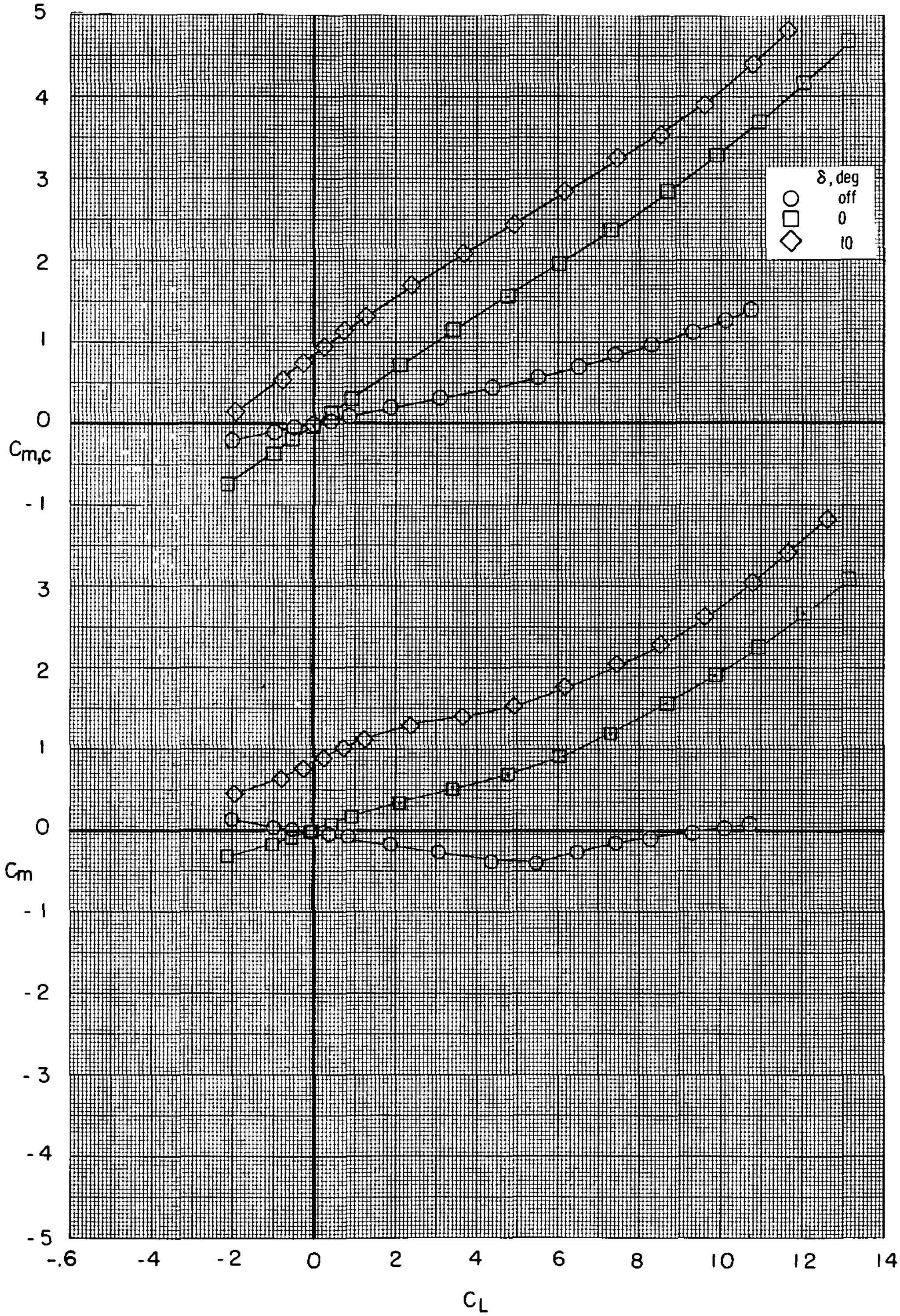

(a) Continued.

Figure 6.- Continued.

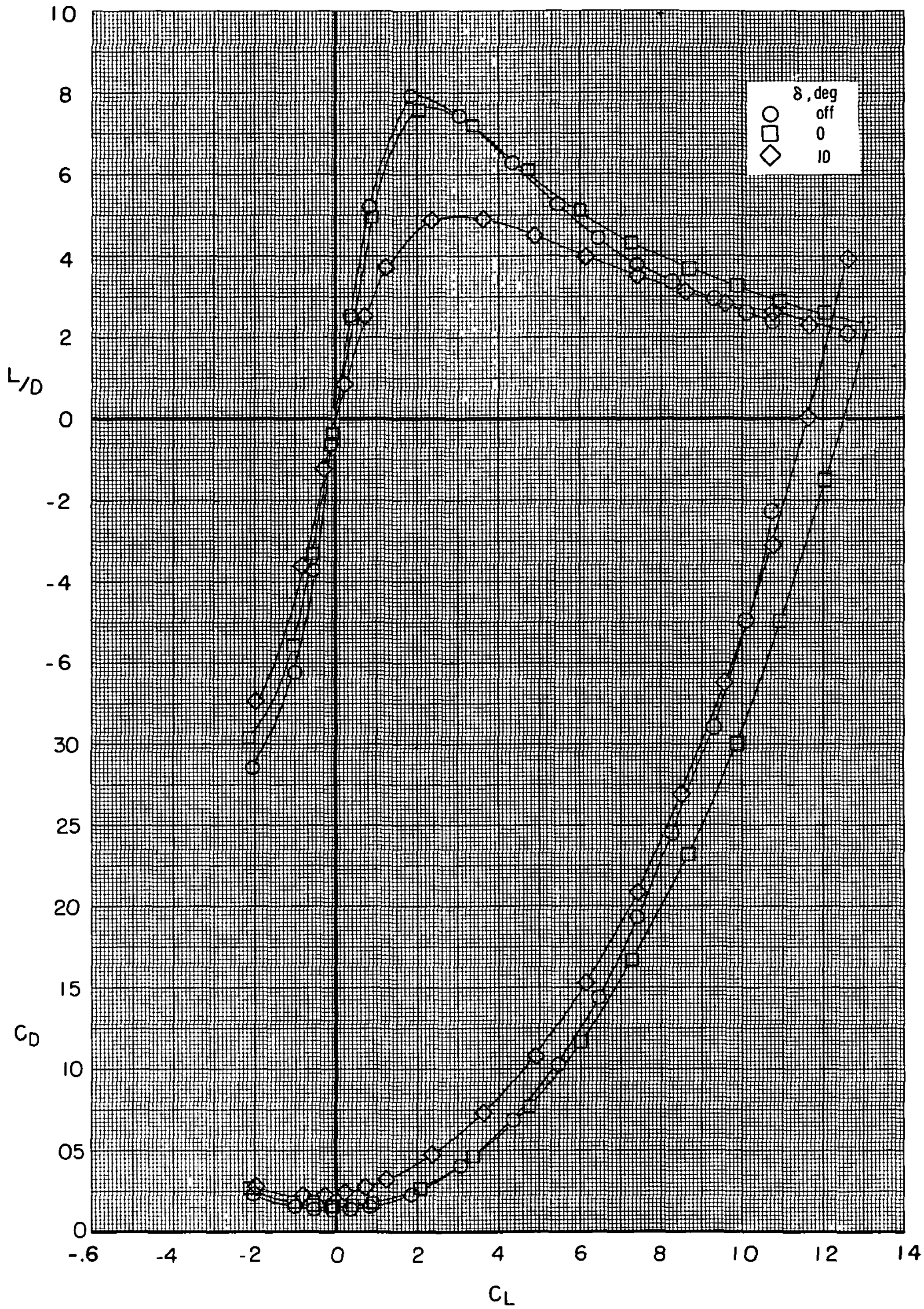

(a) Concluded.

Figure 6.- Continued.

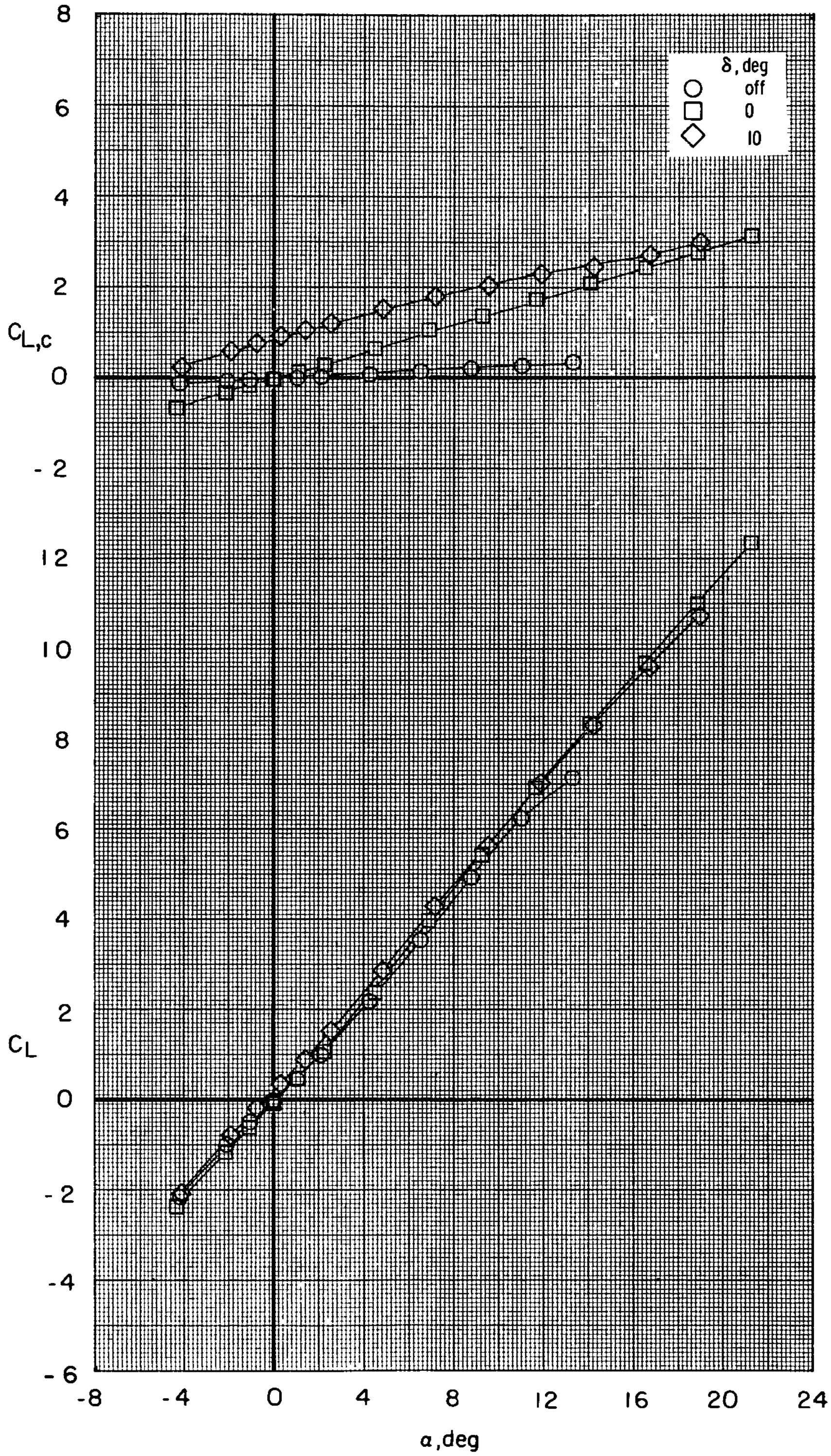

(b) M = 0.70

Figure 6.- Continued.

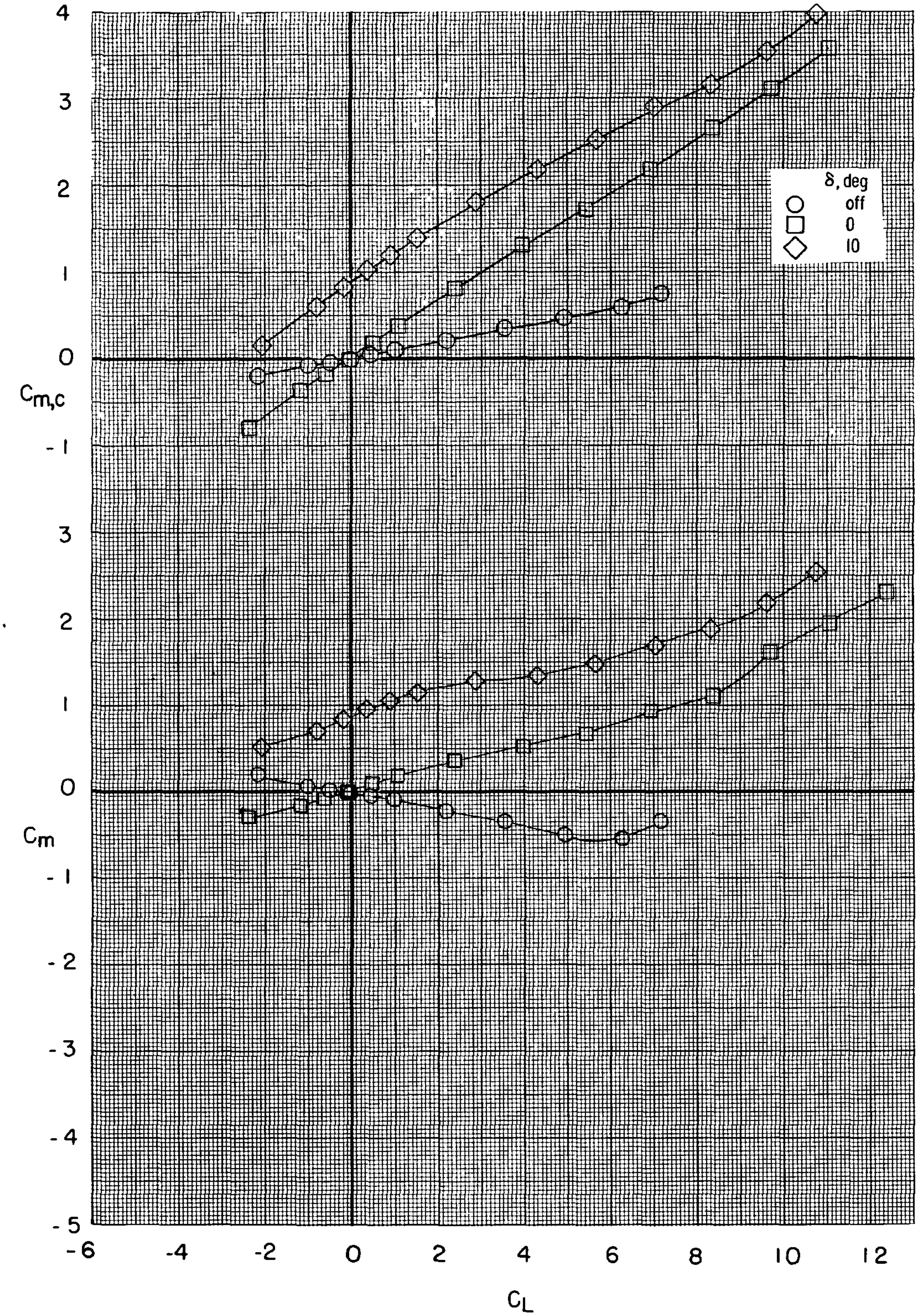

(b) Continued.

Figure 6.- Continued.

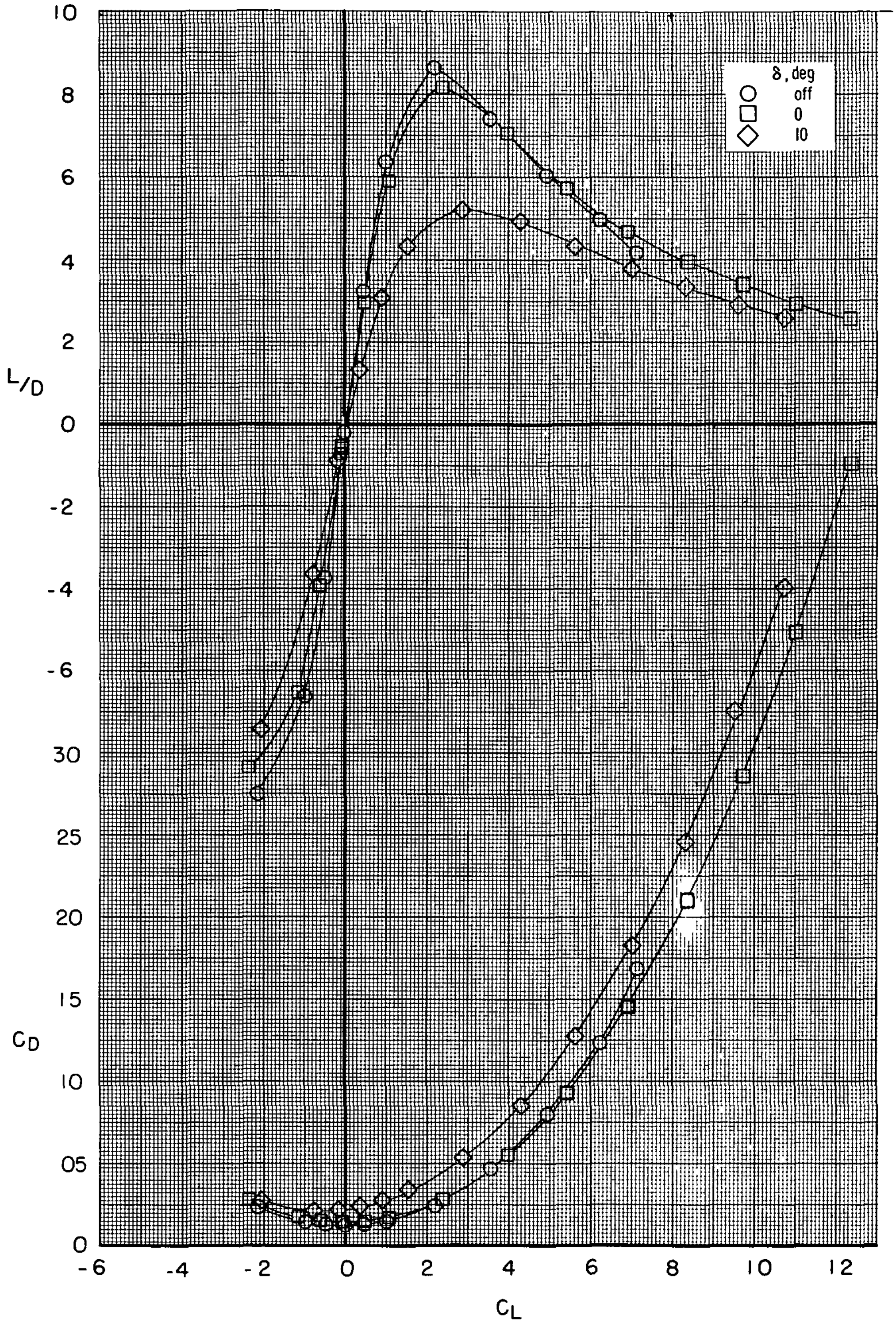

(b) Concluded.

Figure 6.- Continued.

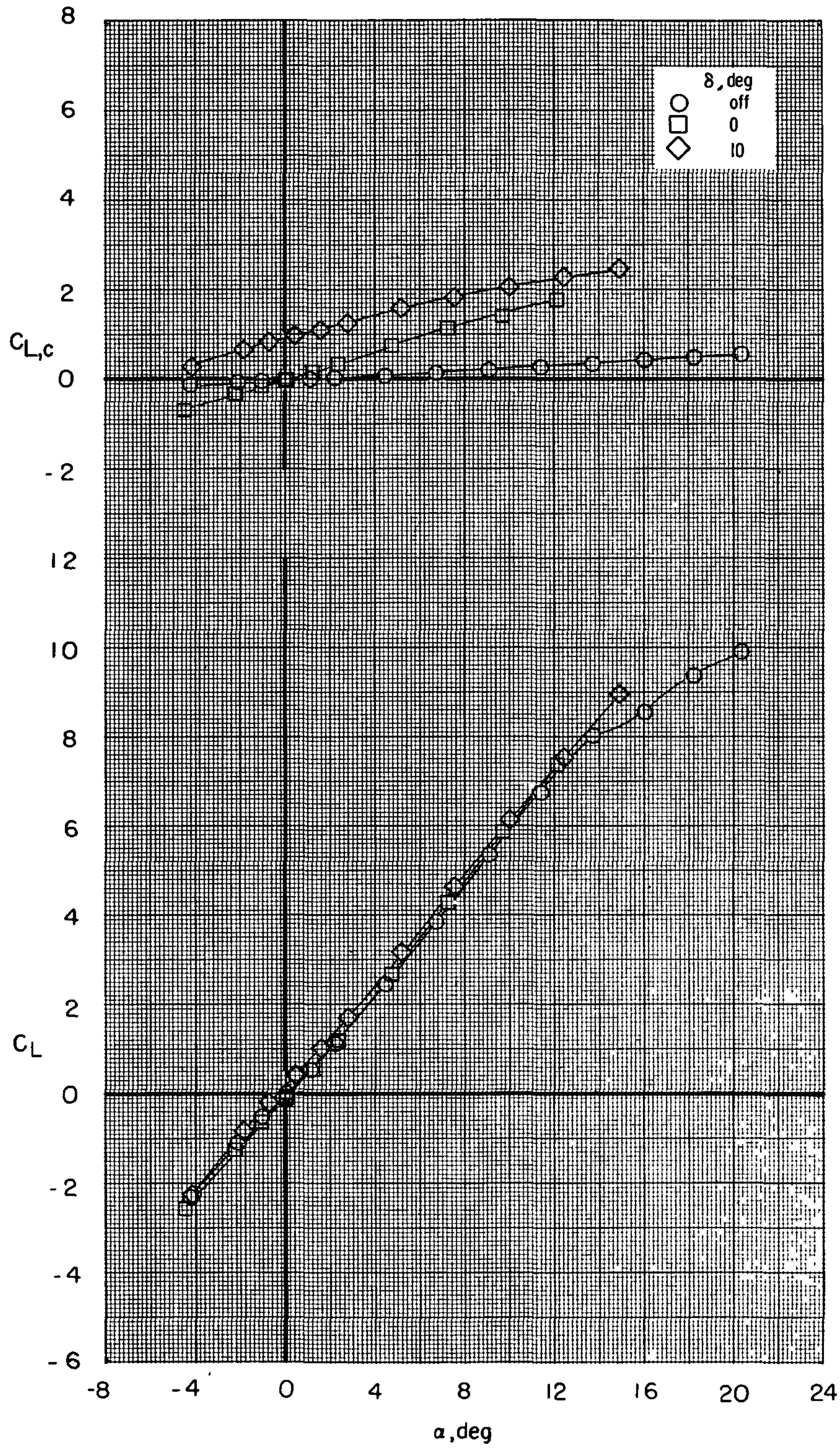

(c) M = 0.85.

Figure 6.- Continued.

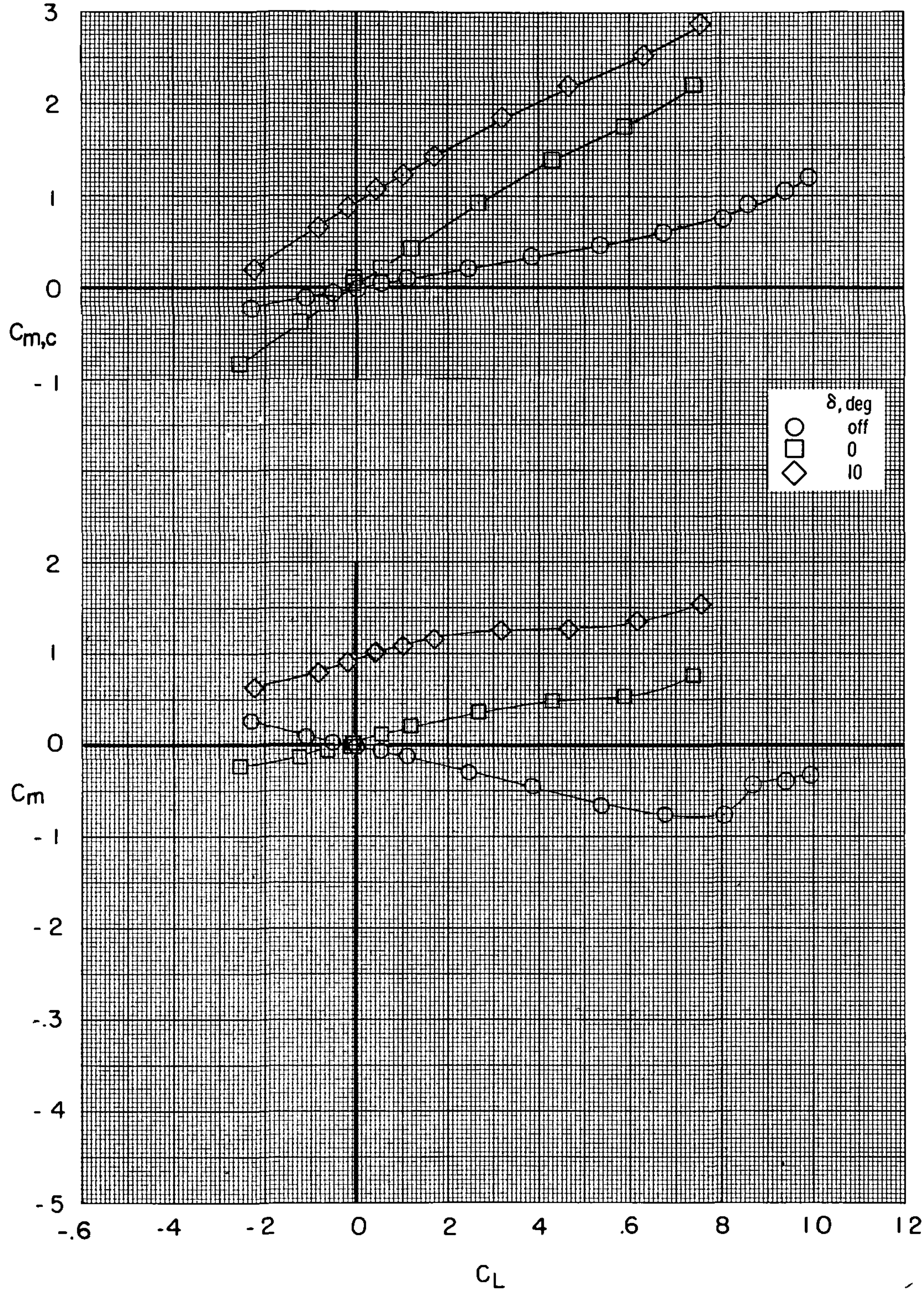

(c) Continued.

Figure 6.- Continued.

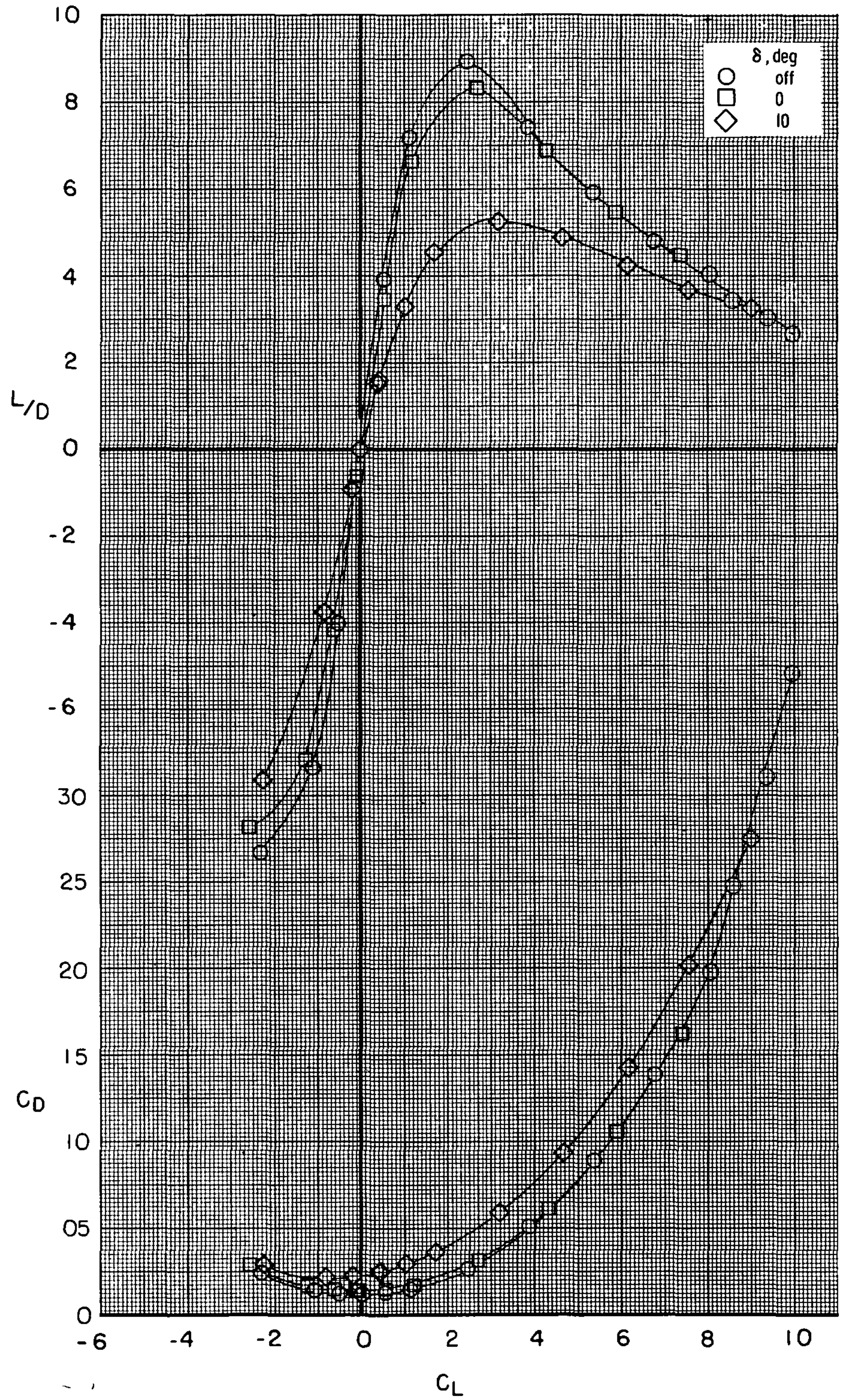

(c) Concluded.

Figure 6.- Concluded.

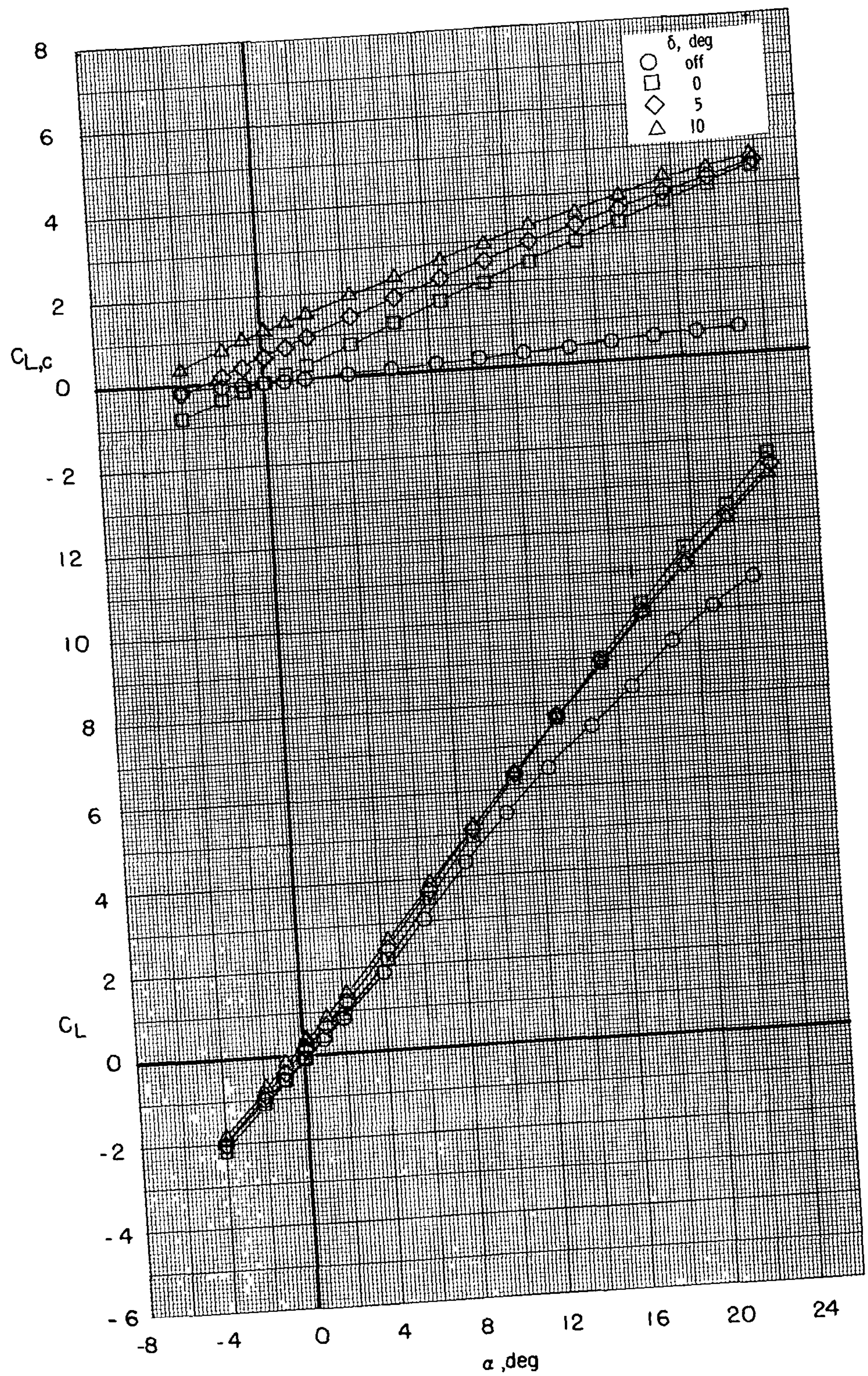

(a) M = 0.40.

Figure 7.- Effect of canard II ($S_c/S_w = 0.22$) deflection on longitudinal characteristics of wing I ($\Lambda_w = 60^\circ$) for $z/\bar{c} = 0.185$.

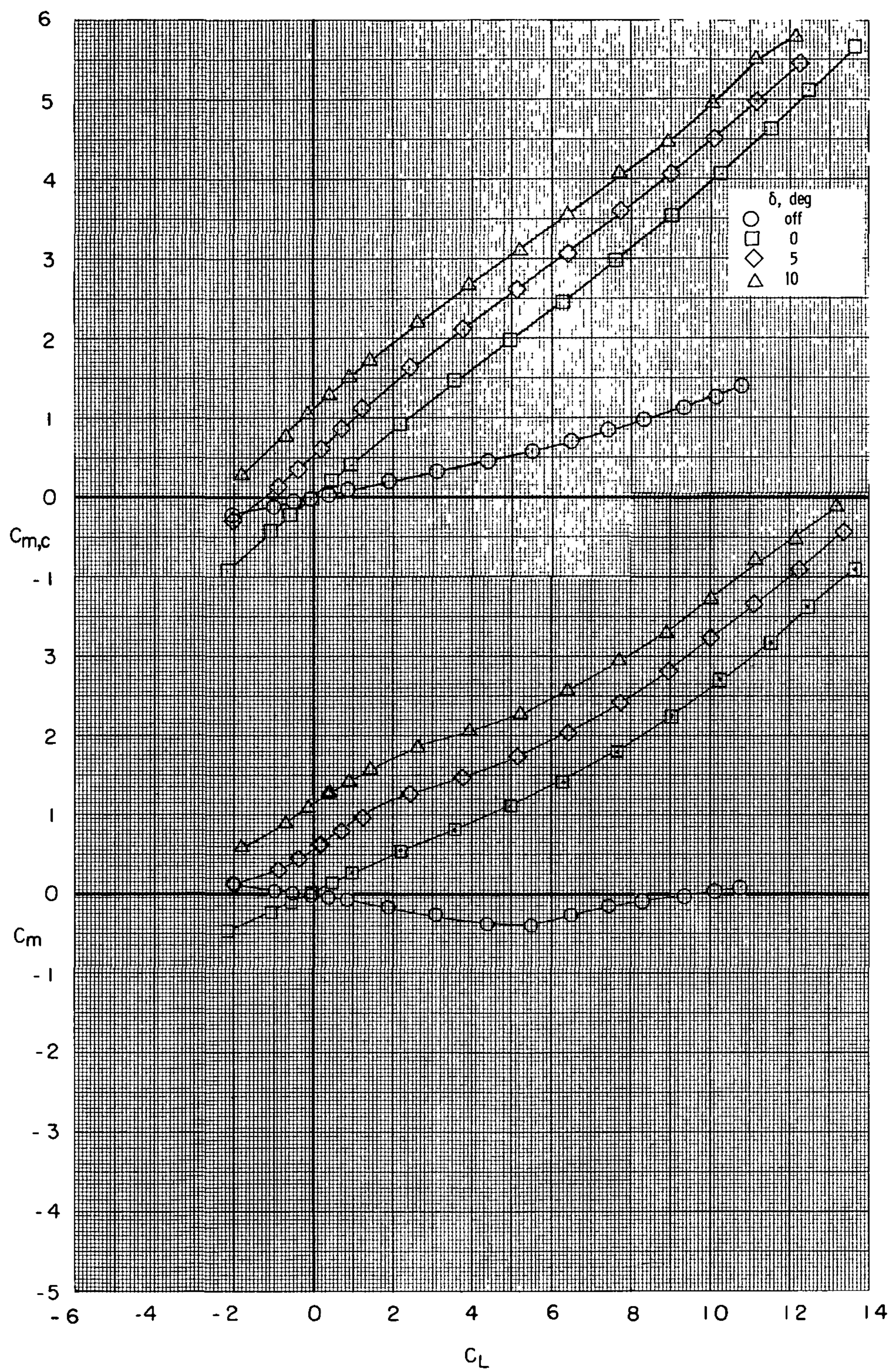

(a) Continued.

Figure 7.- Continued.

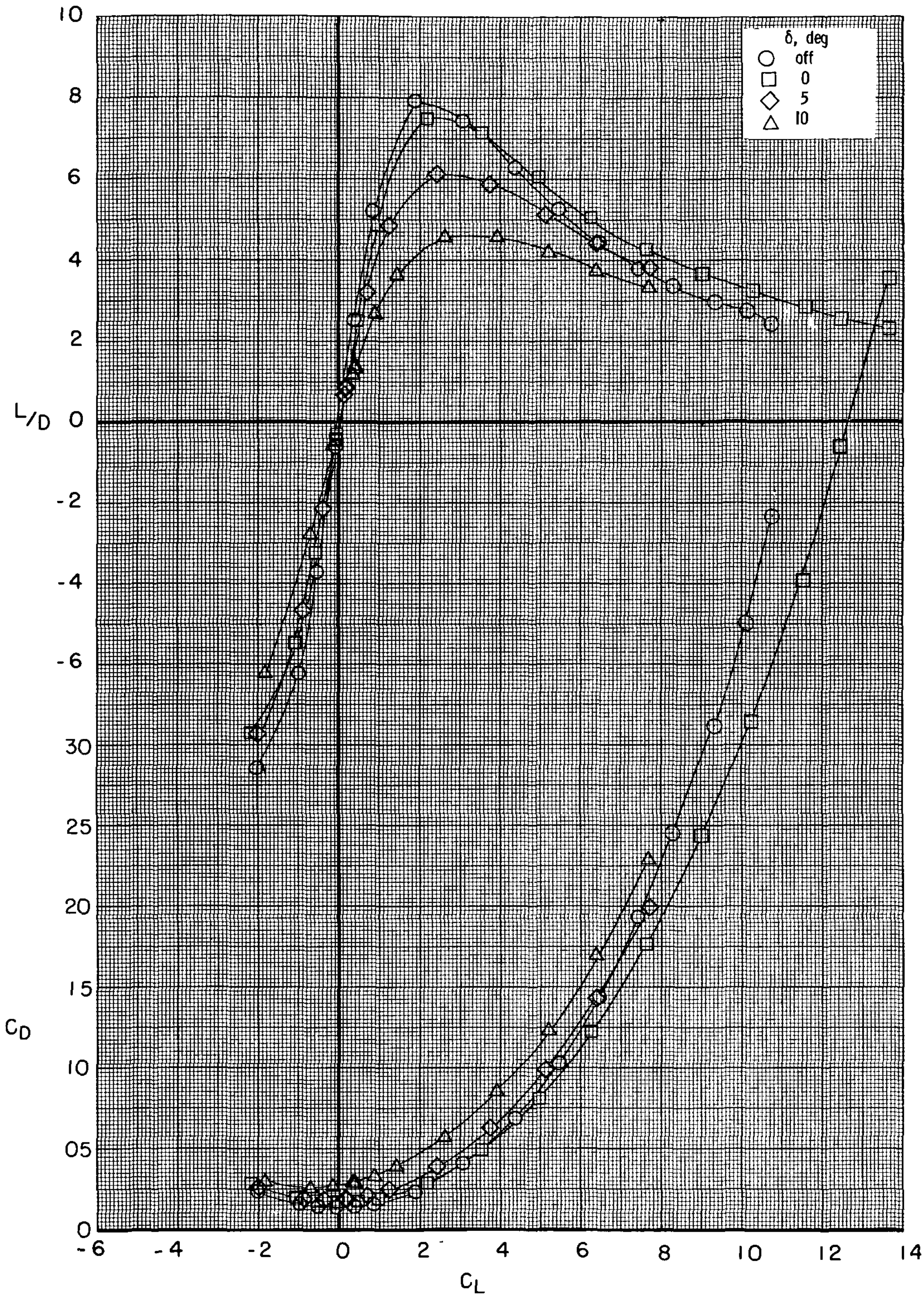

(a) Concluded.

Figure 7.- Continued.

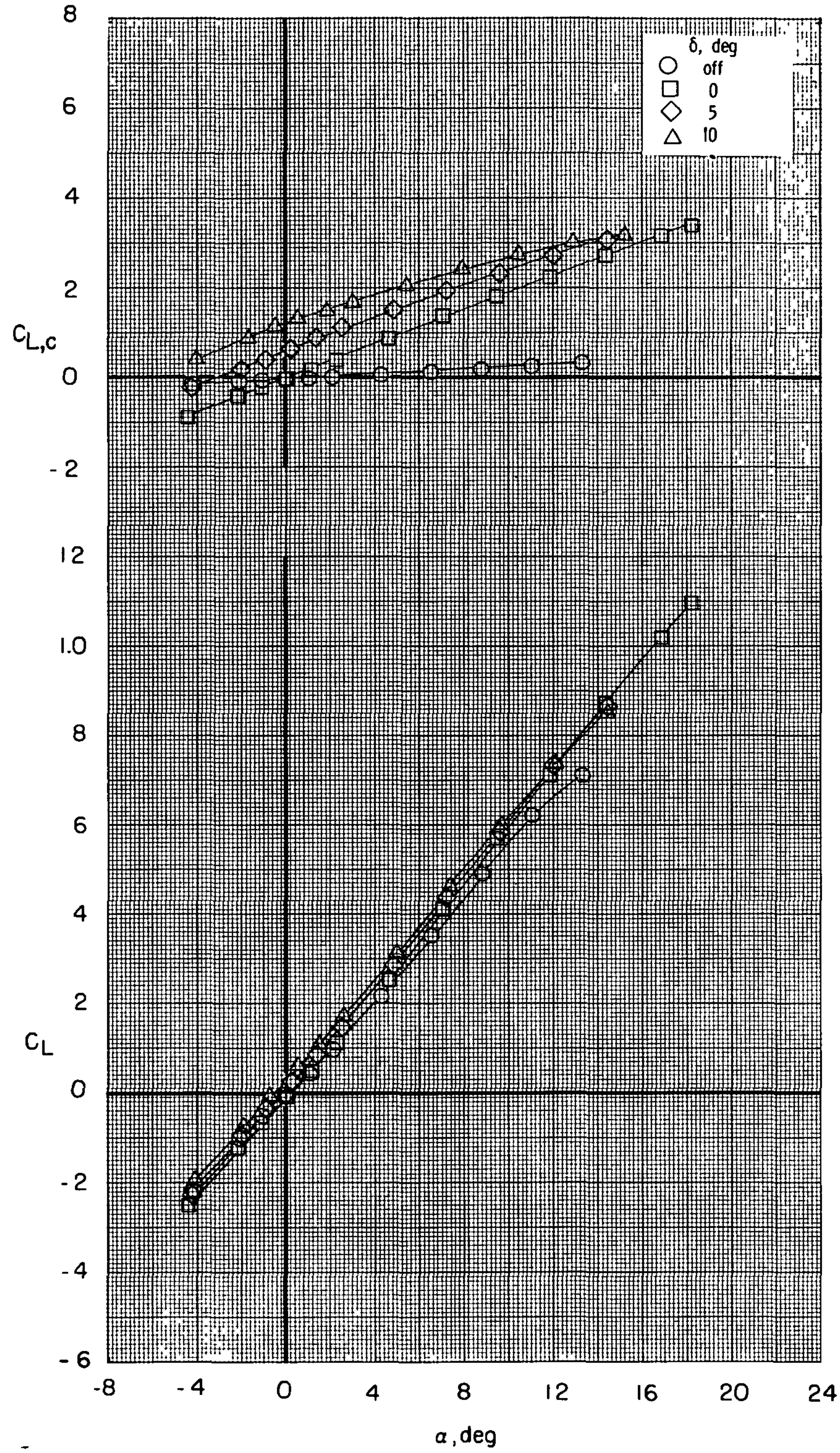

(b) M = 0.70.

Figure 7.- Continued.

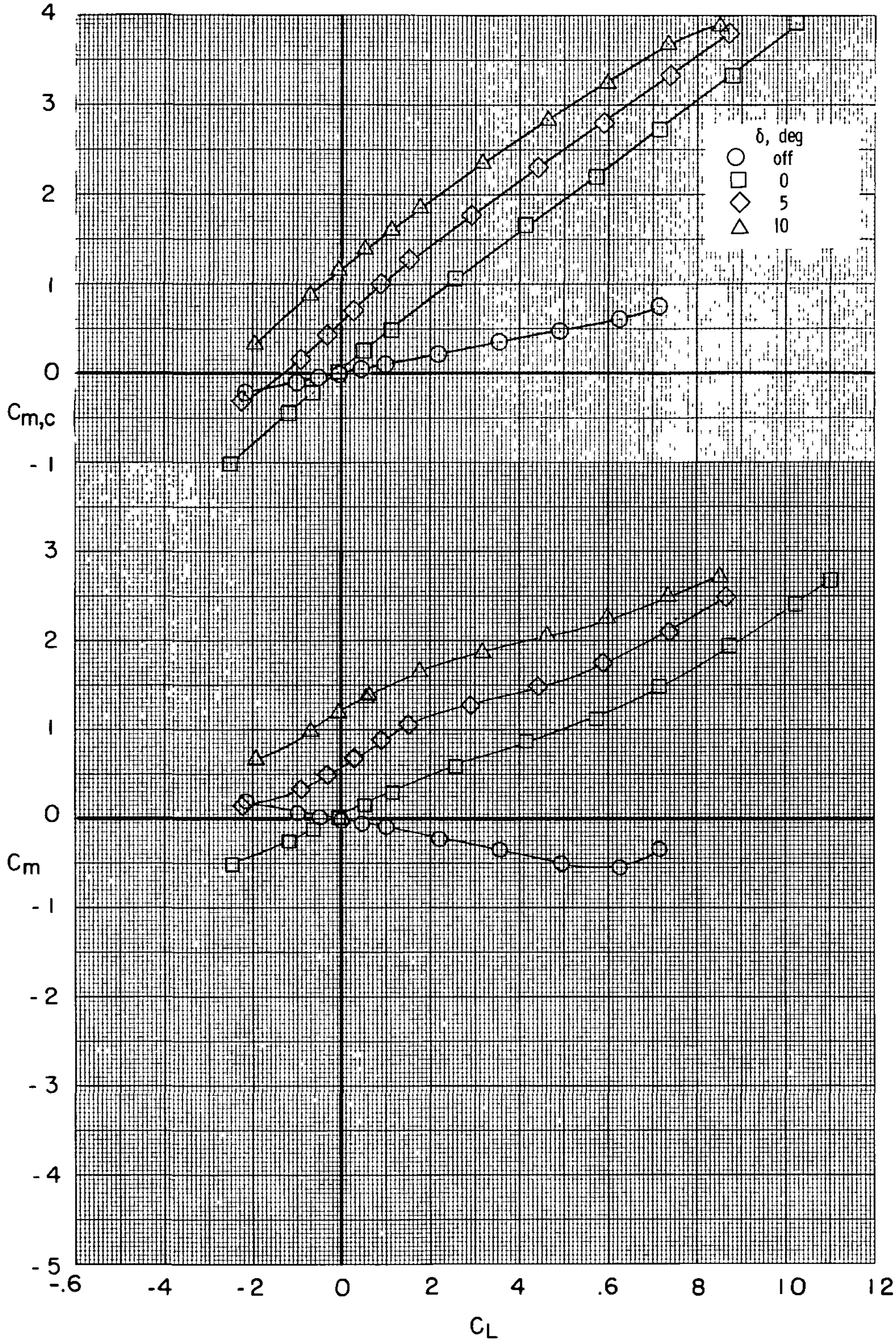

(b) Continued.

Figure 7.- Continued.

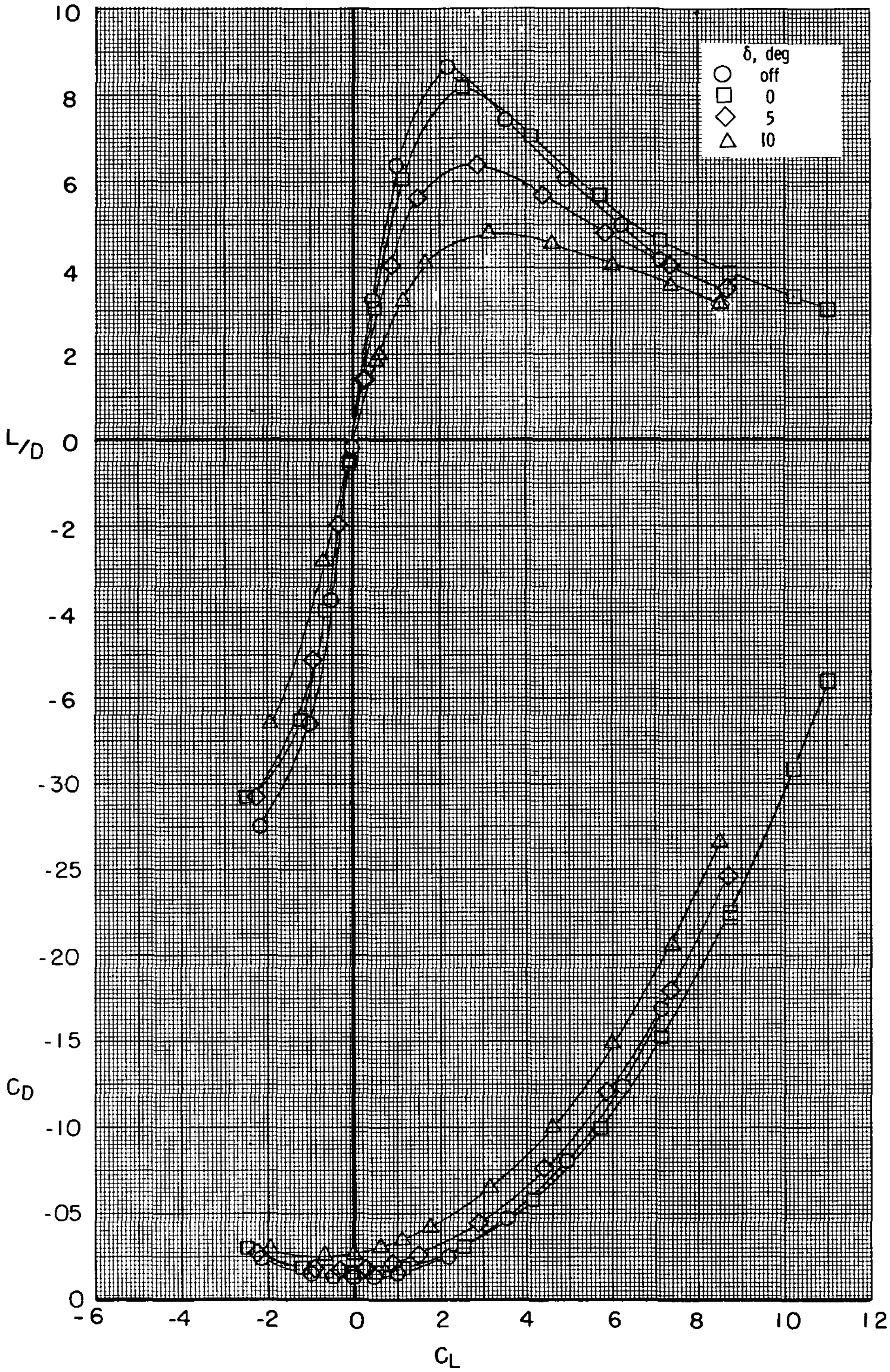

(b) Concluded.

Figure 7.- Continued.

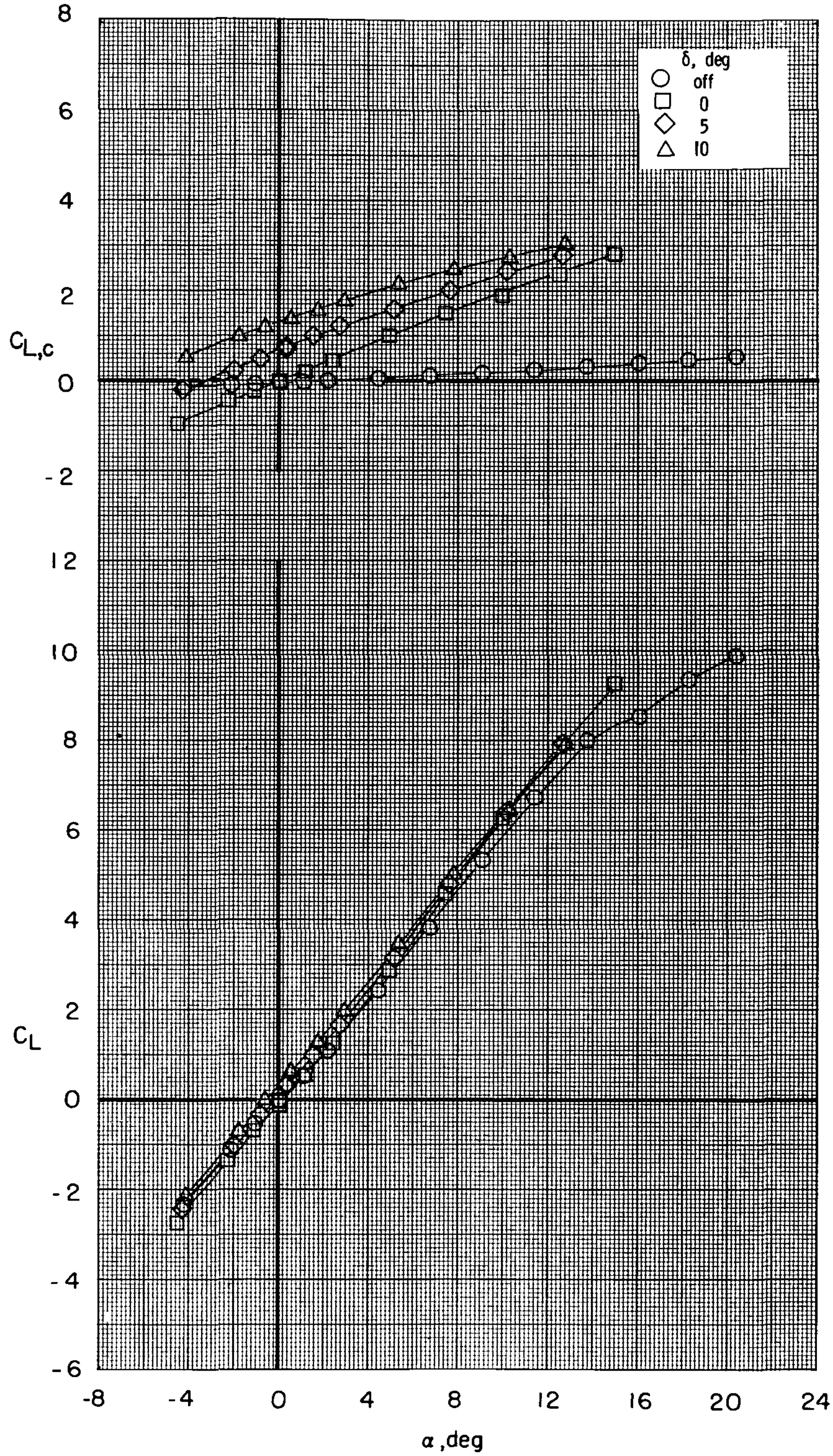

(c) M = 0.85.

Figure 7.- Continued.

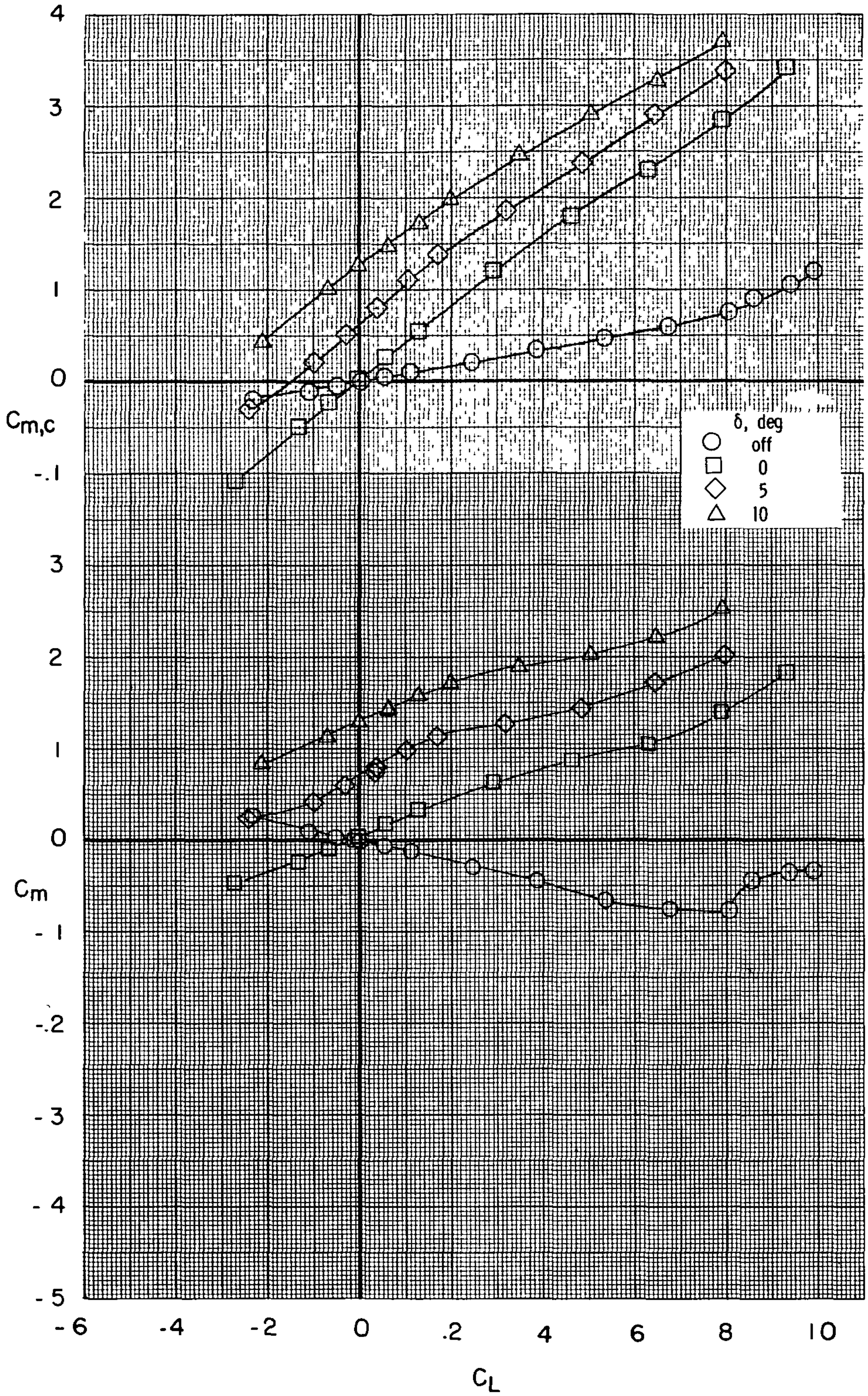

(c) Continued.

Figure 7.- Continued.

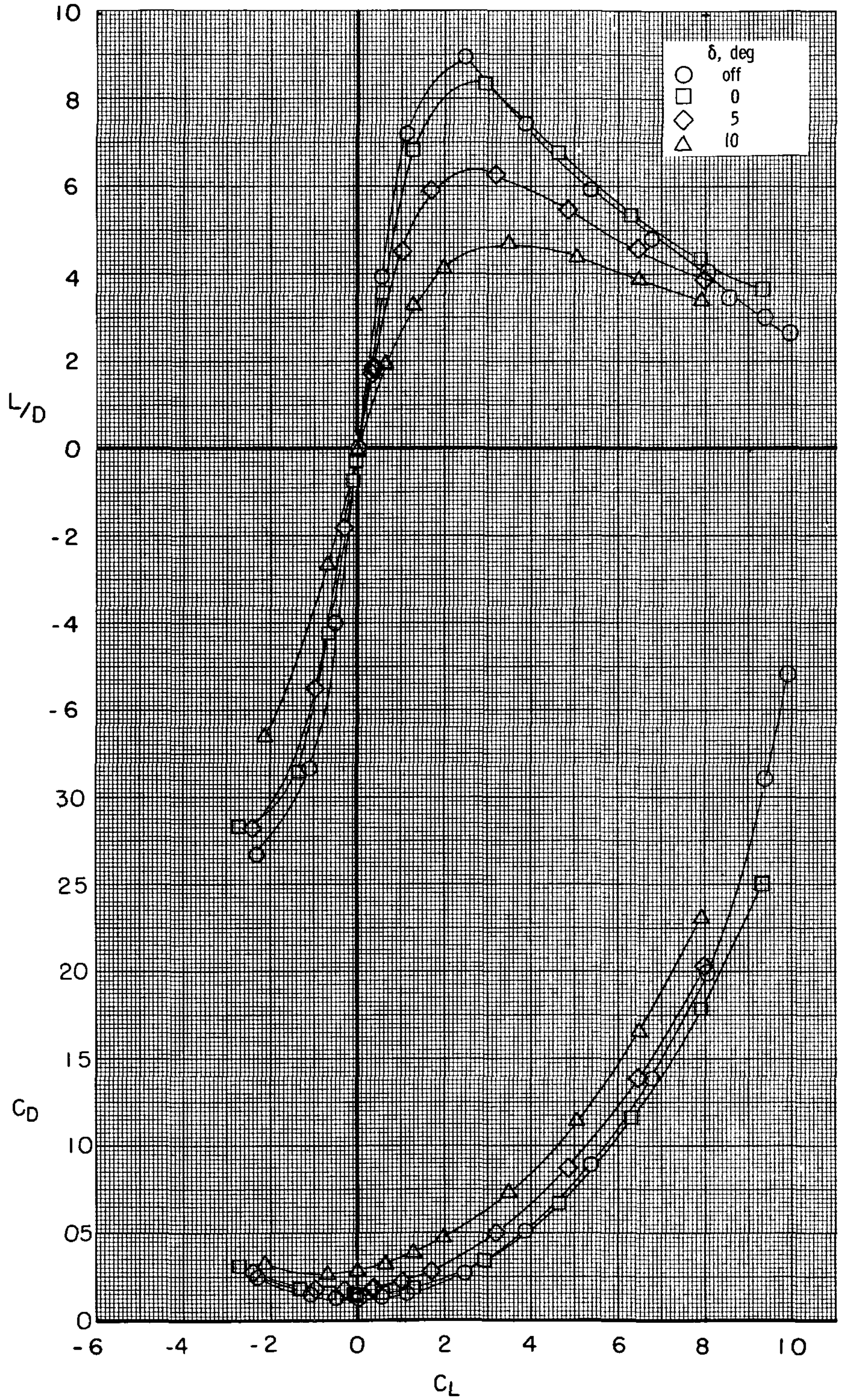

(c) Concluded.

Figure 7.- Concluded.

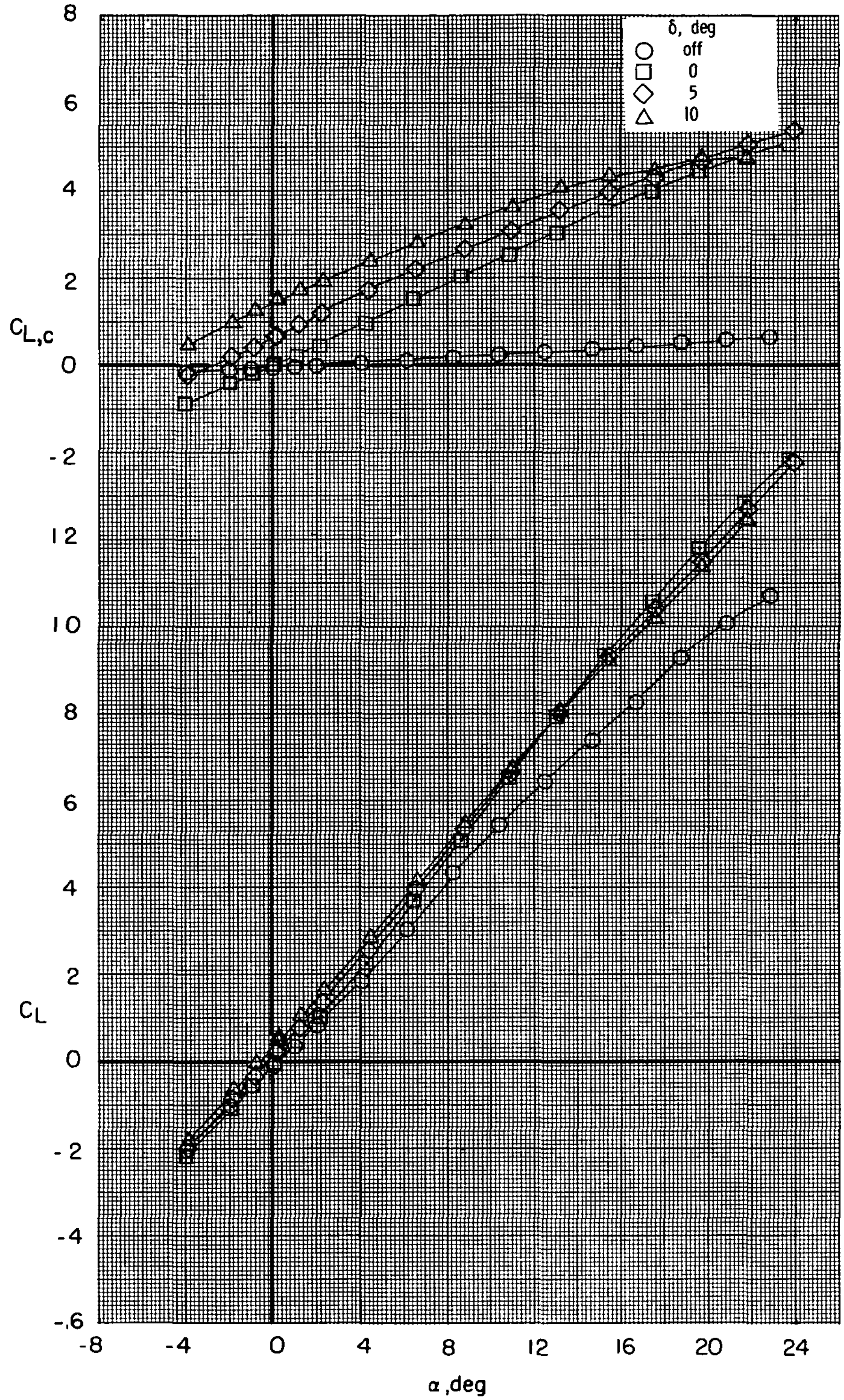

(a) M = 0.40.

Figure 8.- Effect of canard III (S_c/S_W = 0.28) deflection on longitudinal characteristics of wing I (Λ_W = 60°) for $z/\bar{c}$ = 0.185.

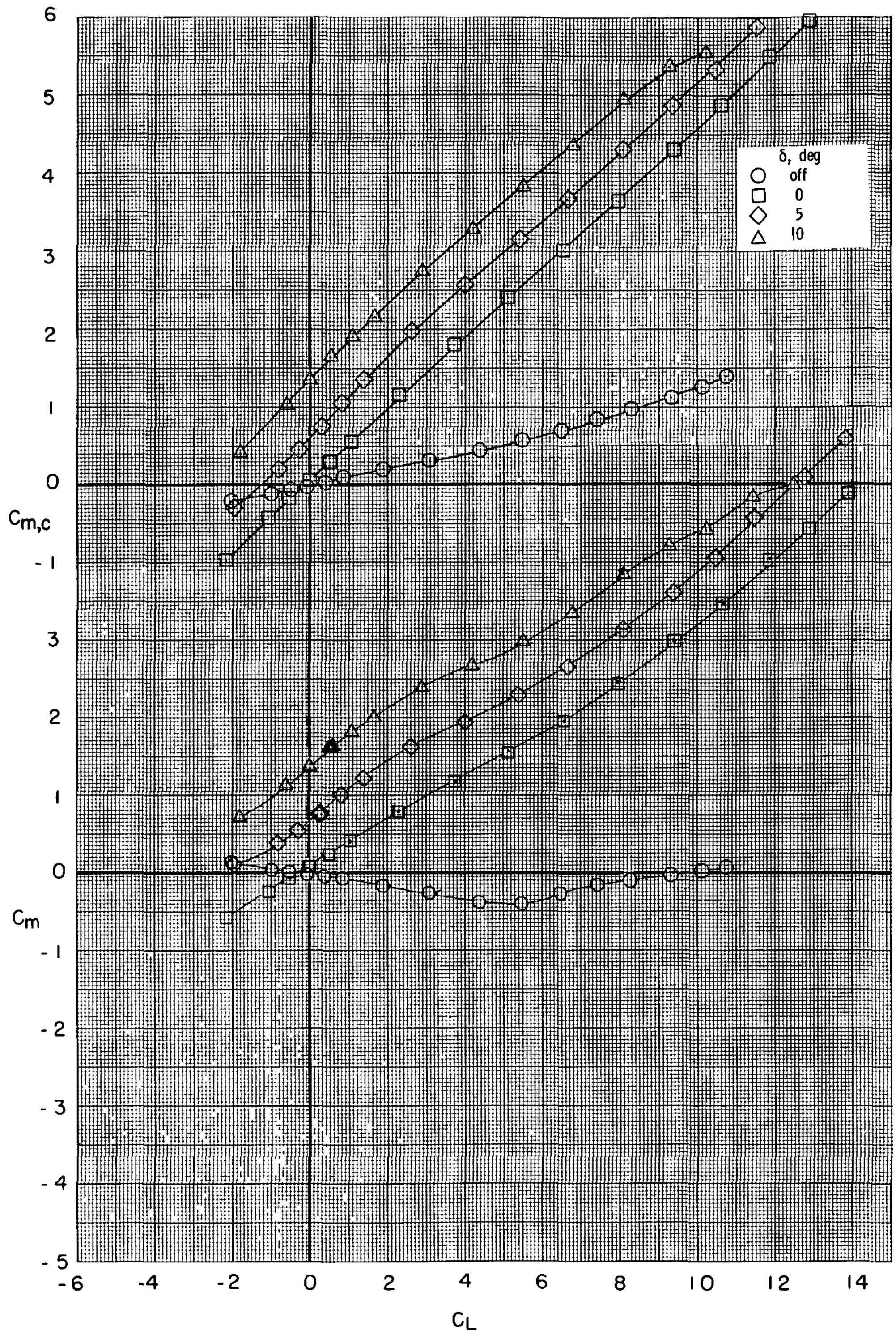

(a) Continued.

Figure 8.- Continued.

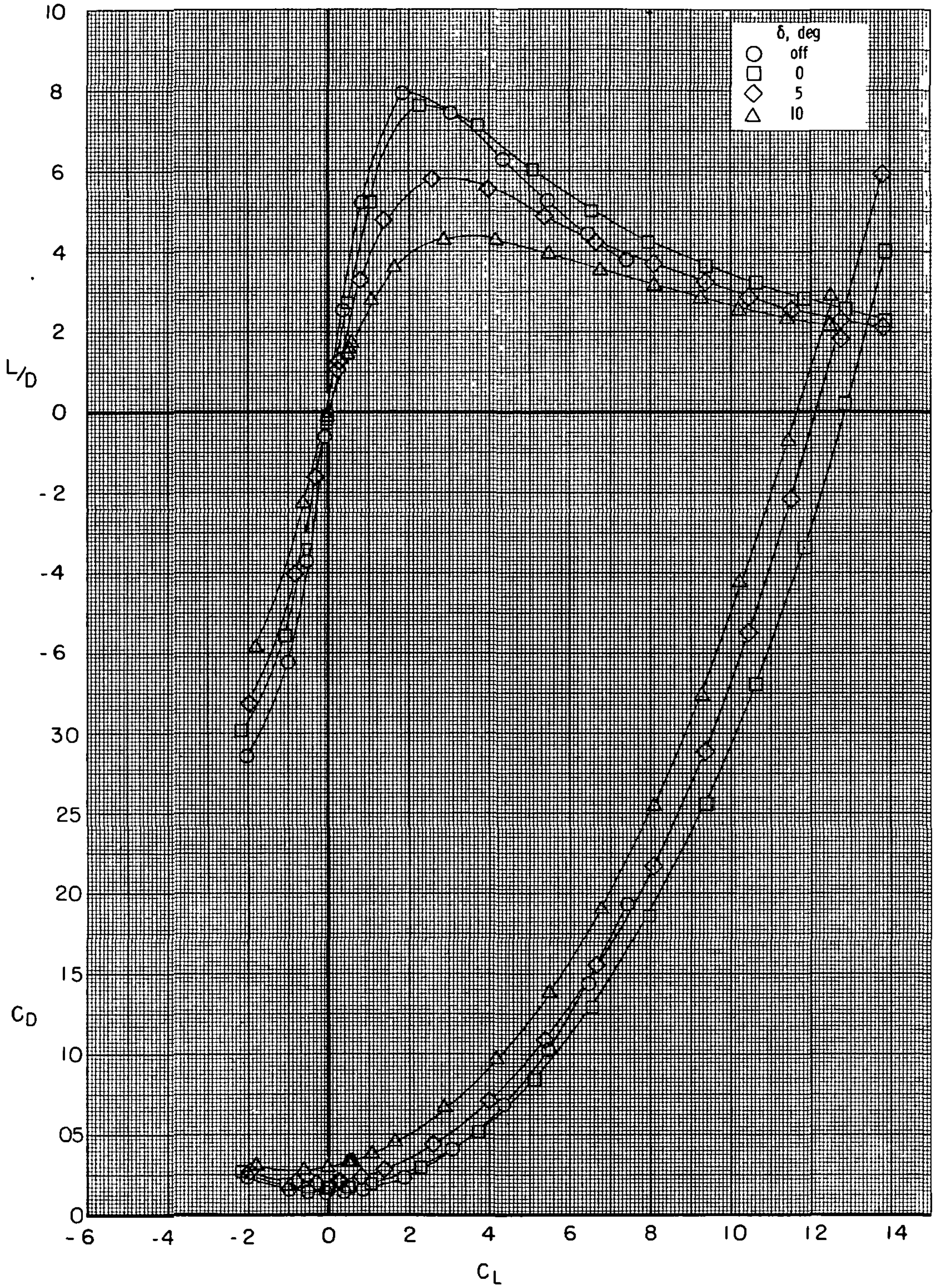

(a) Concluded.

Figure 8.- Continued.

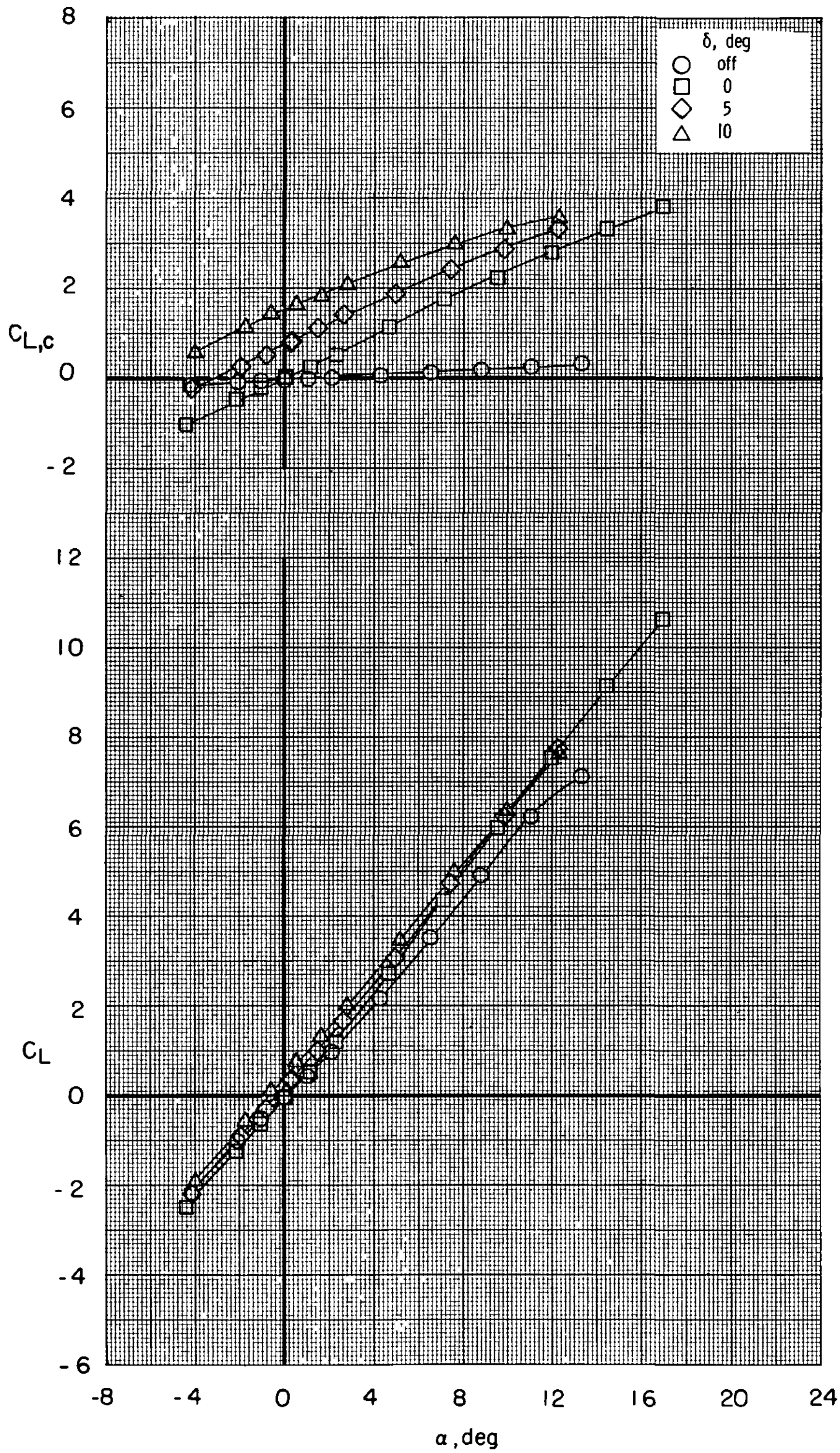

(b) M = 0.70.

Figure 8.- Continued.

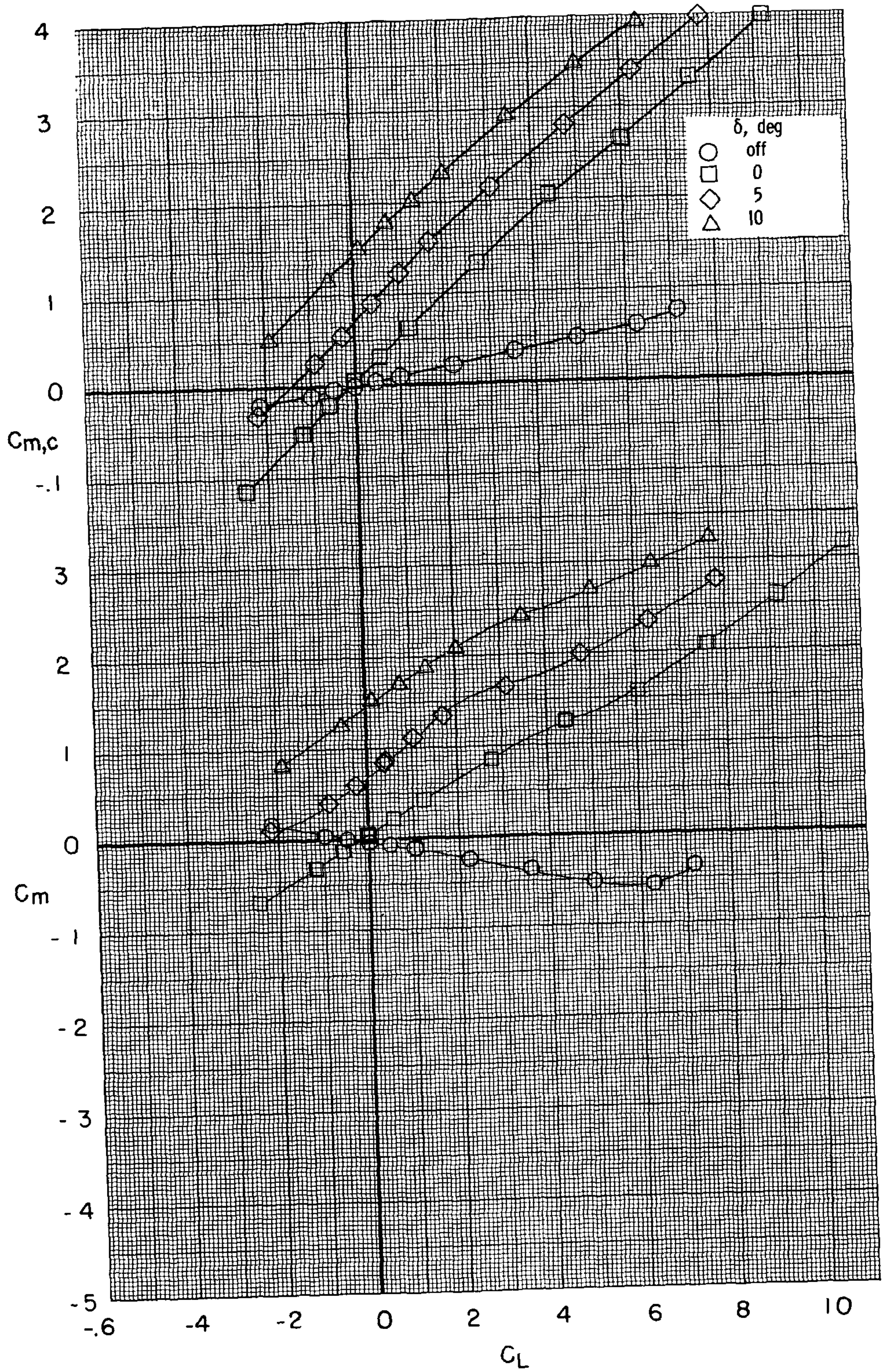

(b) Continued.

Figure 8.- Continued.

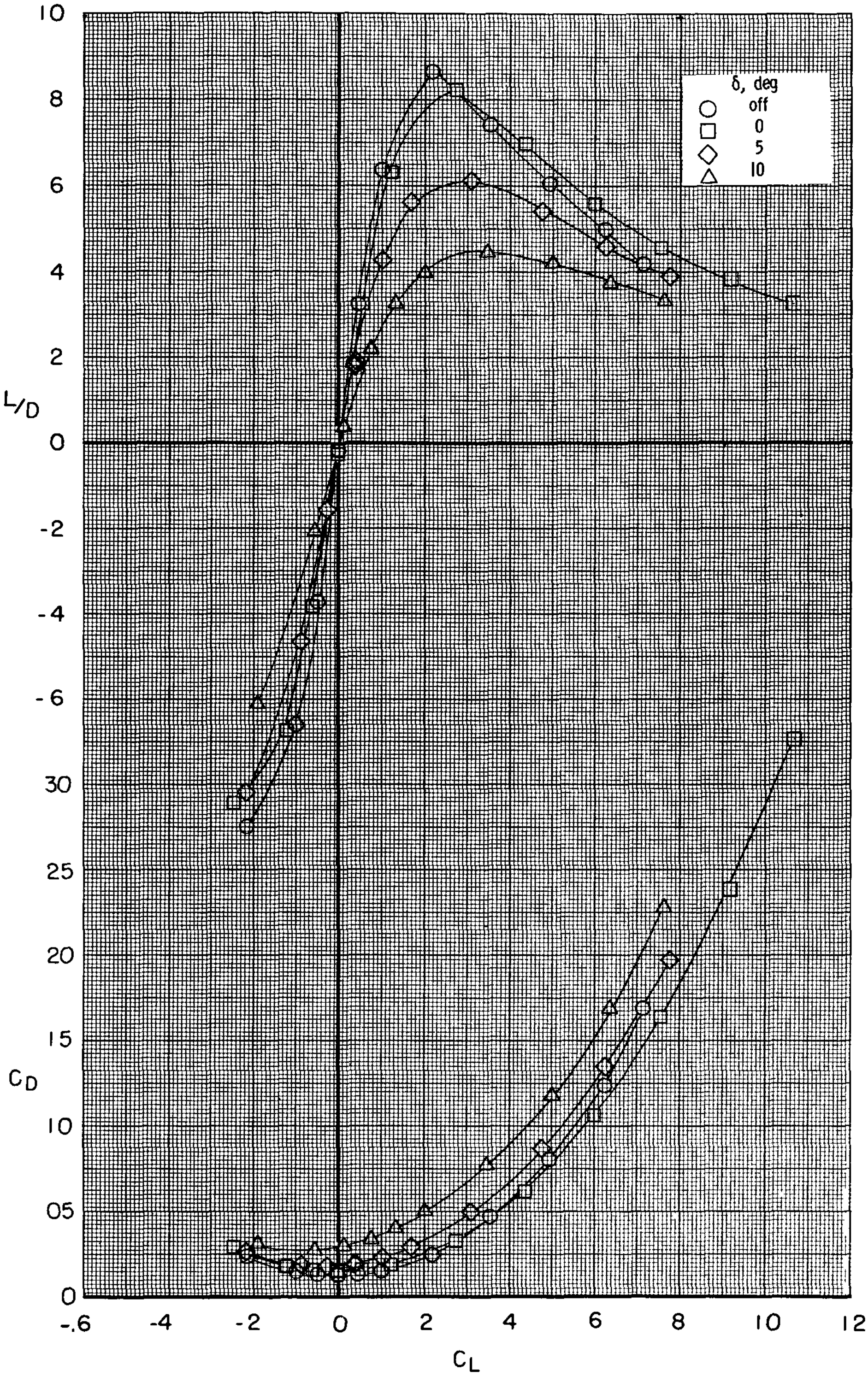

(b) Concluded.

Figure 8.- Continued.

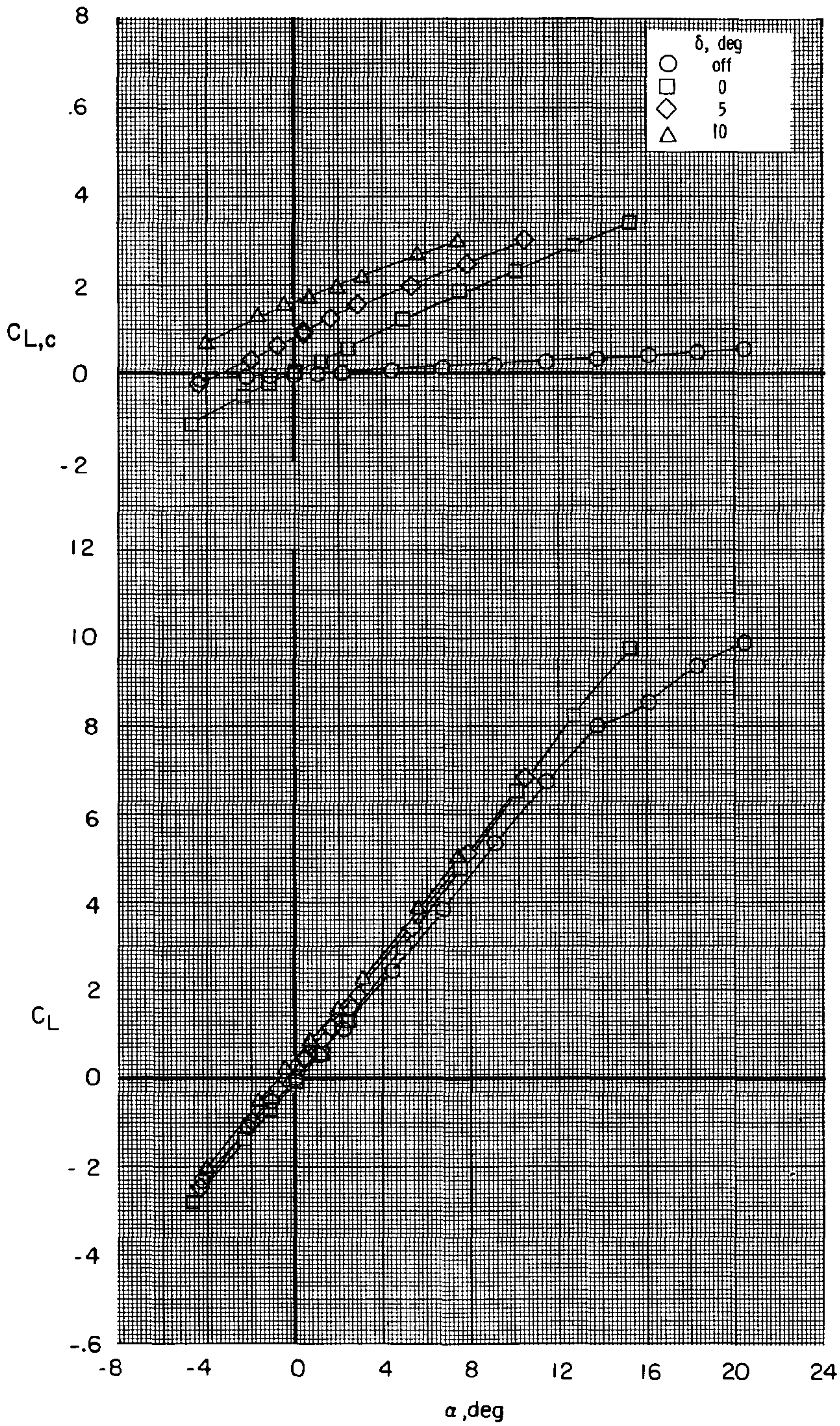

(c) M = 0.85.

Figure 8.- Continued.

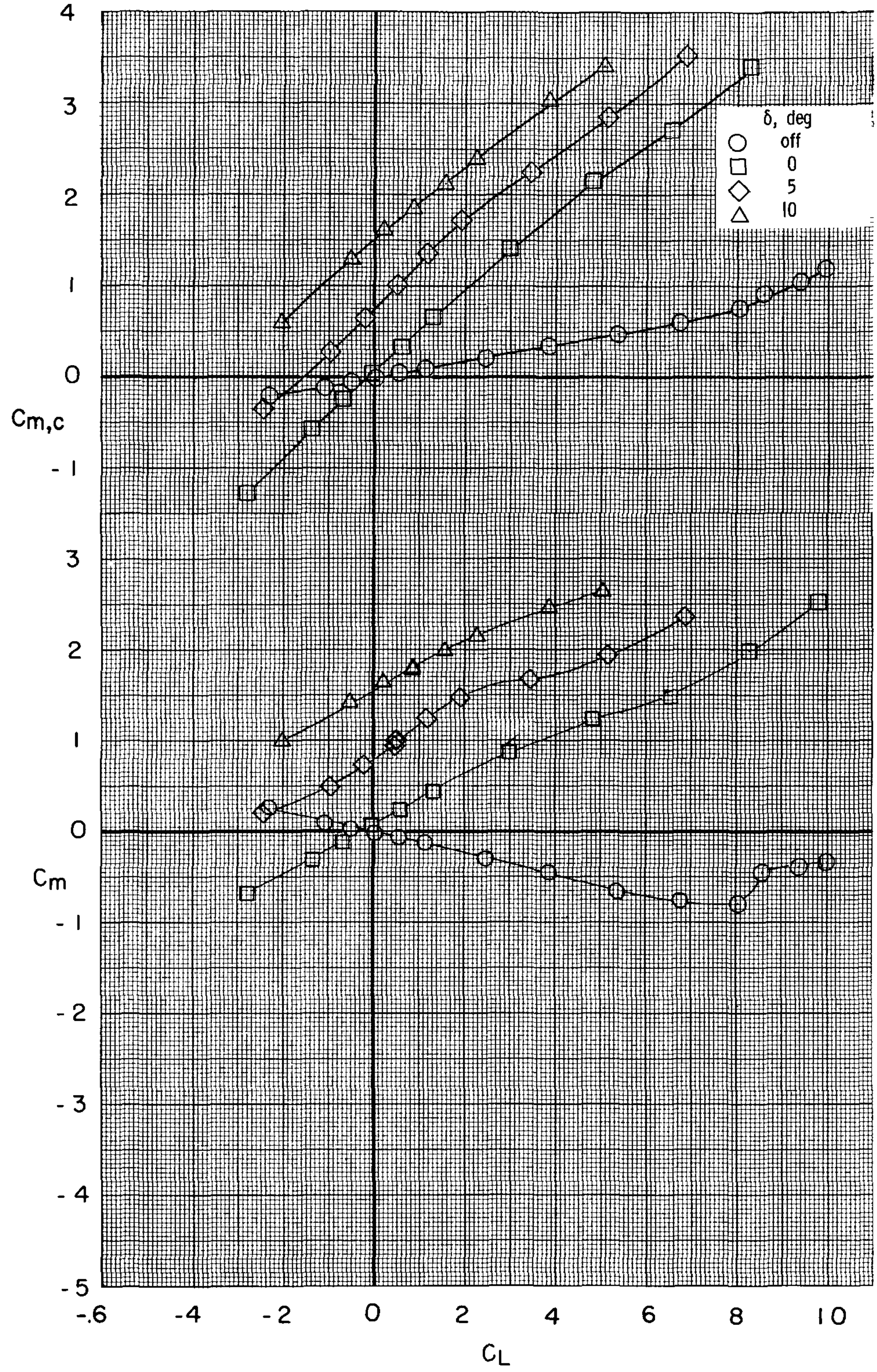

(c) Continued.

Figure 8.- Continued.

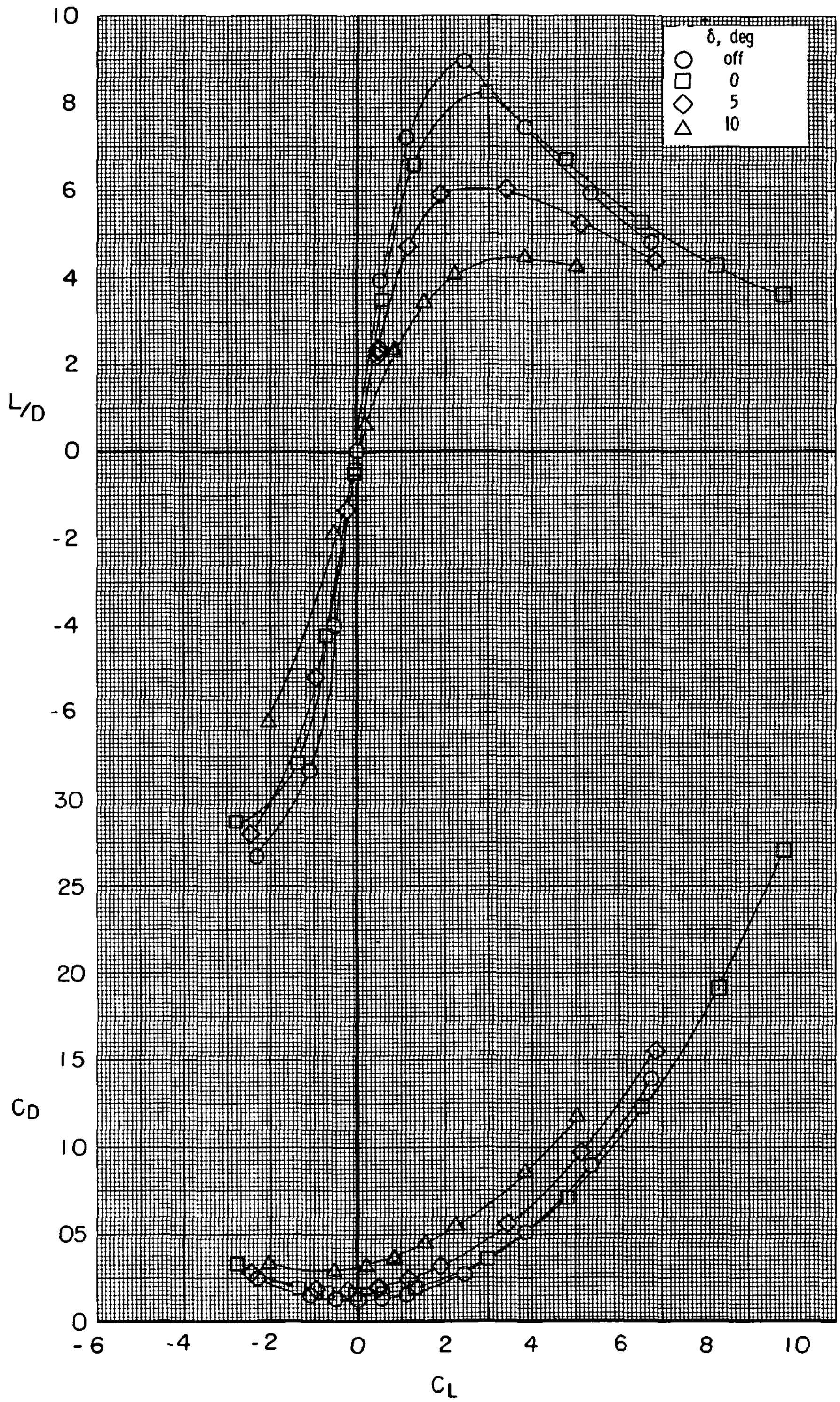

(c) Concluded.

Figure 8.- Concluded.

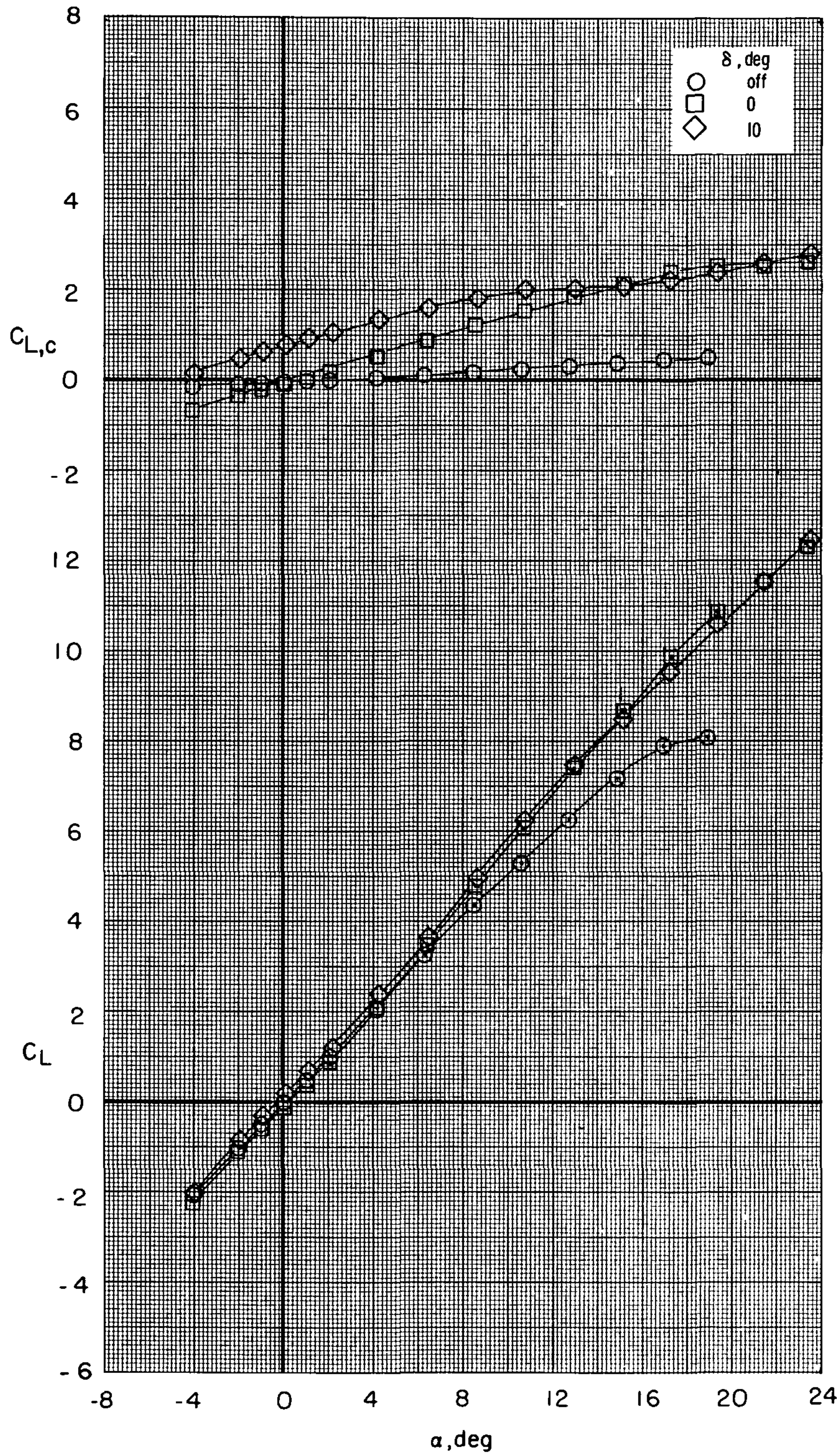

(a) M = 0.40.

Figure 9.- Effect of canard I (S_c/S_w = 0.16) deflection on longitudinal characteristics of wing II (Λ_w = 44°) for $z/\bar{c}$ = 0.0.

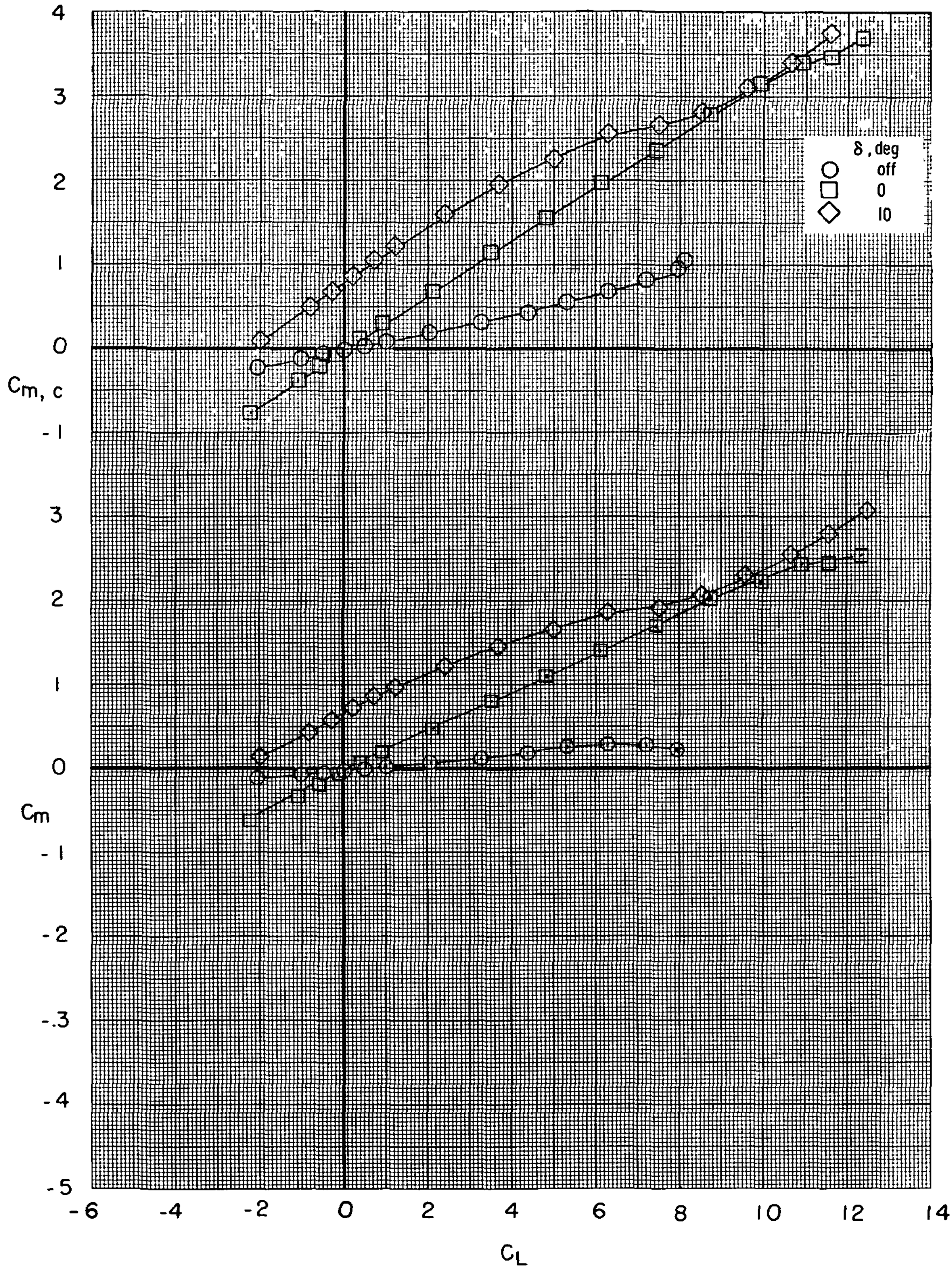

(a) Continued.

Figure 9.- Continued.

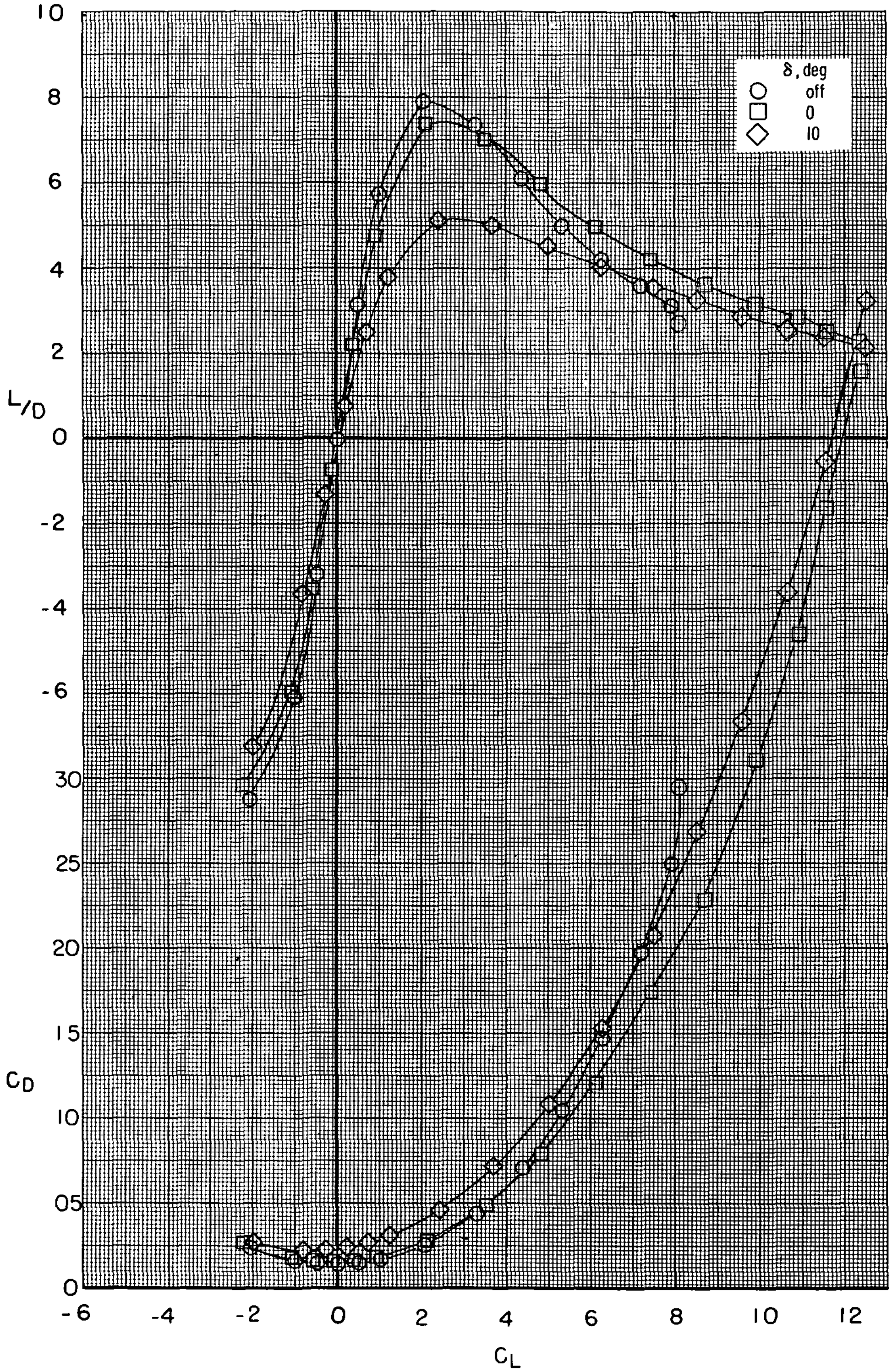

(a) Concluded.

Figure 9.- Continued.

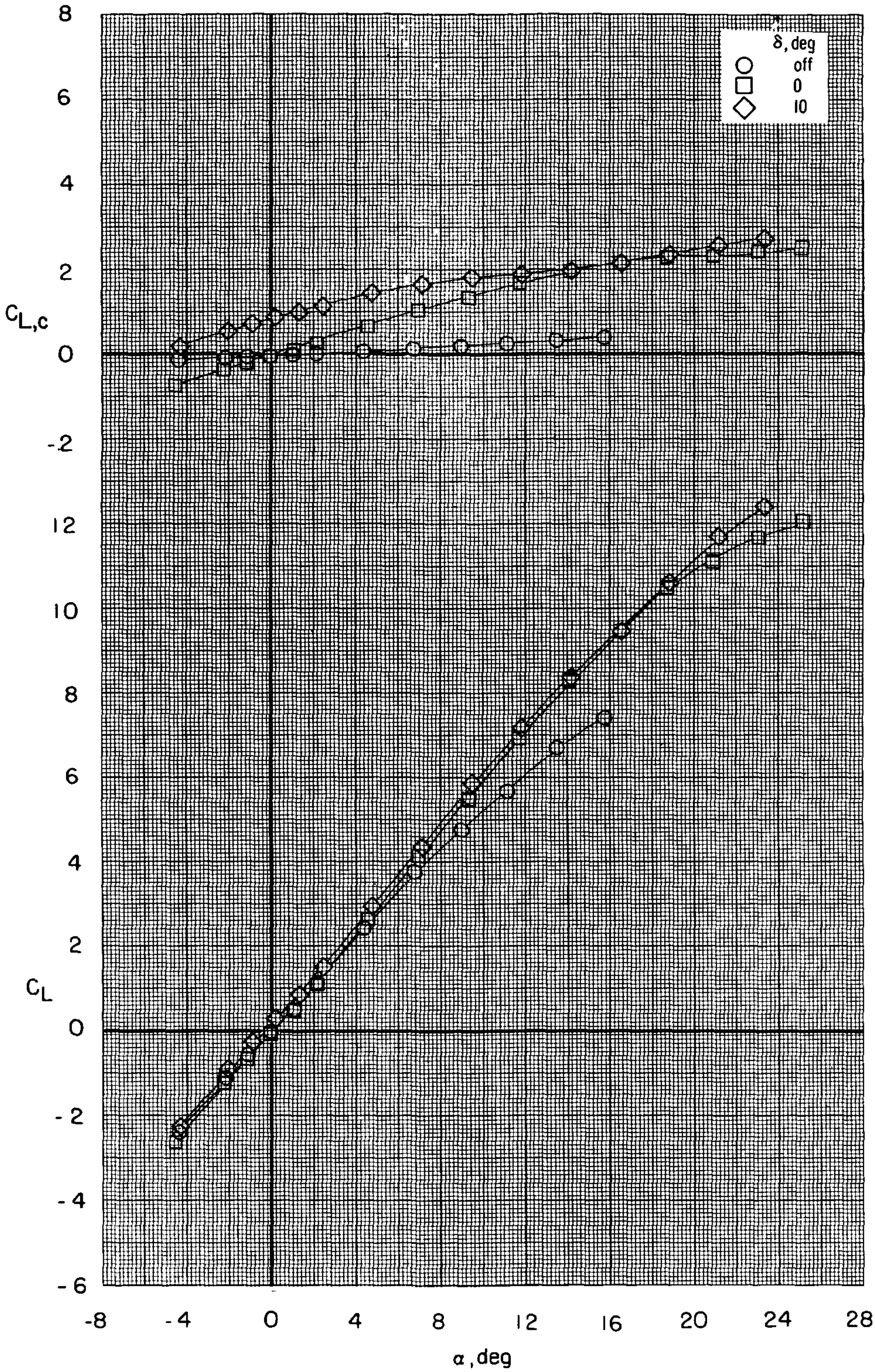

(b) M = 0.70.

Figure 9.- Continued.

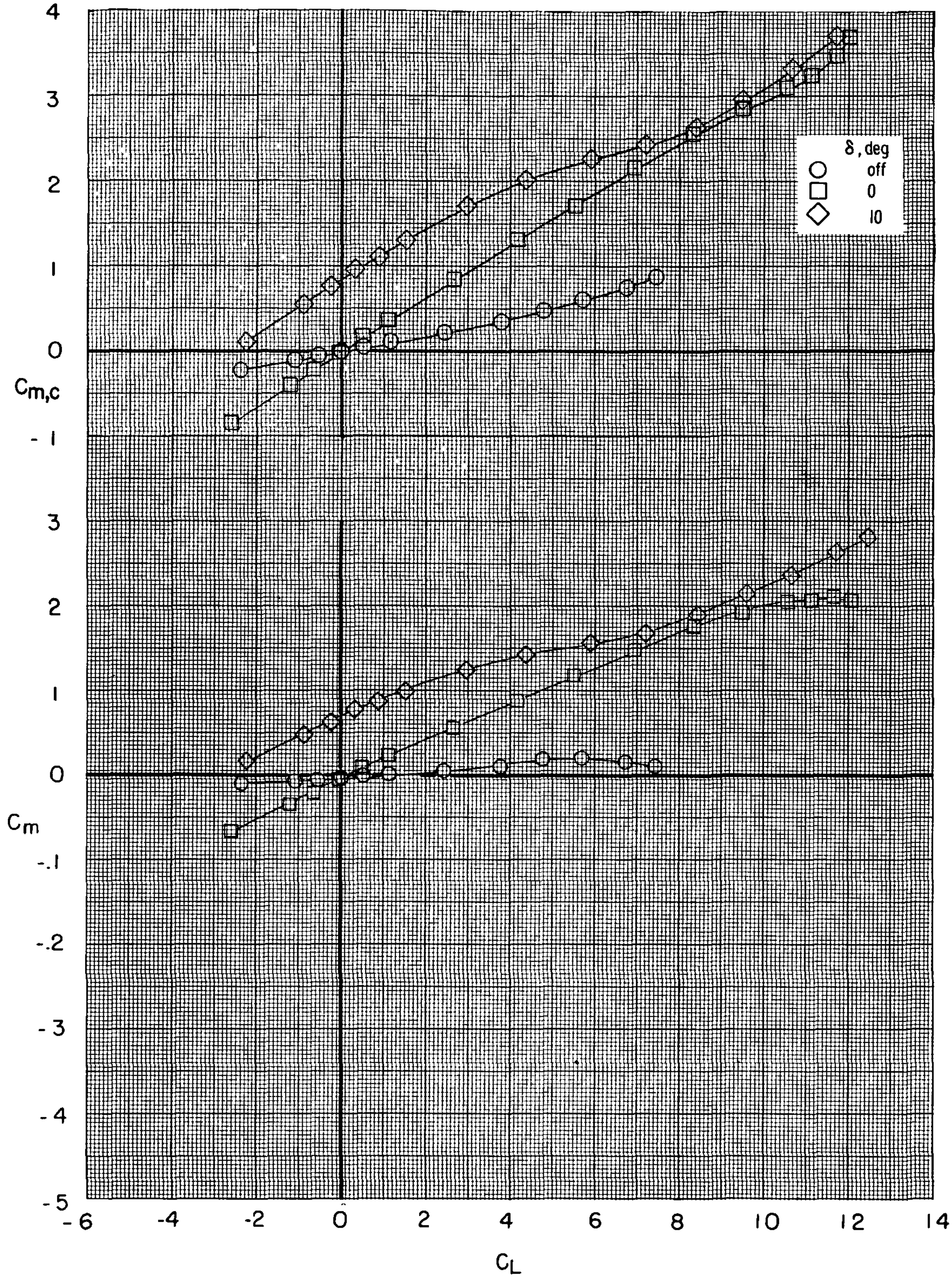

(b) Continued.

Figure 9.- Continued.

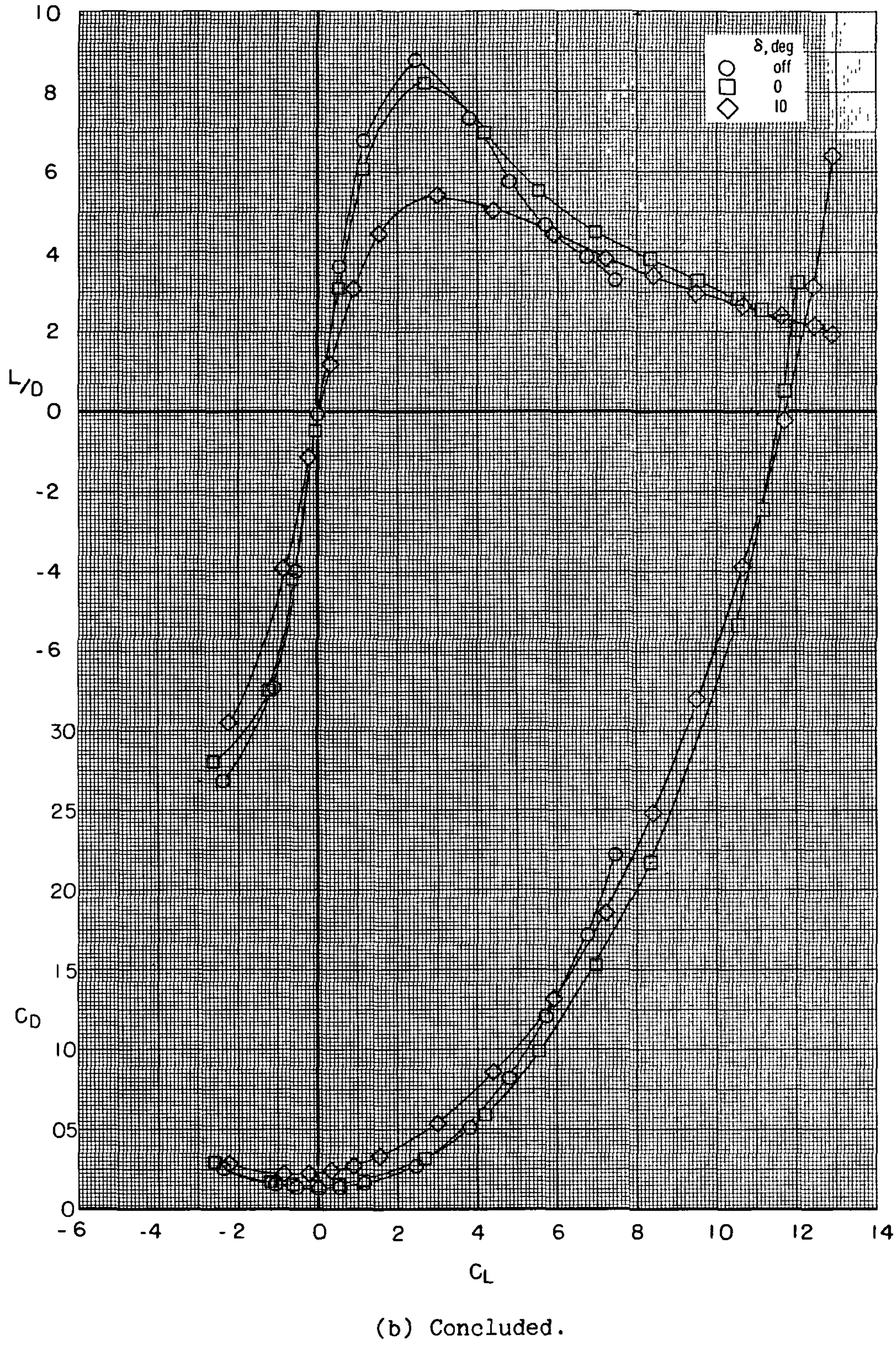

(b) Concluded.

Figure 9.- Continued.

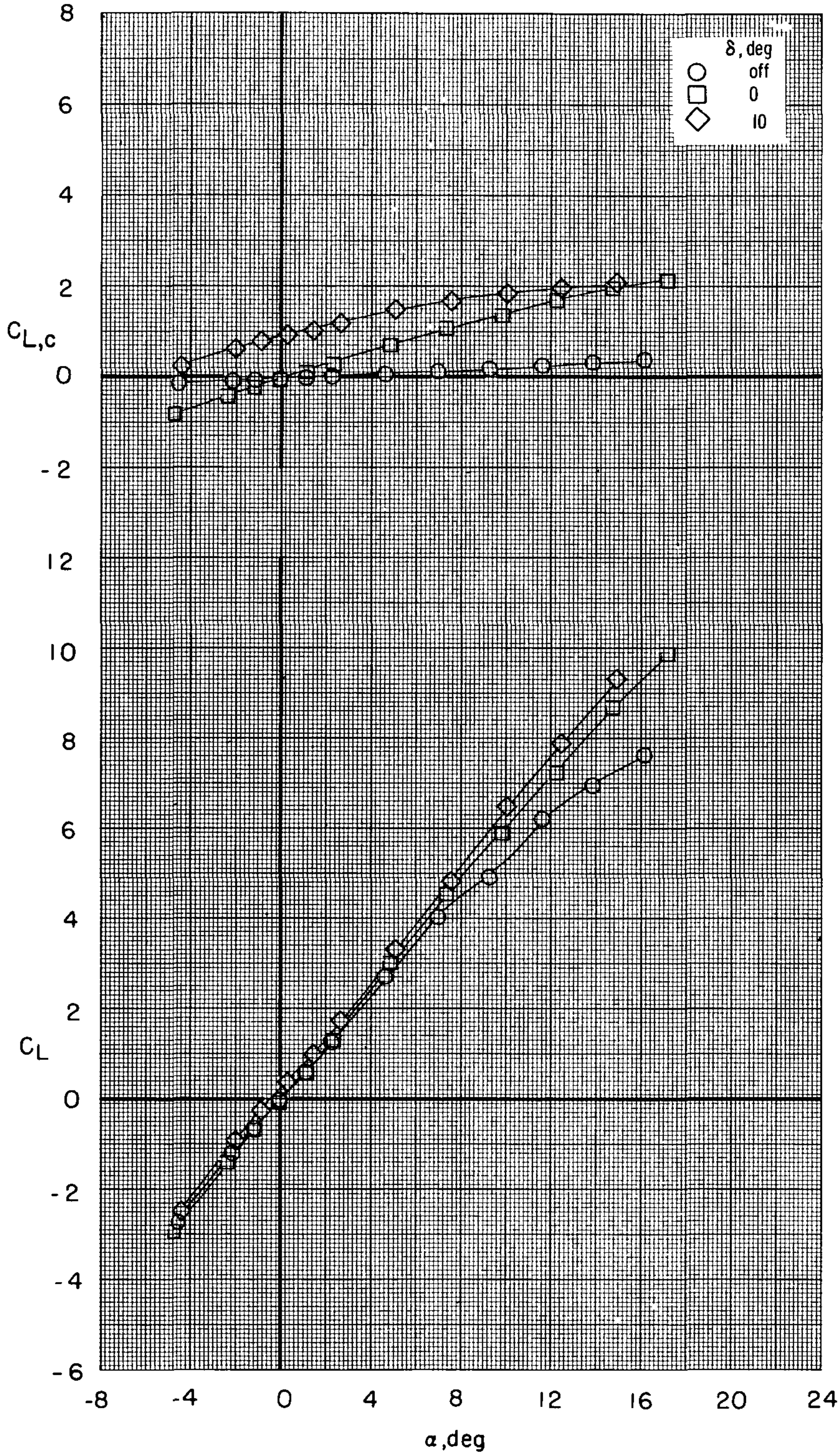

(c) M = 0.85.

Figure 9.- Continued.

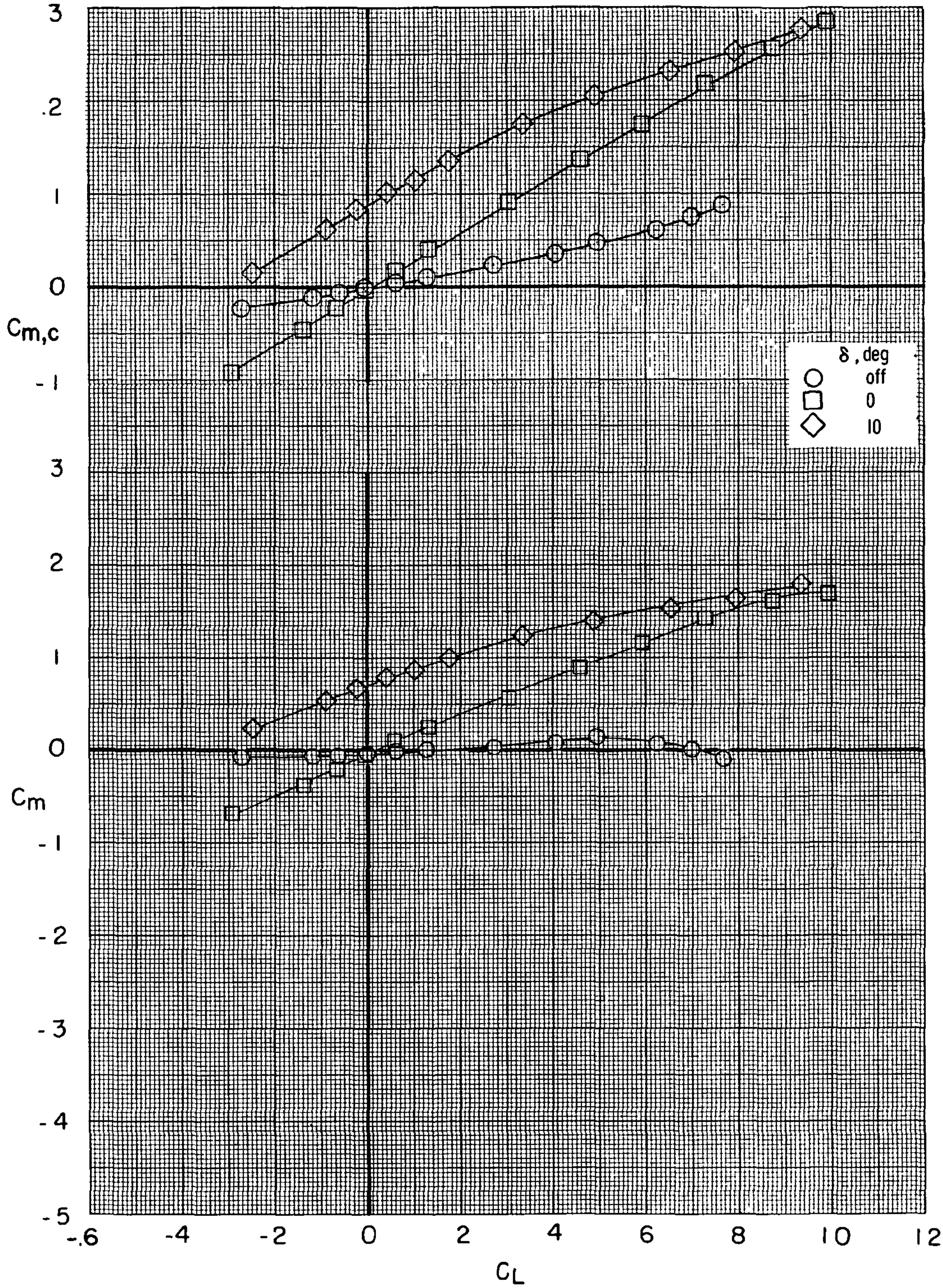

(c) Continued.

Figure 9.- Continued.

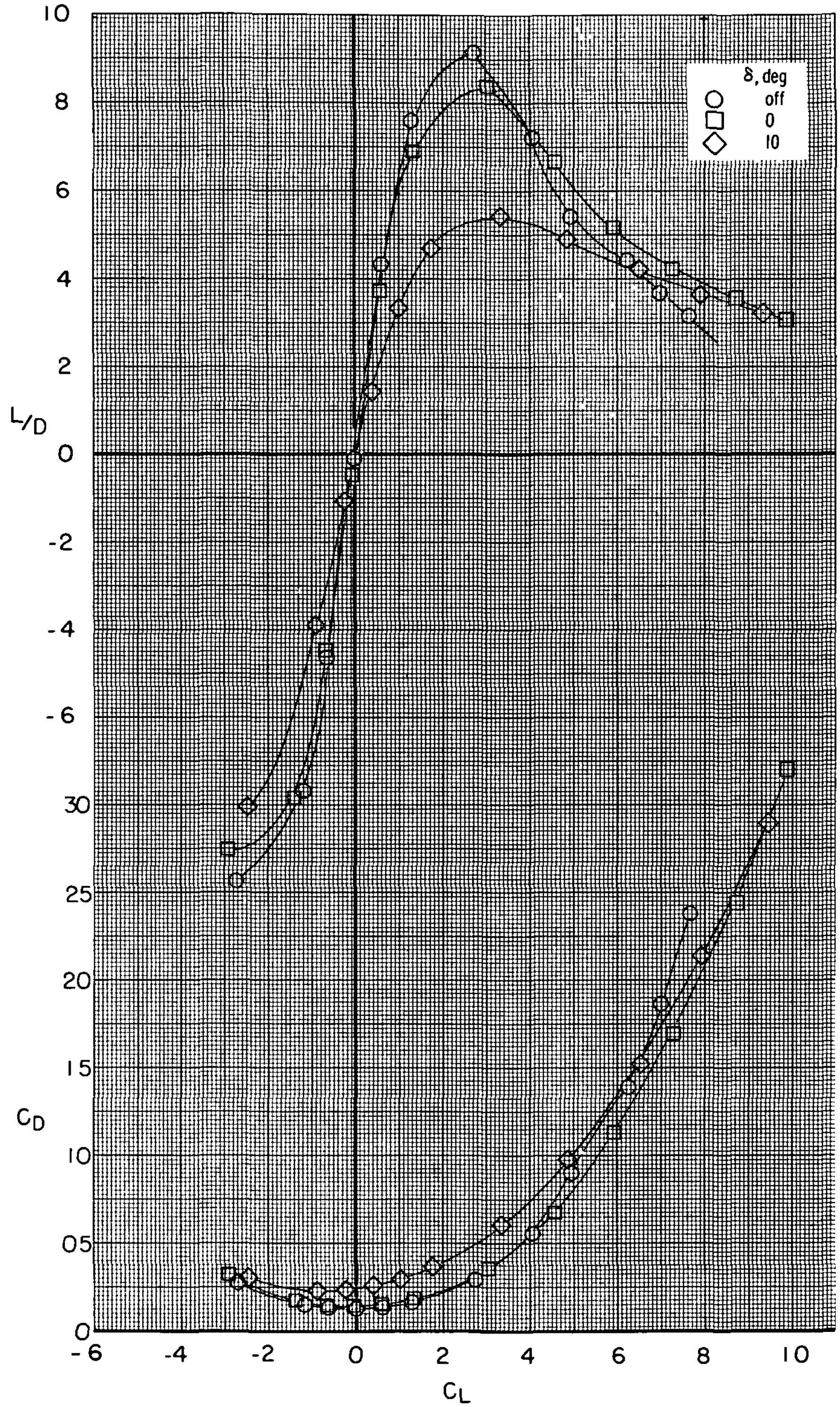

(c) Concluded.

Figure 9.- Concluded.

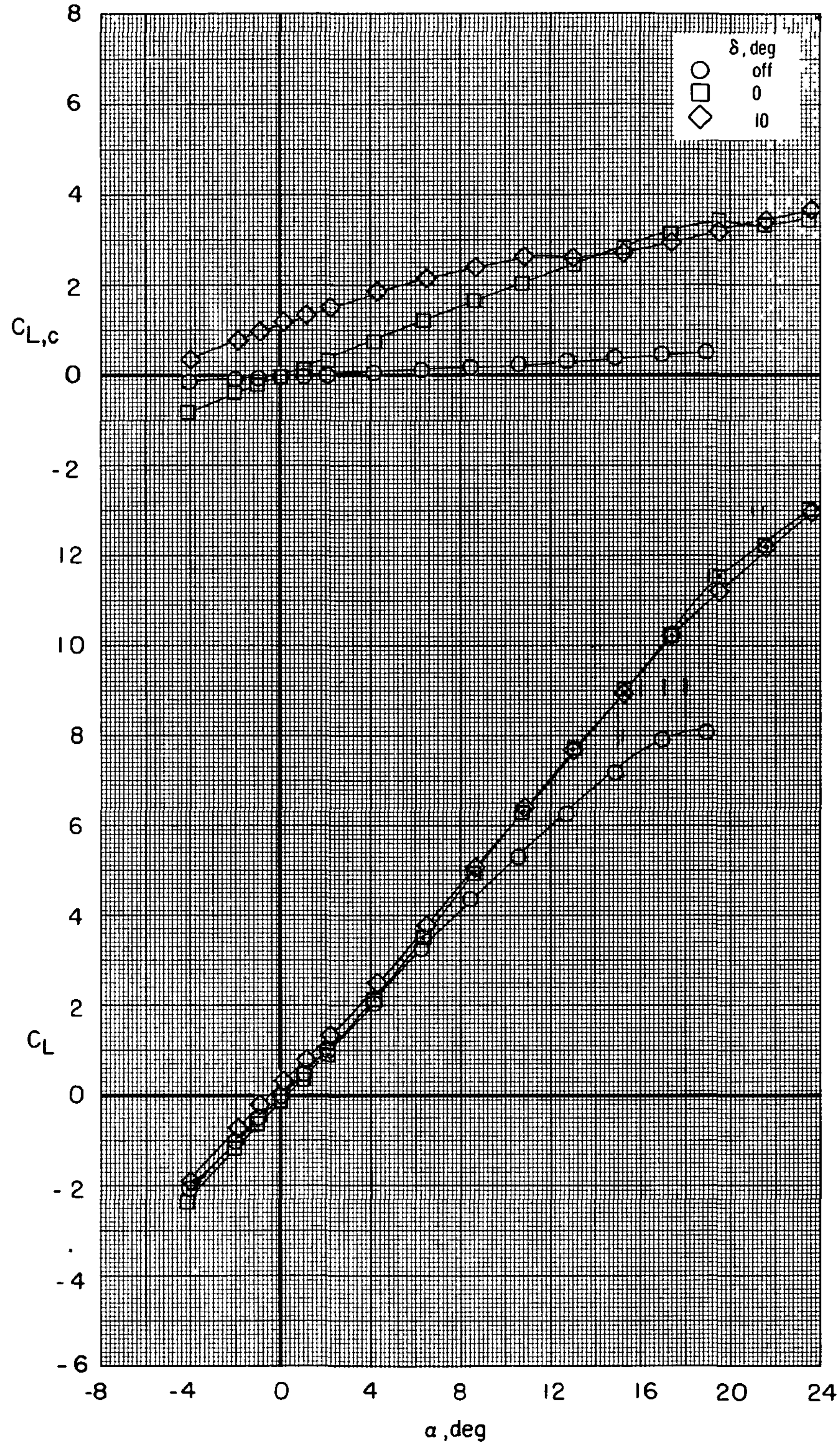

(a) M = 0.40.

Figure 10.- Effect of canard II (S_c/S_w = 0.22) deflection on longitudinal characteristics for wing II (Λ_w = 44°), $z/\bar{c}$ = 0.0.

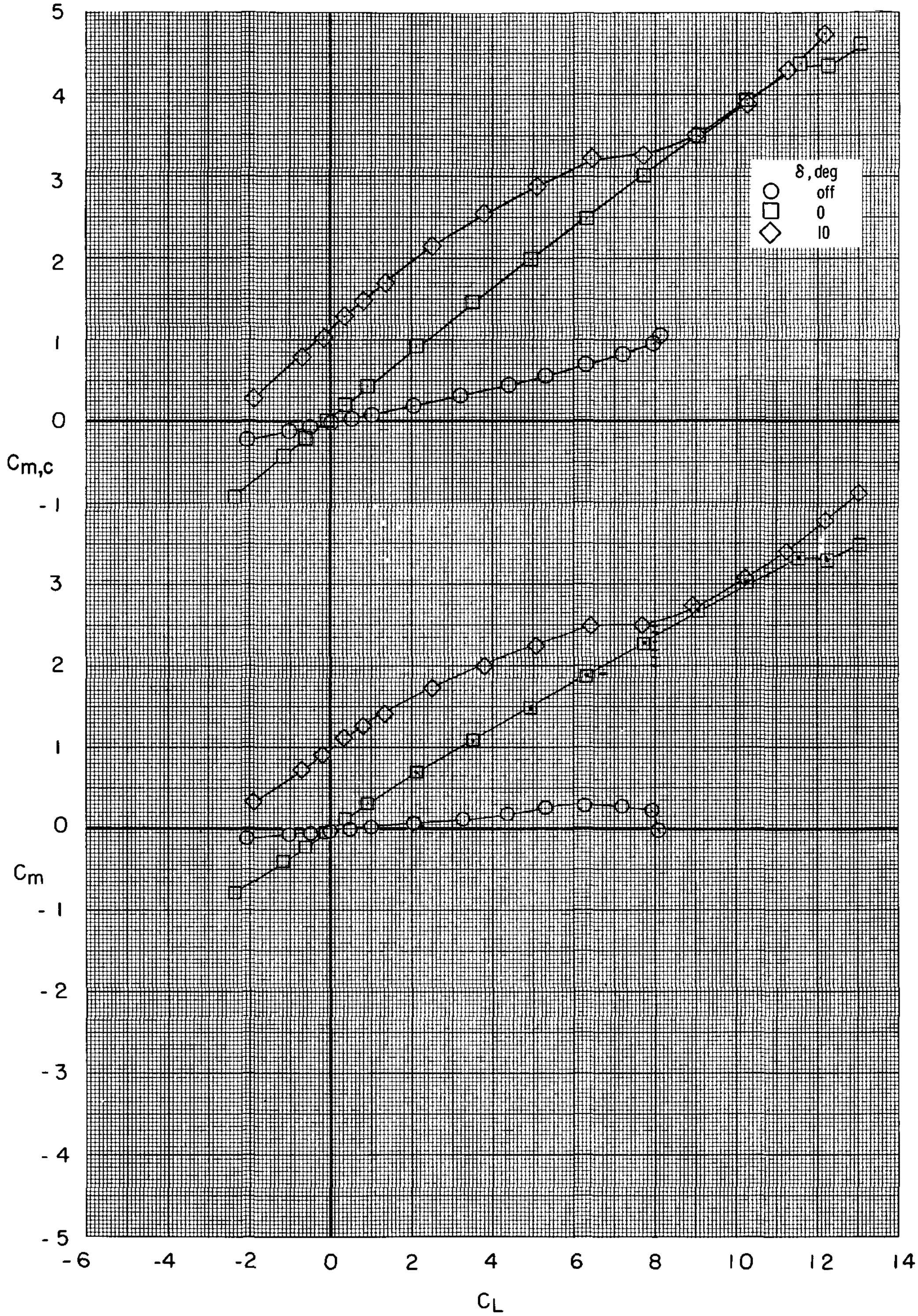

(a) Continued.

Figure 10.- Continued.

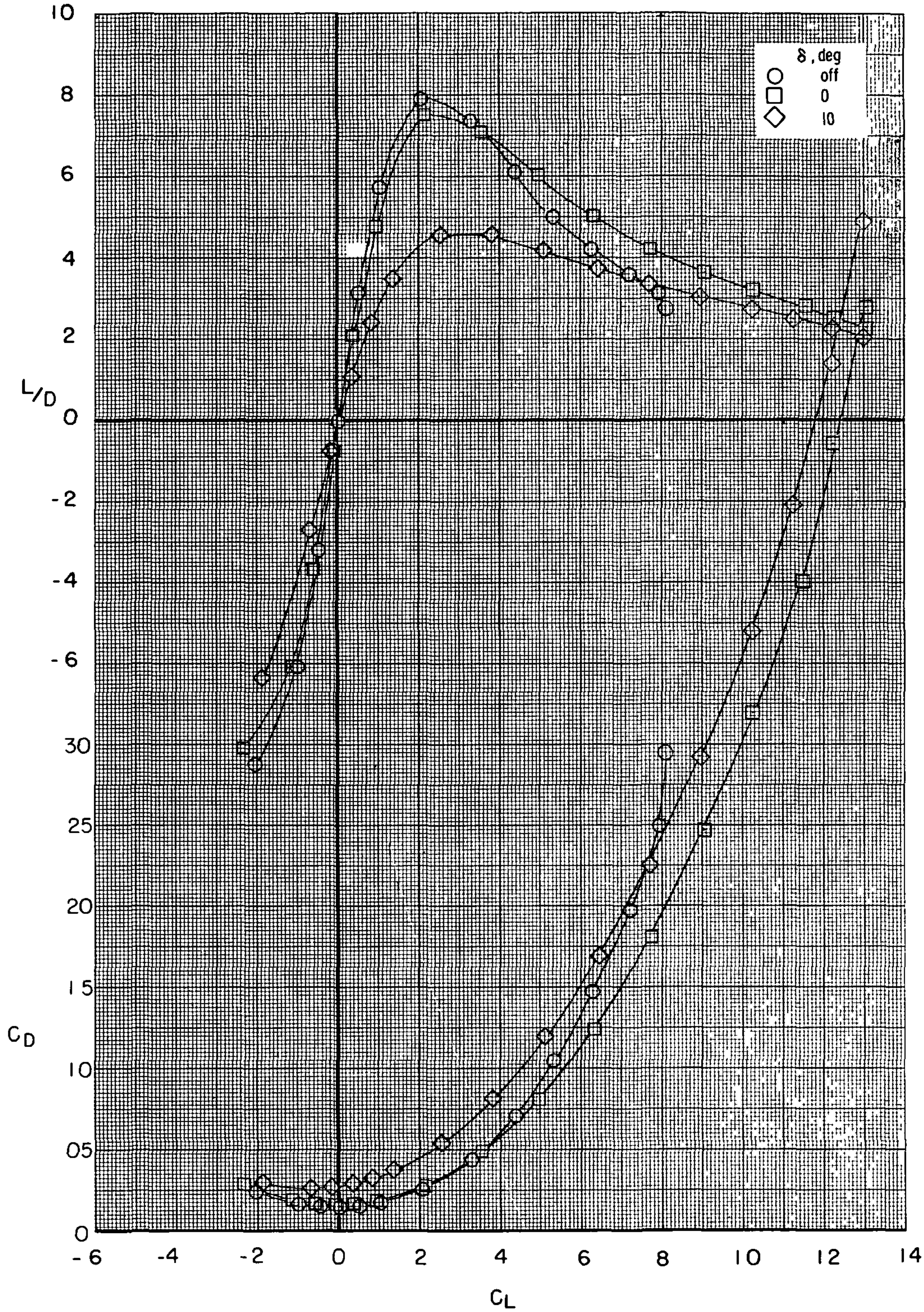

(a) Concluded.

Figure 10.- Continued.

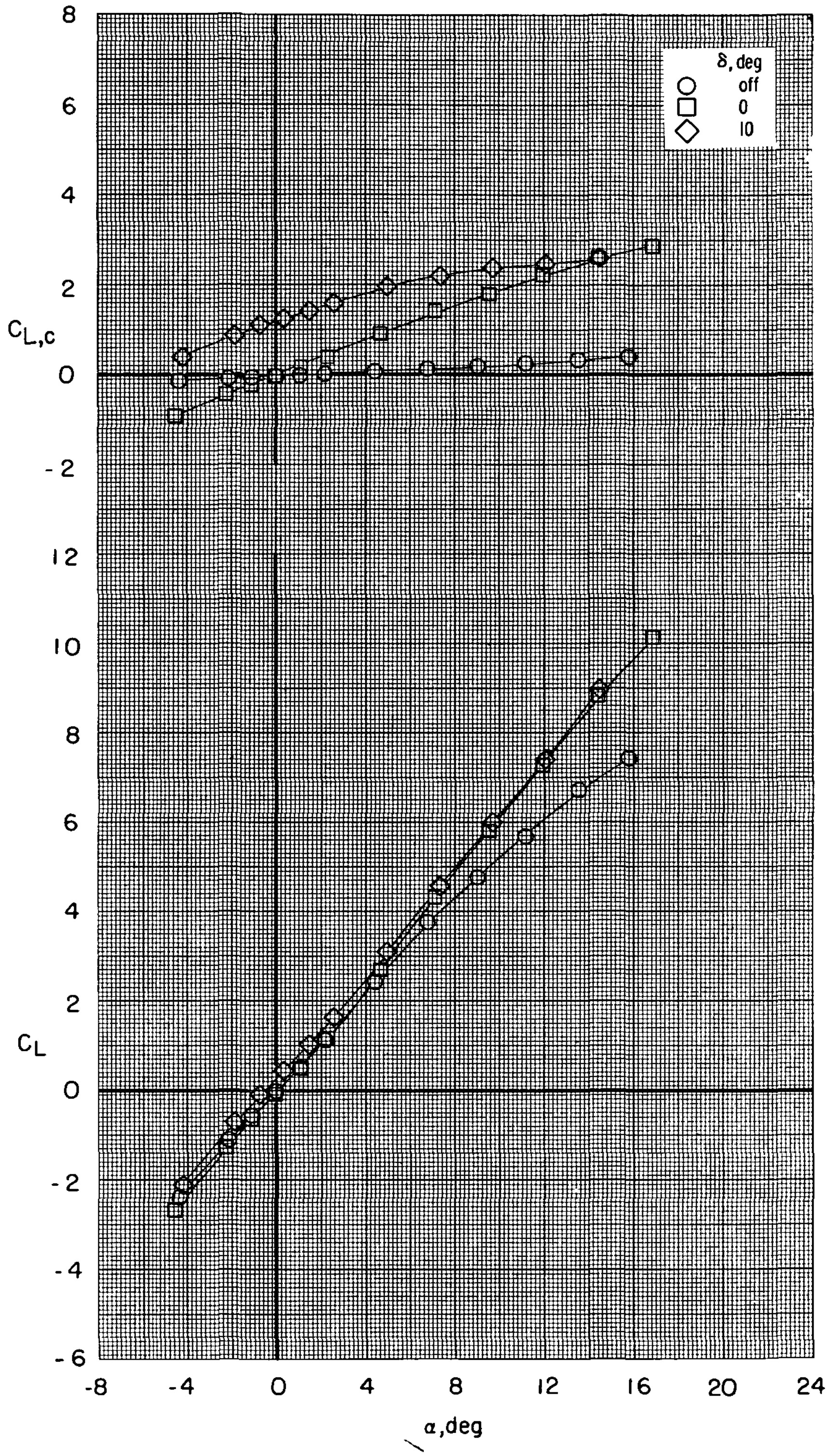

(b) M = 0.70.

Figure 10.- Continued.

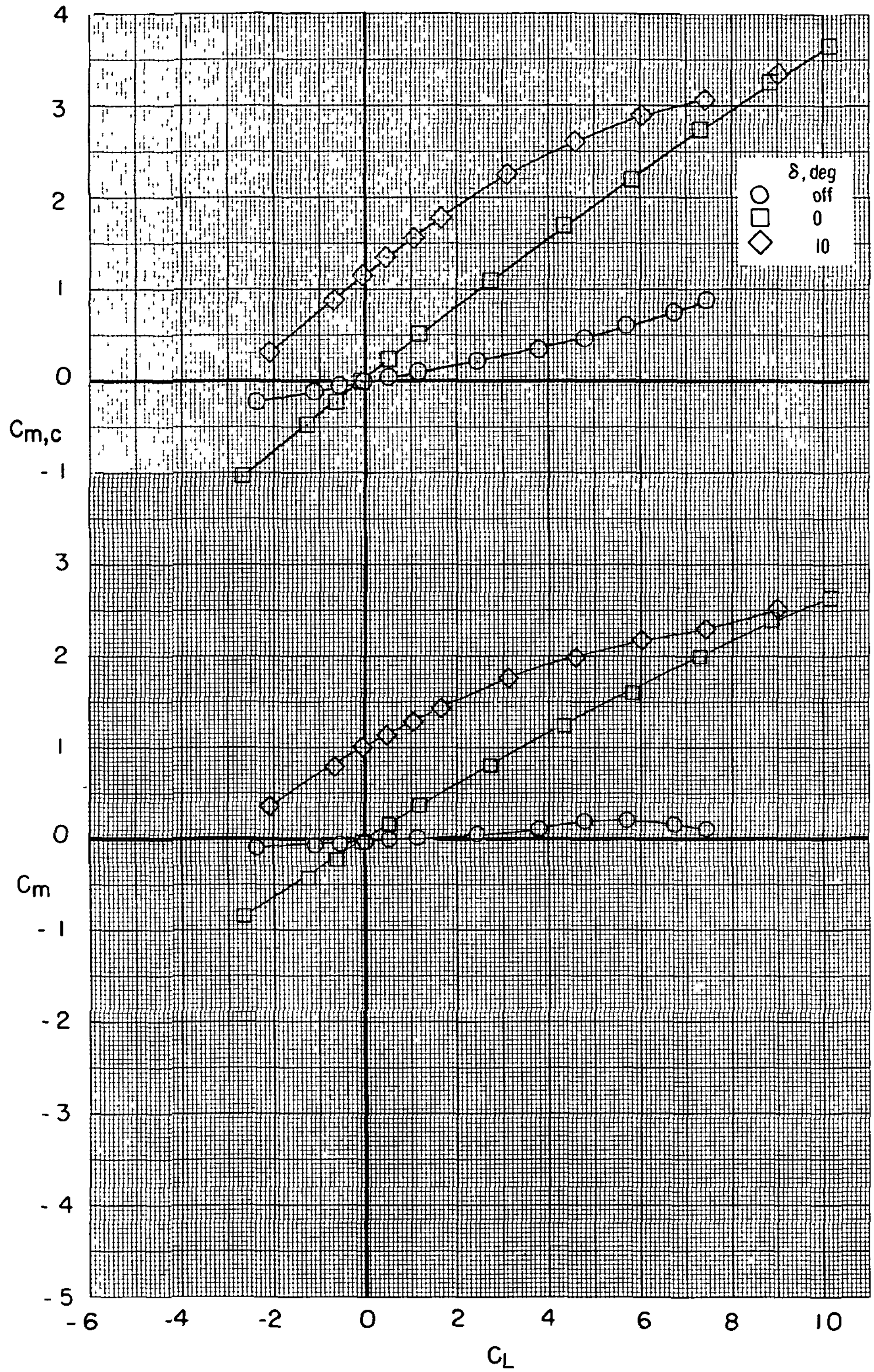

(b) Continued.

Figure 10.- Continued.

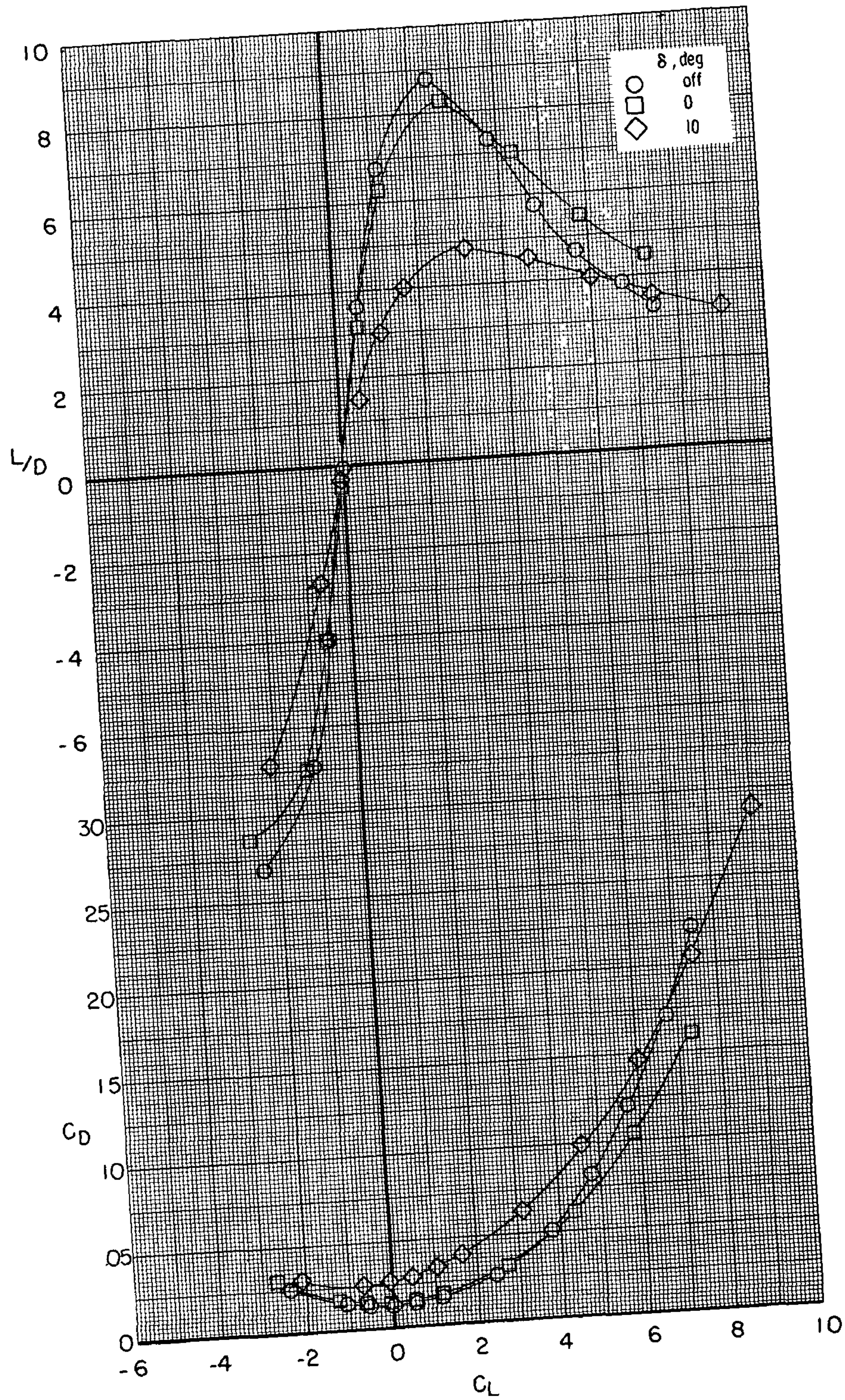

(b) Concluded.

Figure 10.- Continued.

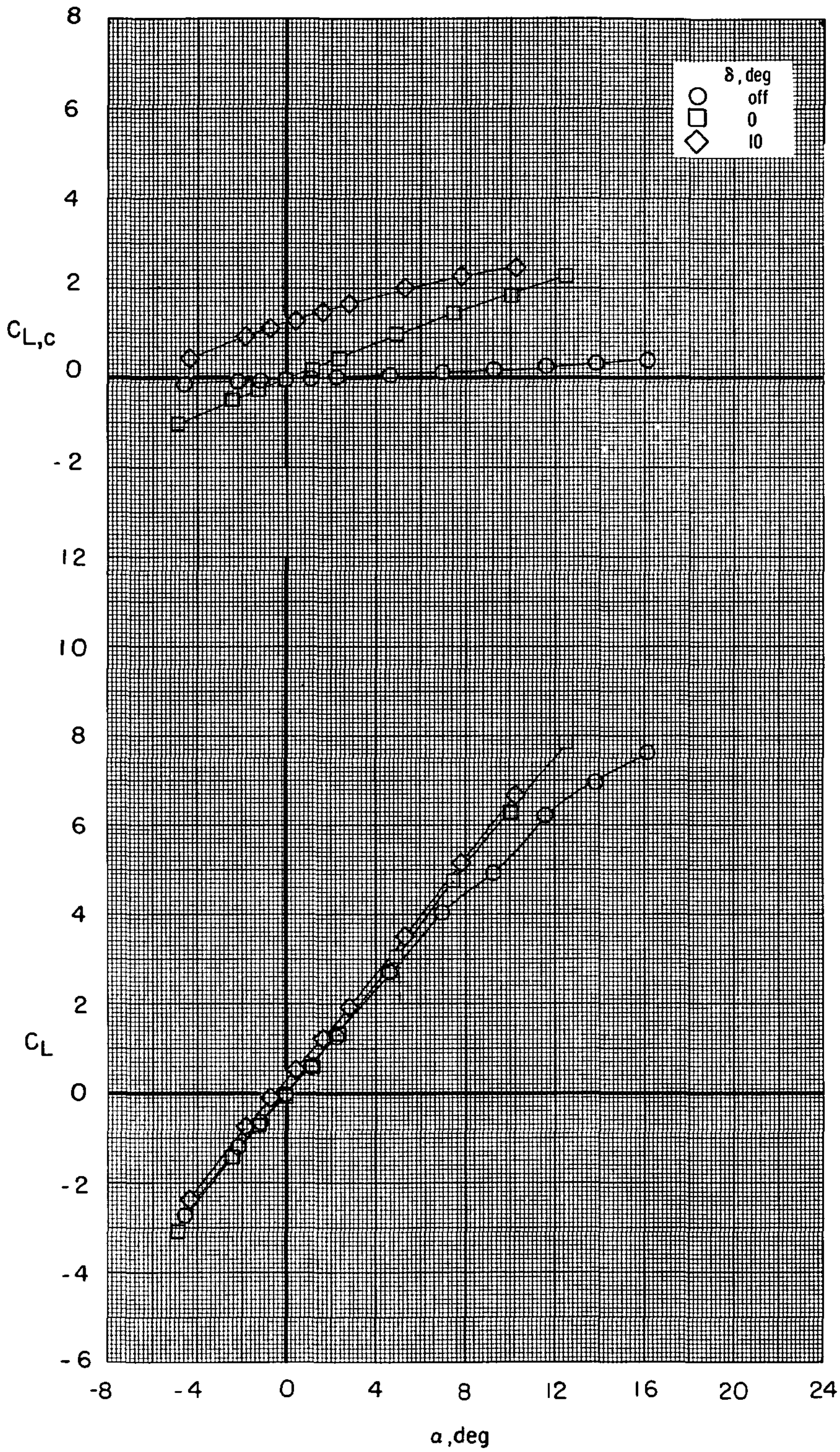

(c) M = 0.85.

Figure 10.- Continued.

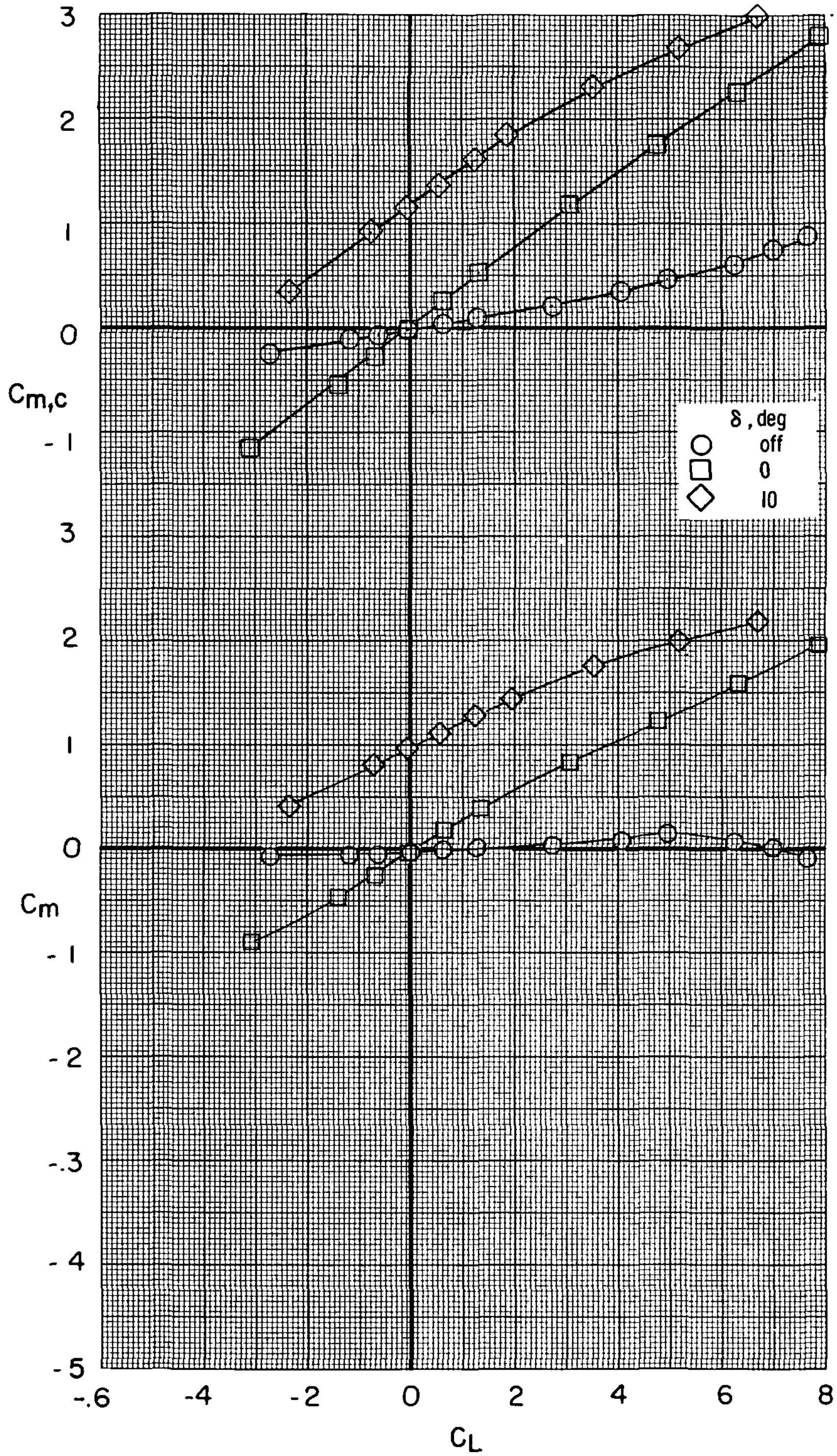

(c) Continued.

Figure 10.- Continued.

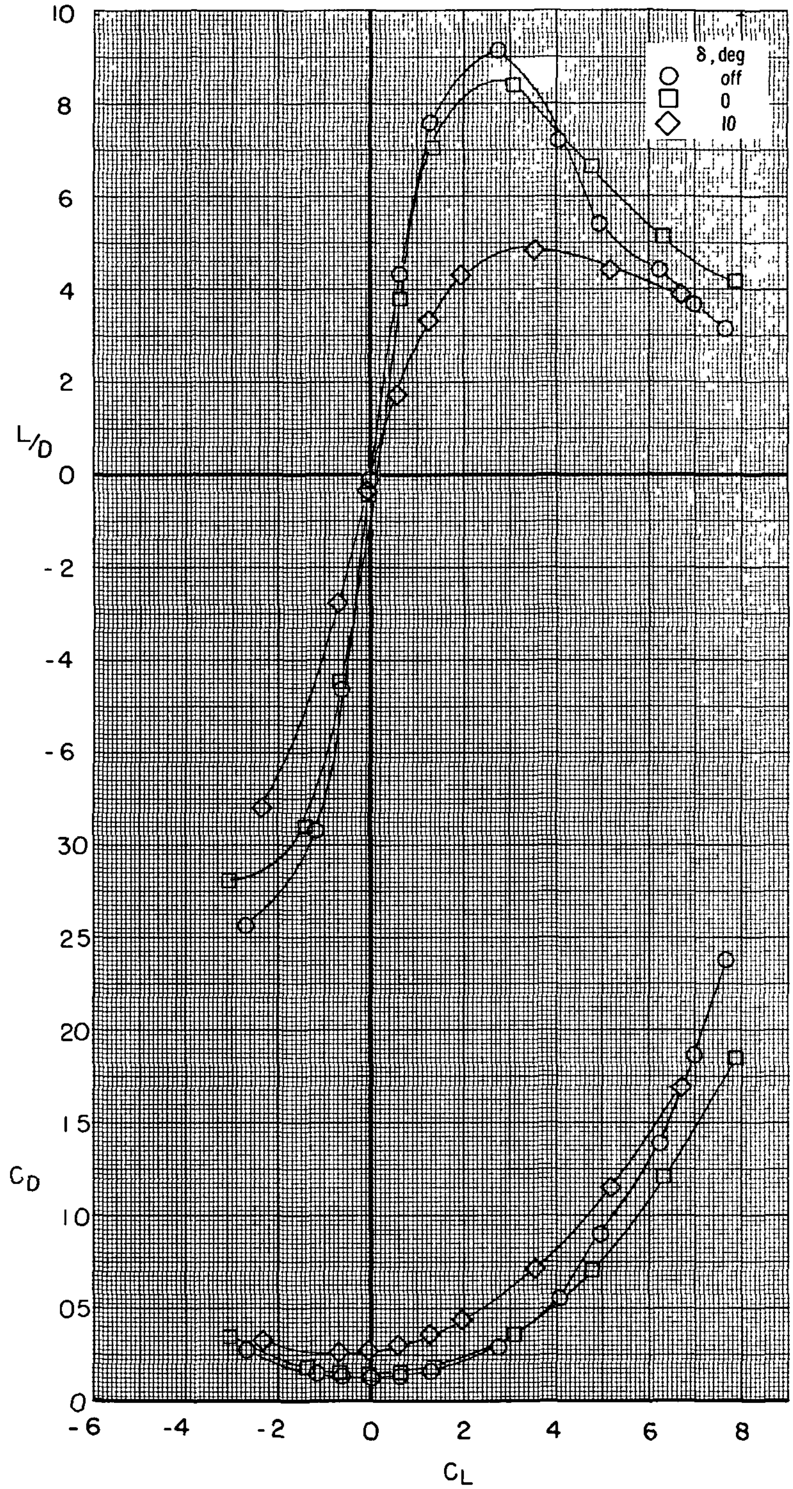

(c) Concluded.

Figure 10.- Concluded.

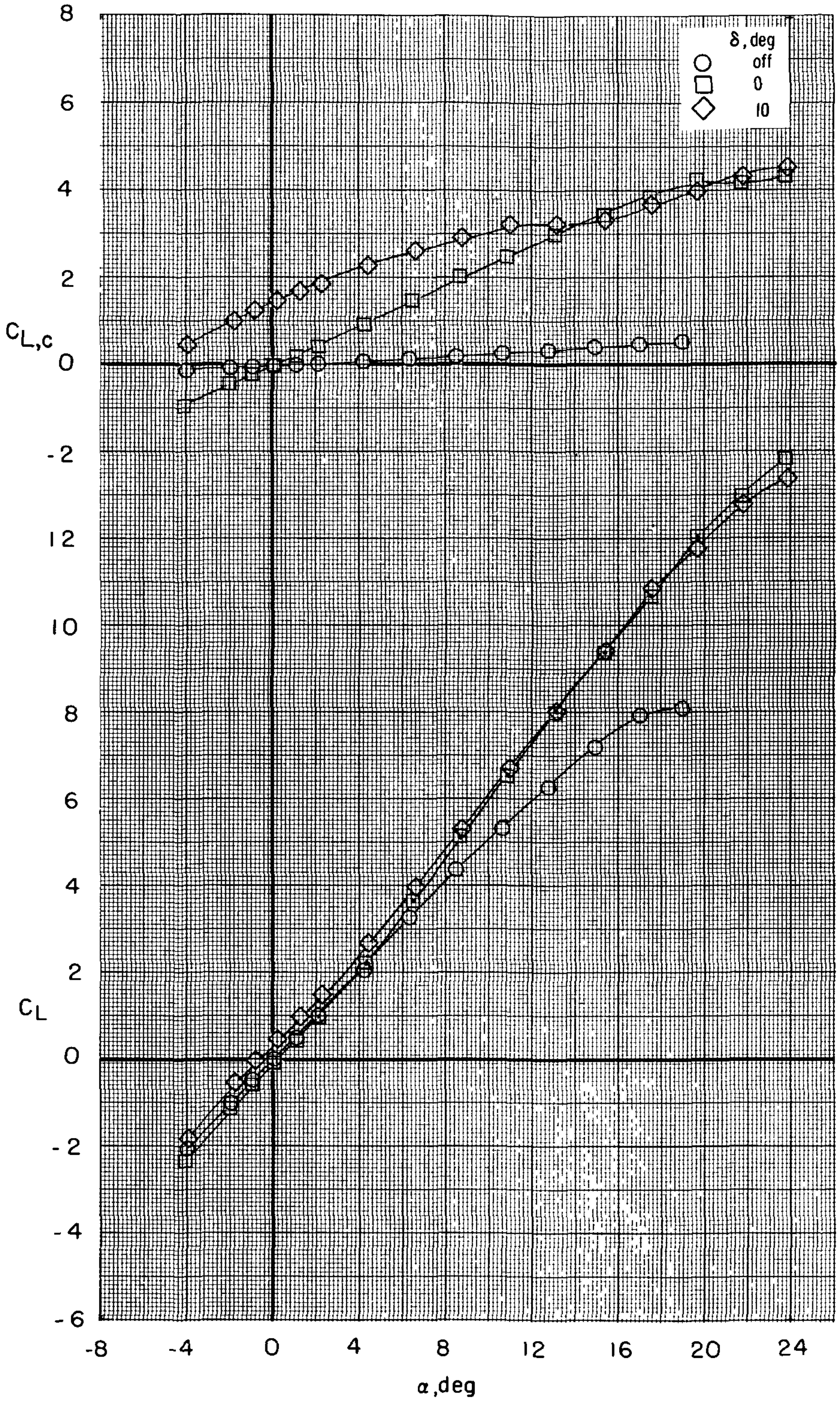

(a) M = 0.40.

Figure 11.- Effect of canard III (S_c/S_w = 0.28) deflection on longitudinal characteristics for wing II (Λ_w = 44°), $z/\bar{c}$ = 0.0.

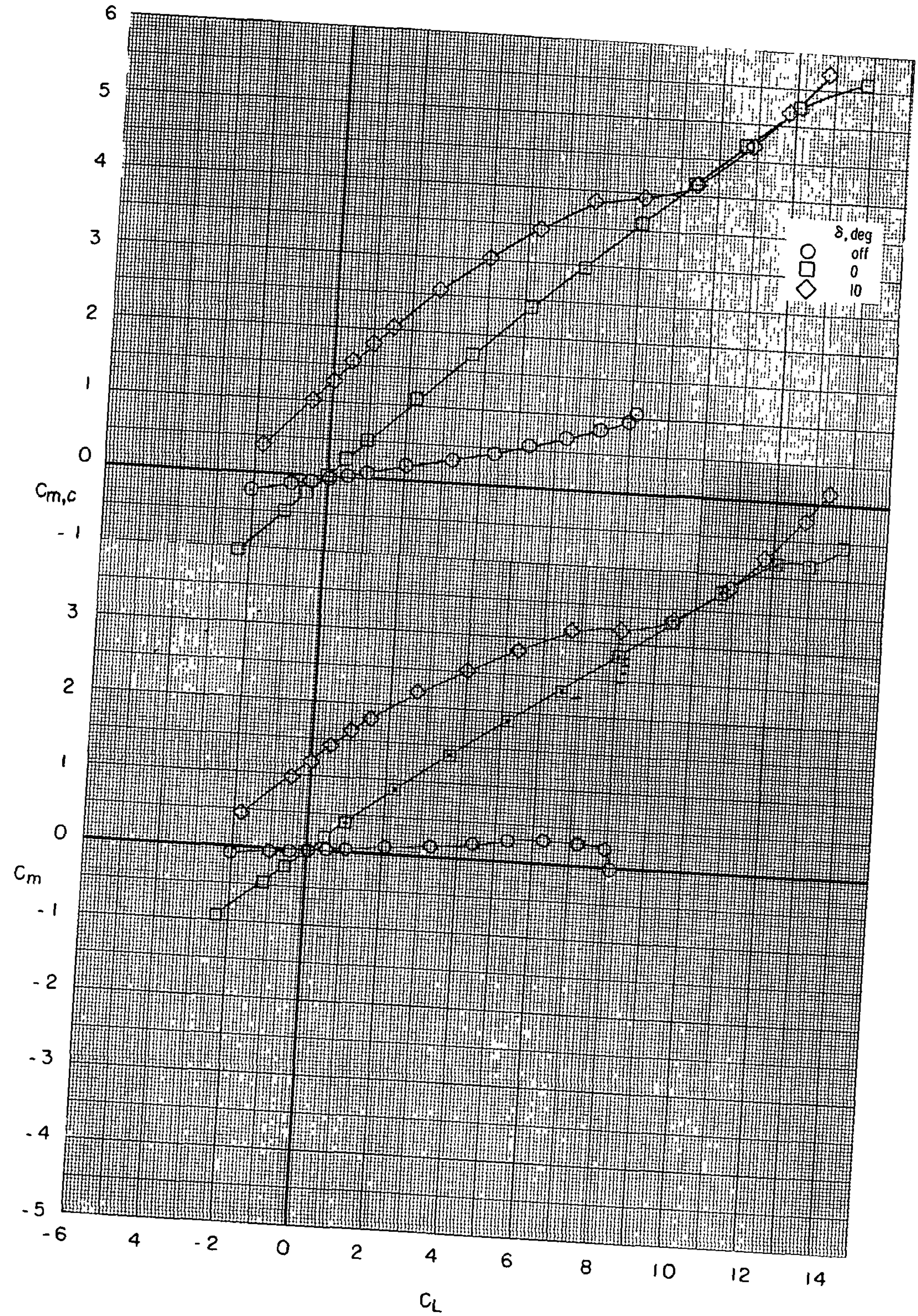

(a) Continued.

Figure 11.- Continued.

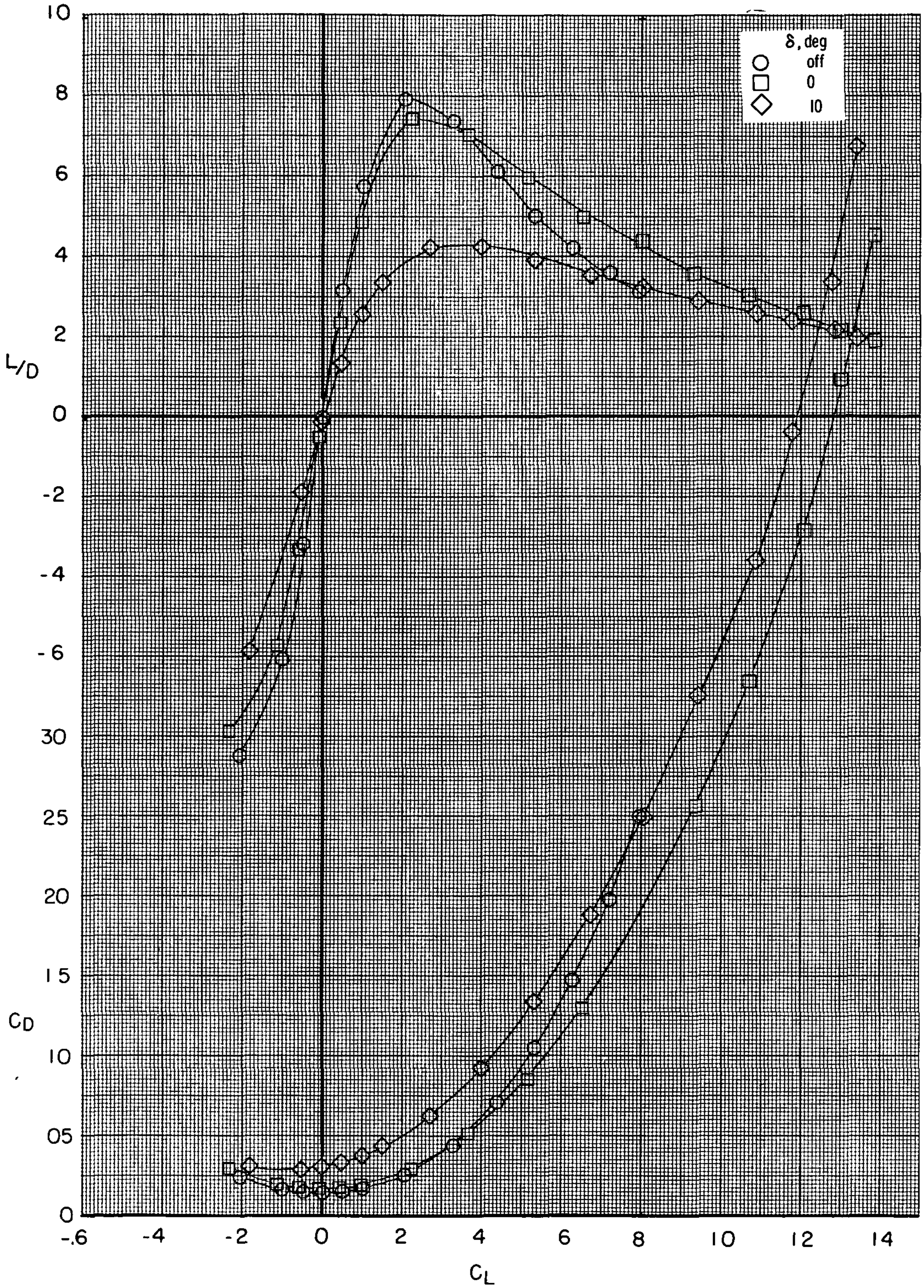

(a) Concluded.

Figure 11.- Continued.

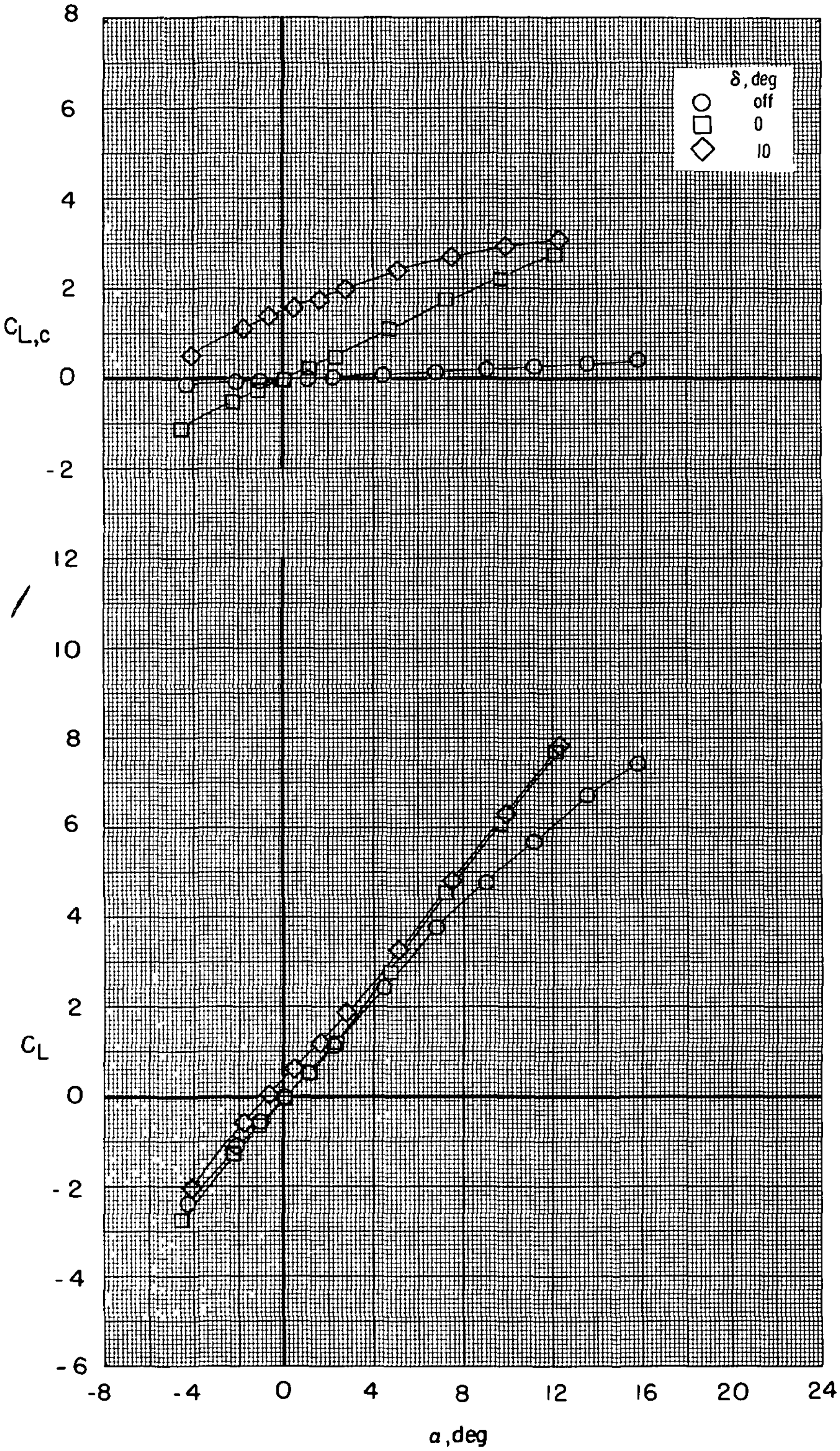

(b) M = 0.70.

Figure 11.- Continued.

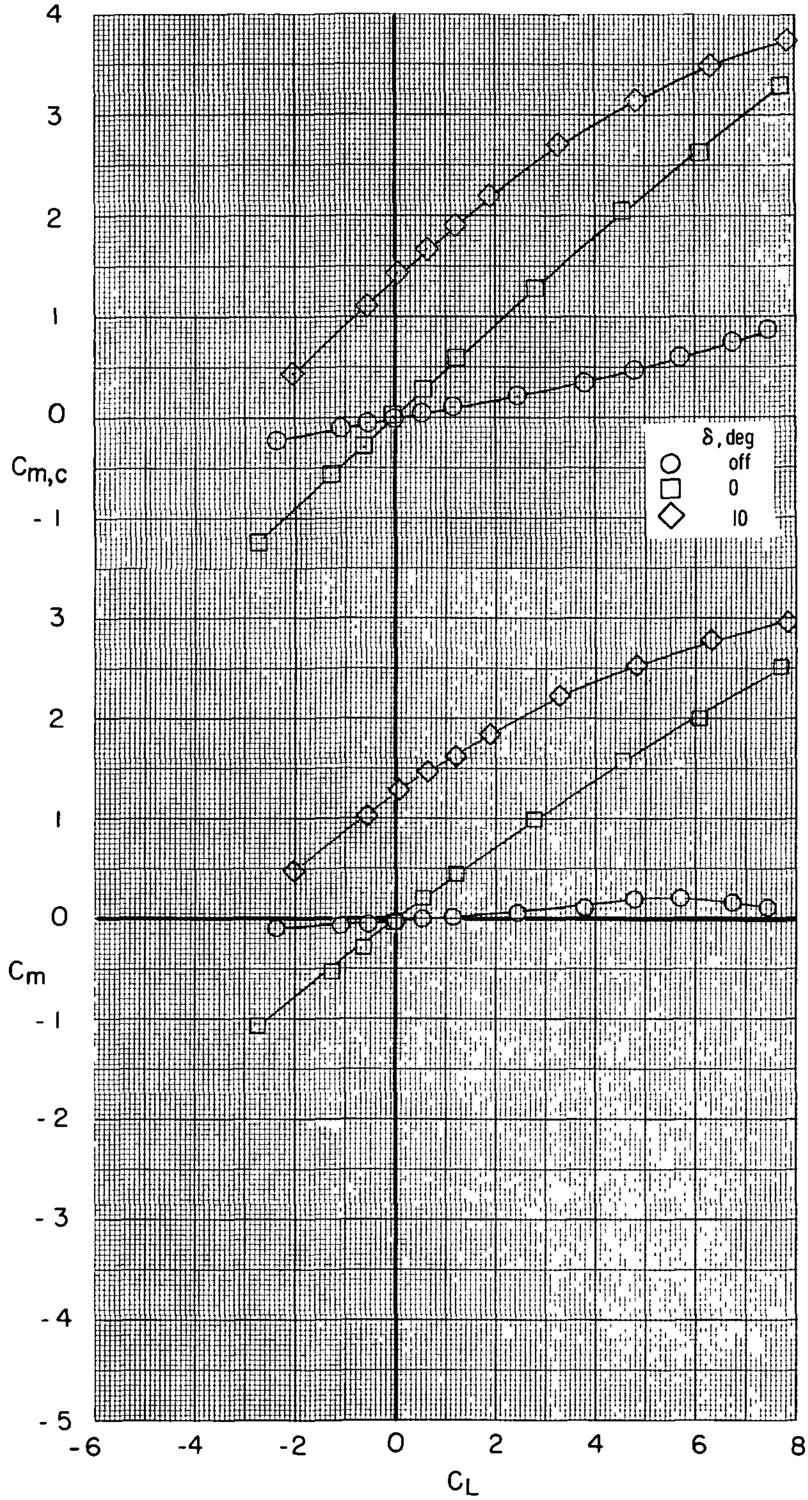

(b) Continued.

Figure 11.- Continued.

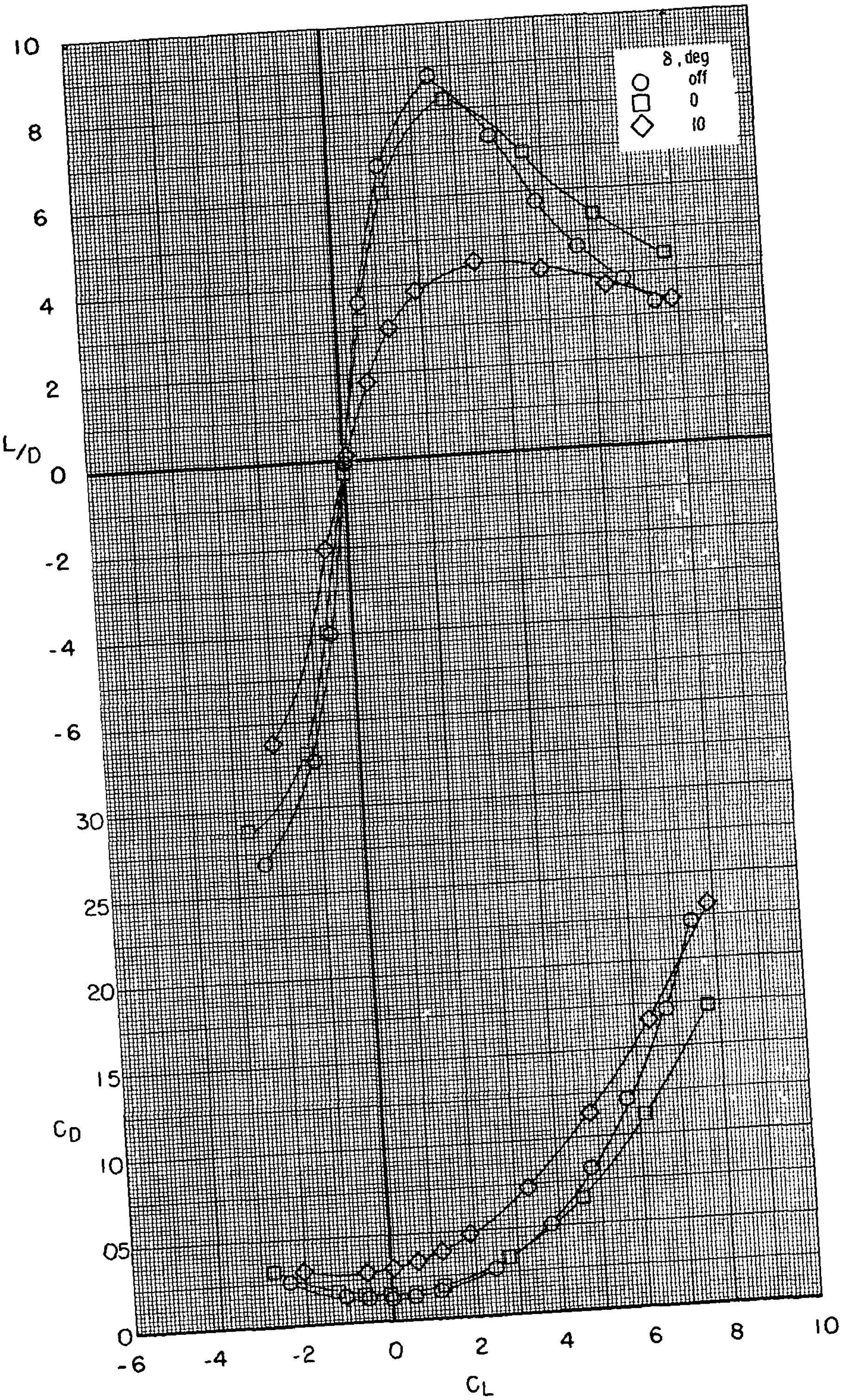

(b) Concluded.

Figure 11.- Continued.

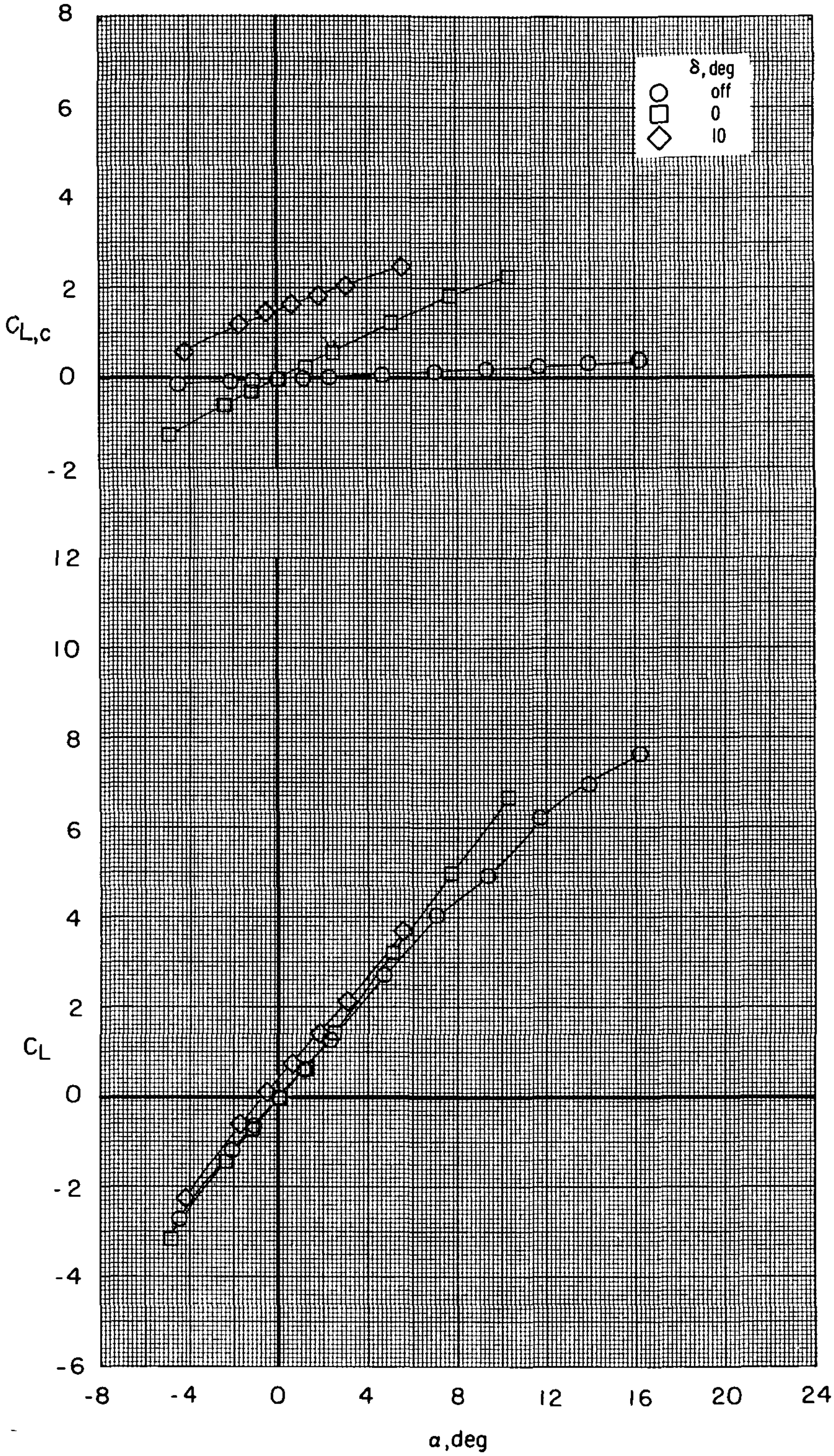

(c) M = 0.85.

Figure 11.- Continued.

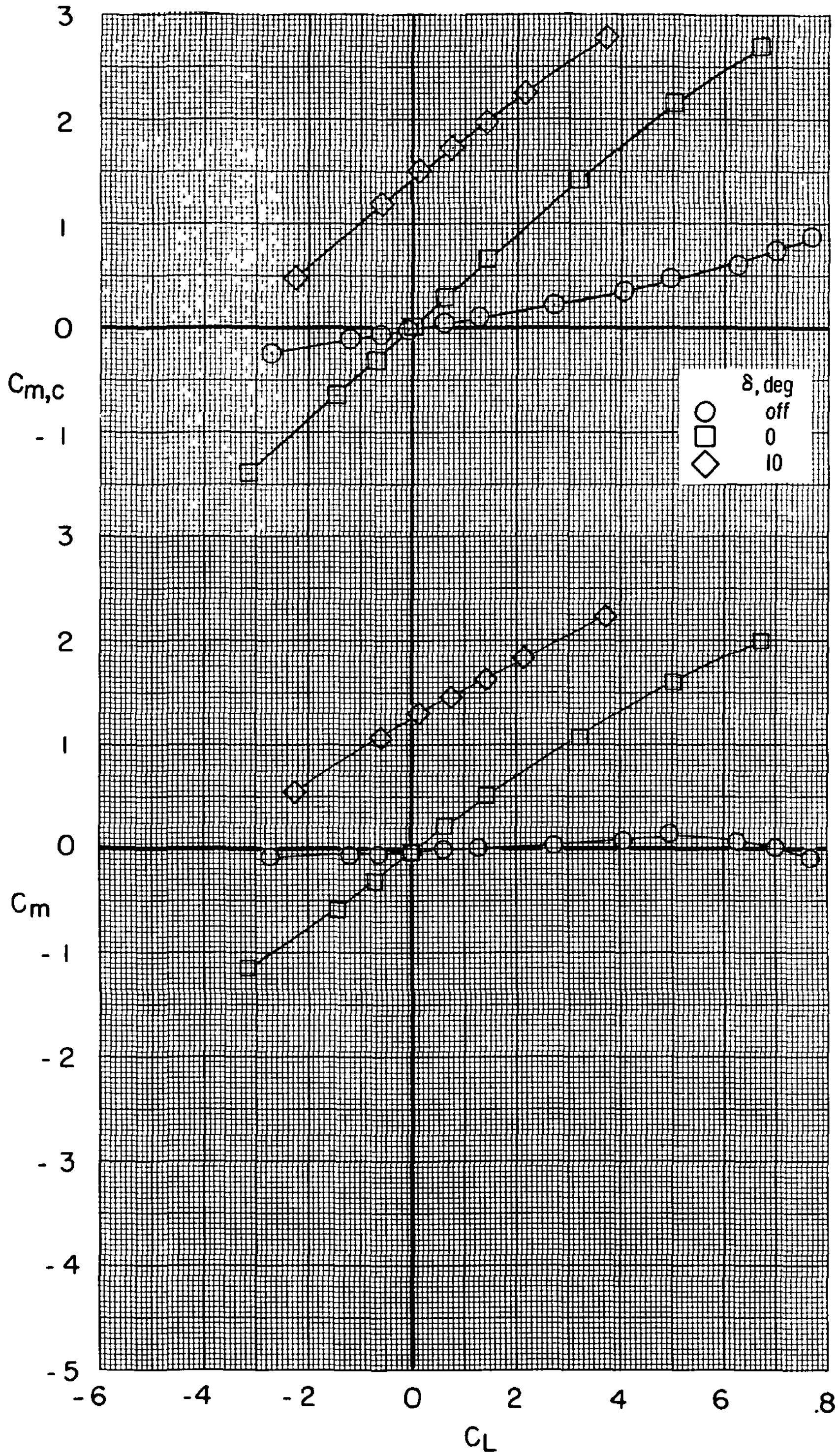

(c) Continued.

Figure 11.- Continued.

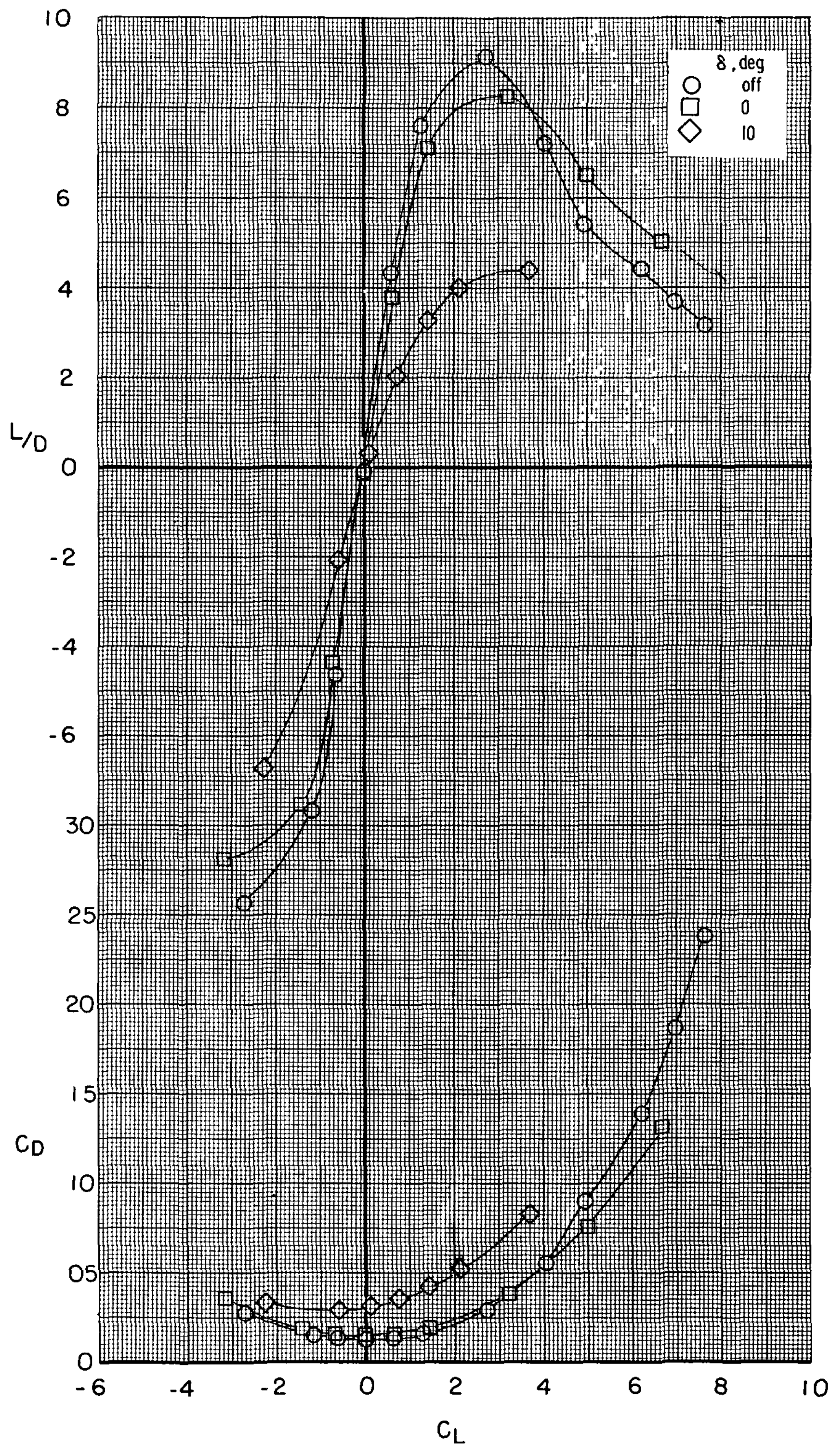

(c) Concluded.

Figure 11.- Concluded.

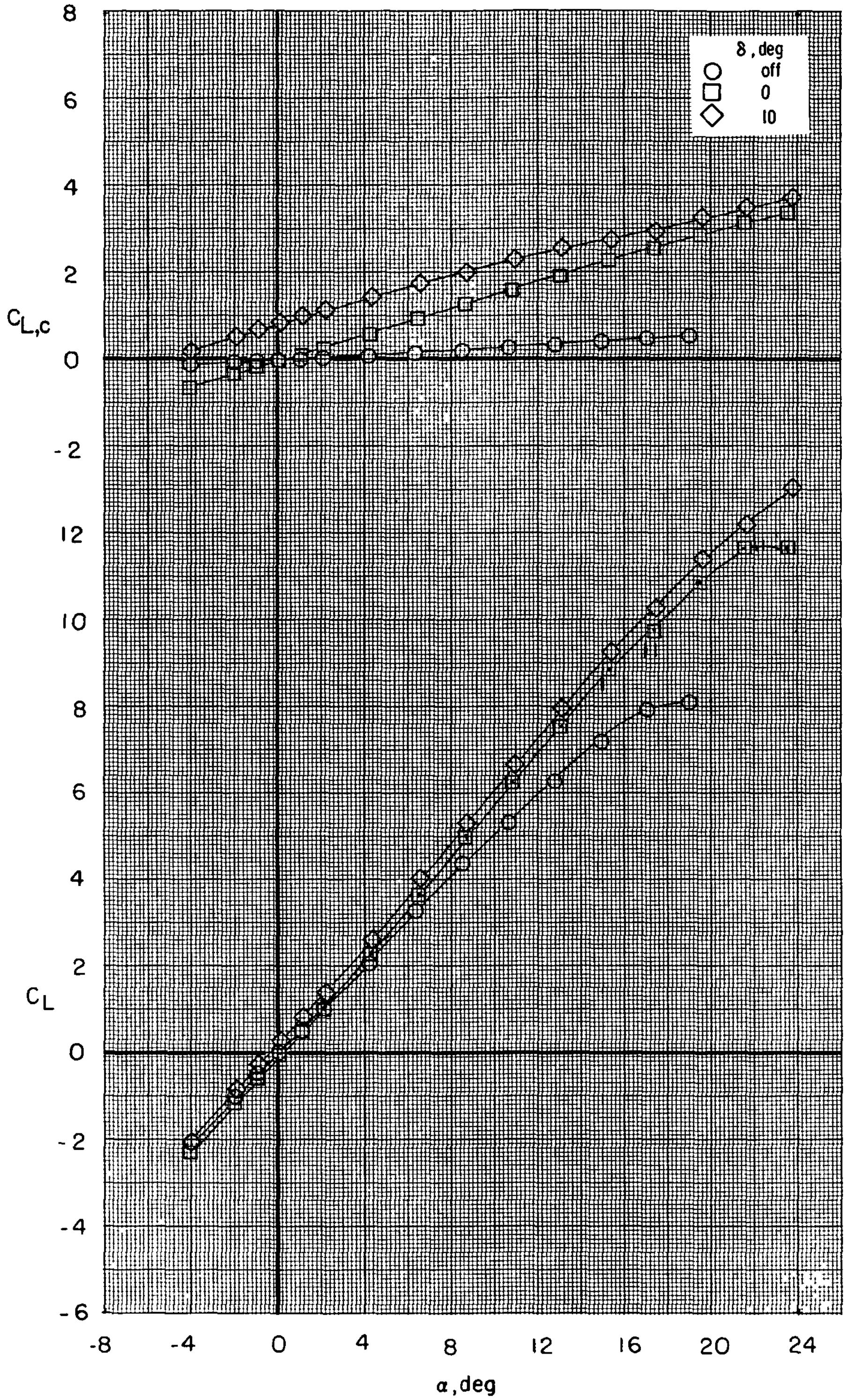

(a) M = 0.40.

Figure 12.- Effect of canard I ($S_c/S_W = 0.16$) deflection on longitudinal characteristics of wing II ($\Lambda_W = 44^o$) for $z/\bar{c} = 0.185$.

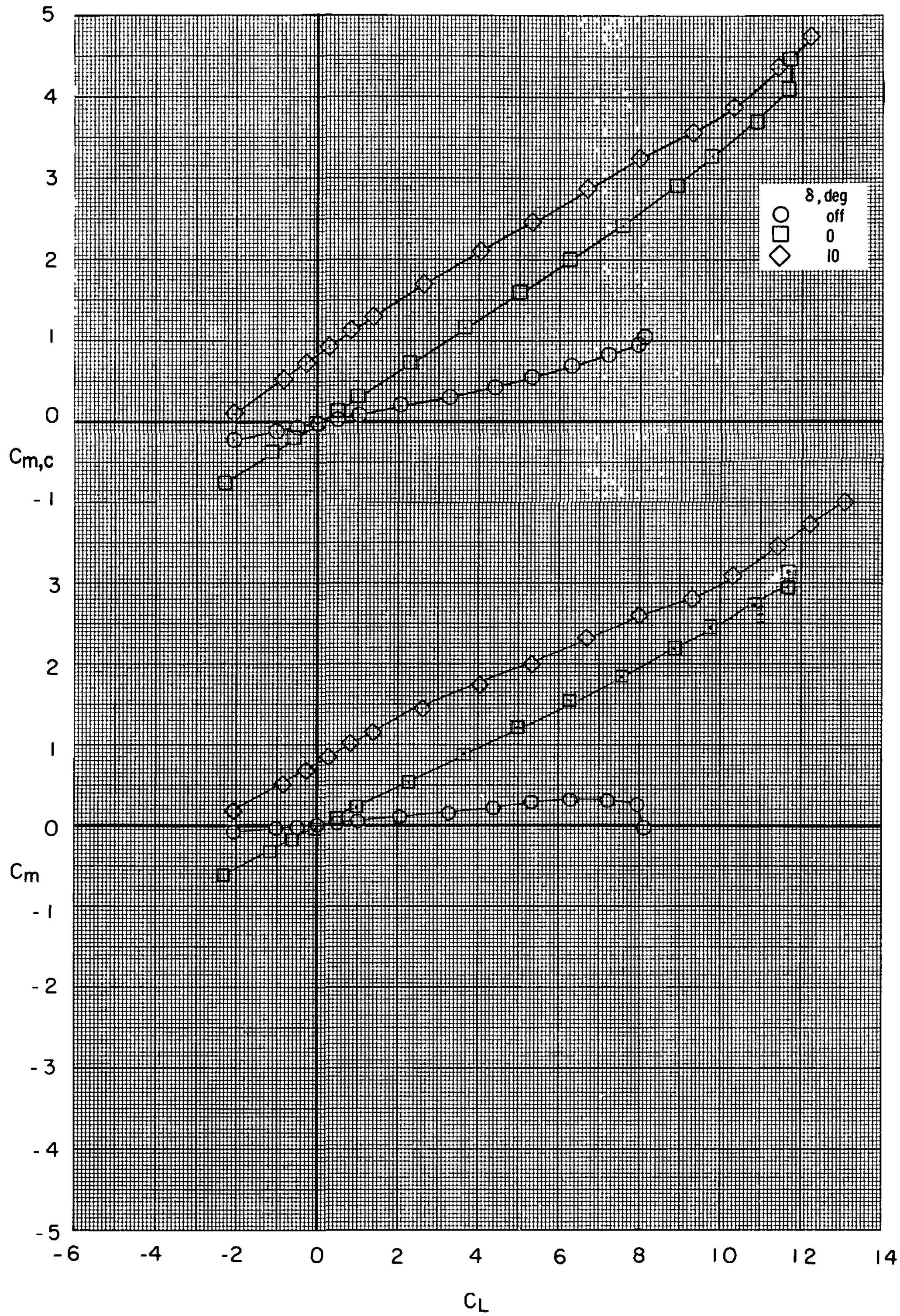

(a) Continued.

Figure 12.- Continued.

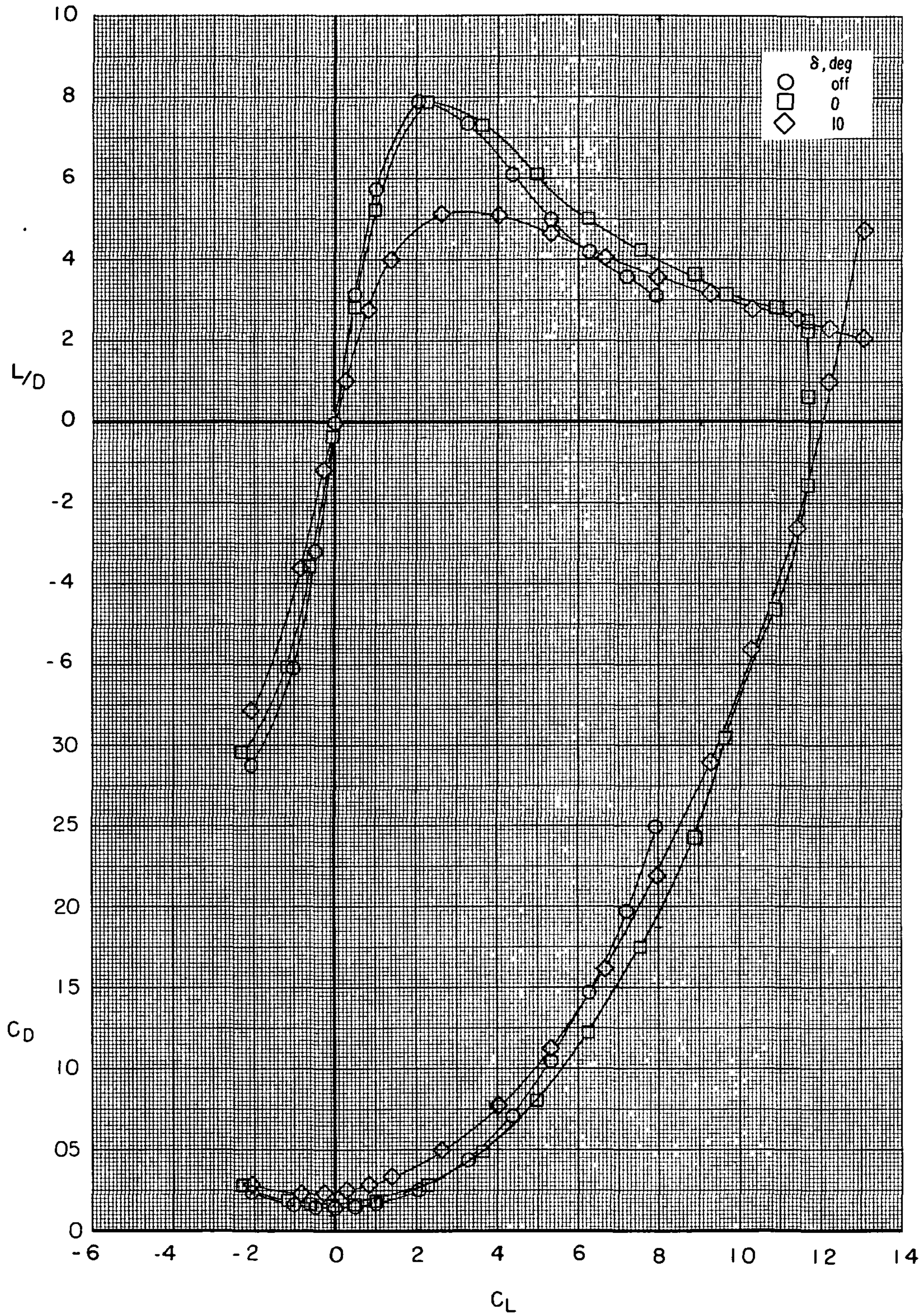

(a) Concluded.

Figure 12.- Continued.

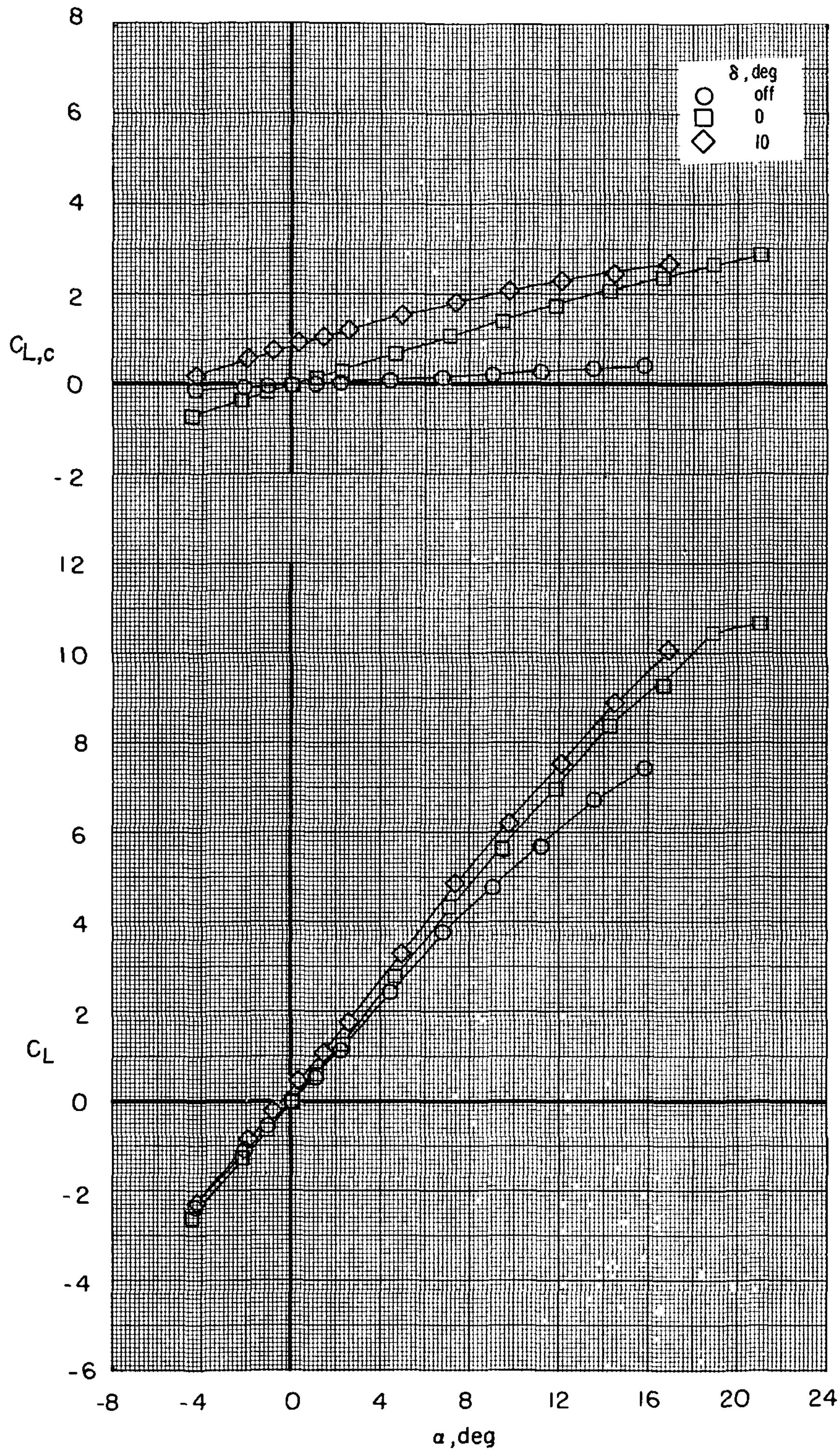

(b) M = 0.70.

Figure 12.- Continued.

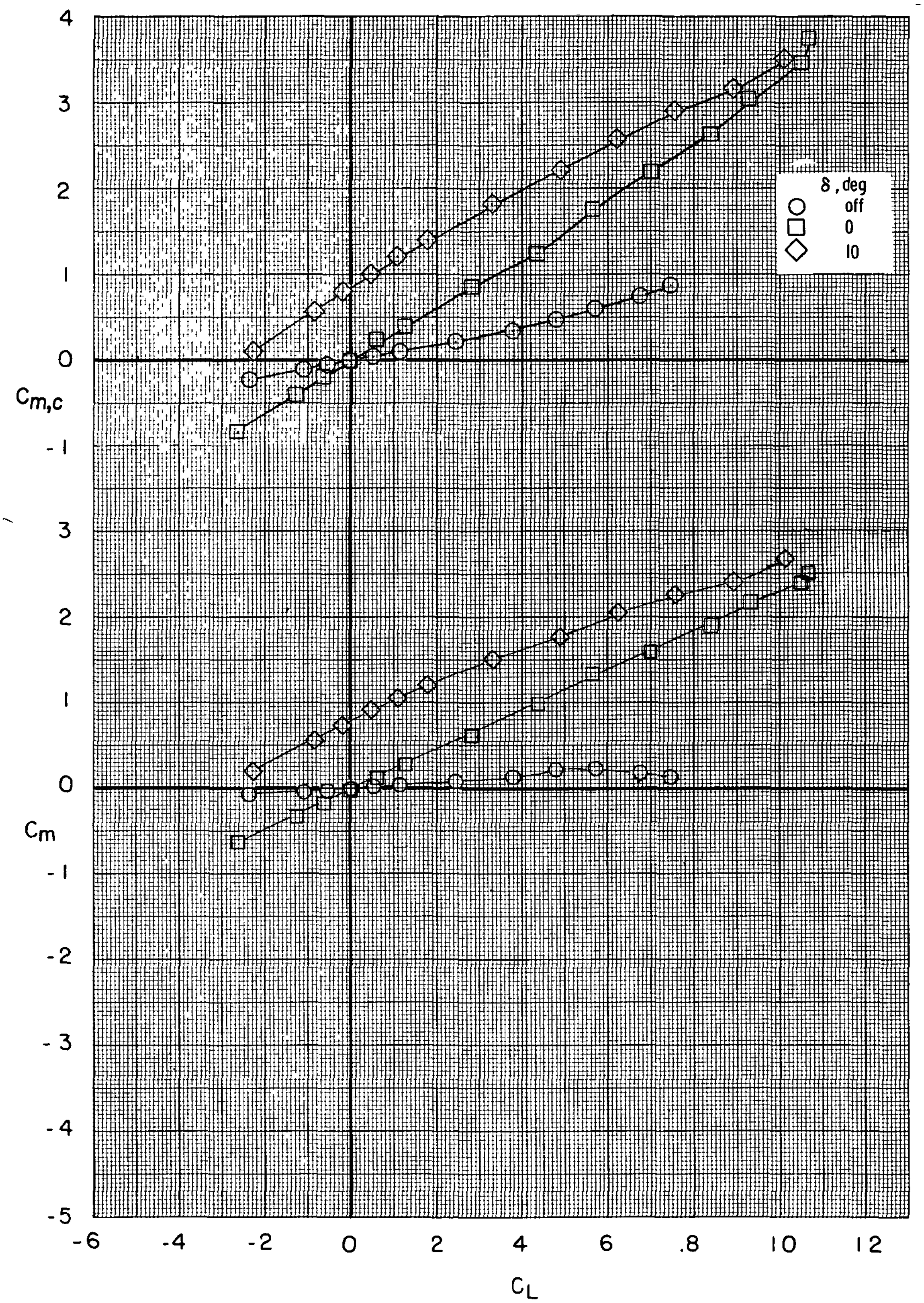

(b) Continued.

Figure 12.- Continued.

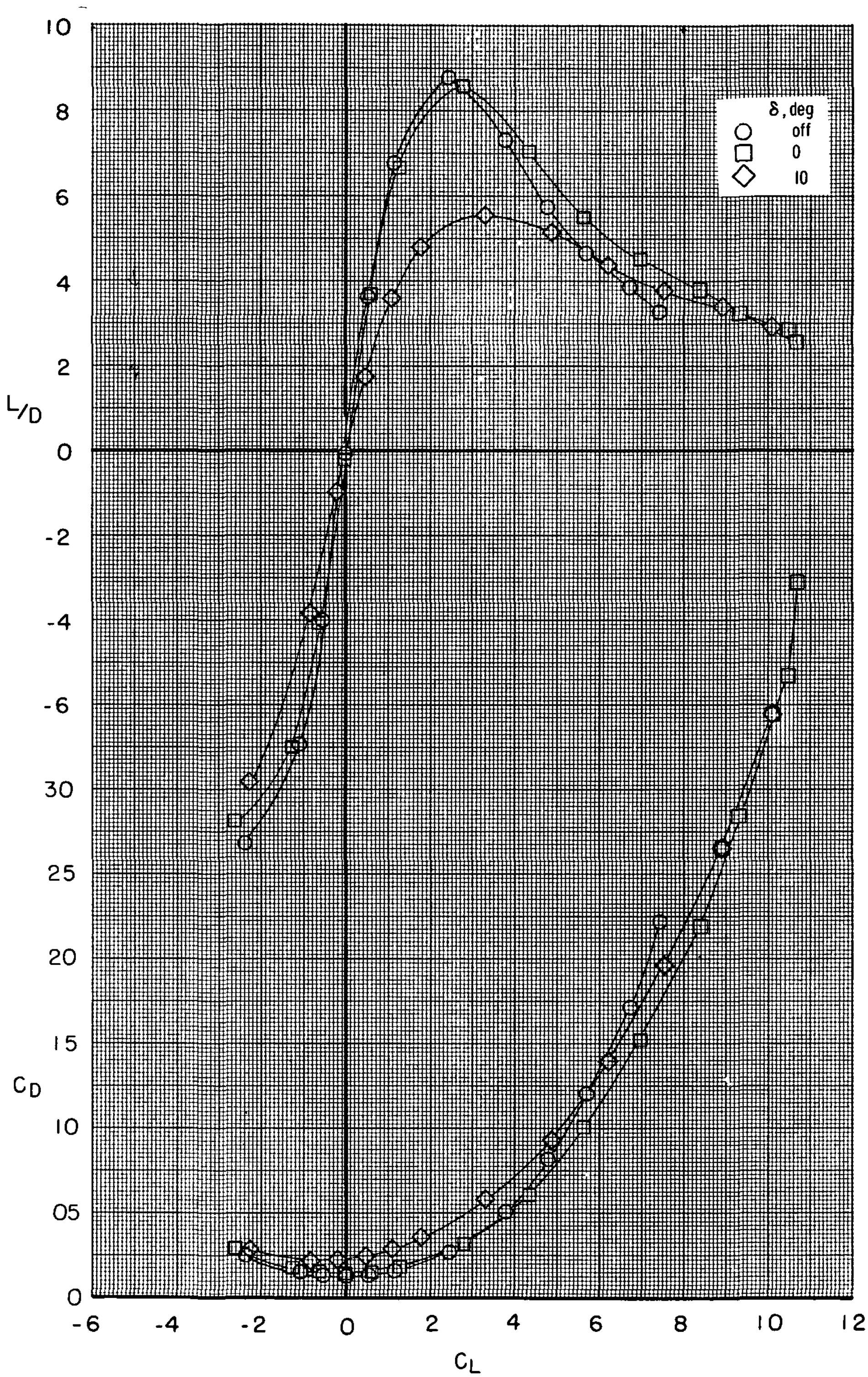

(b) Concluded.

Figure 12.- Continued.

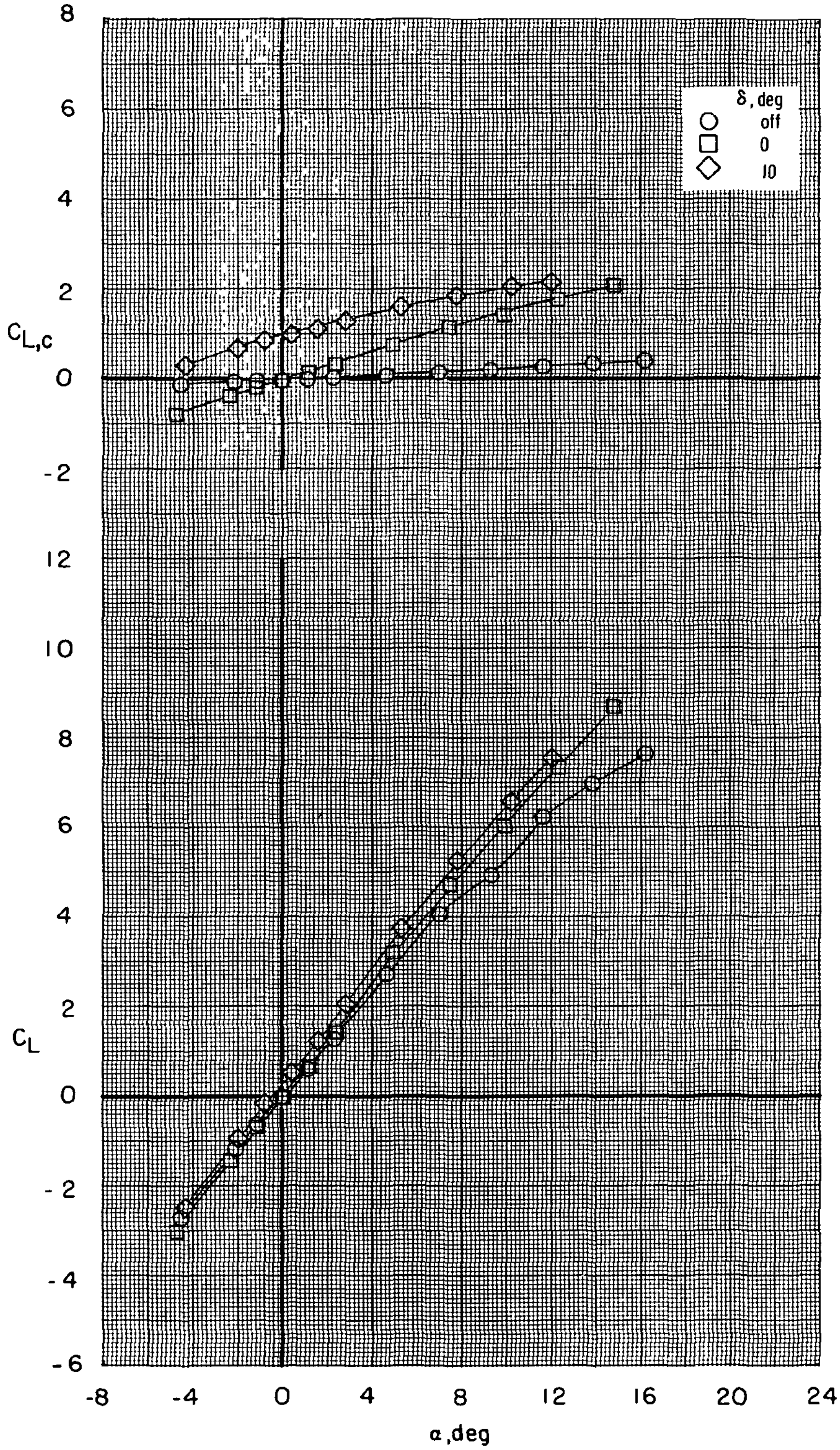

(c) M = 0.85.

Figure 12.- Continued.

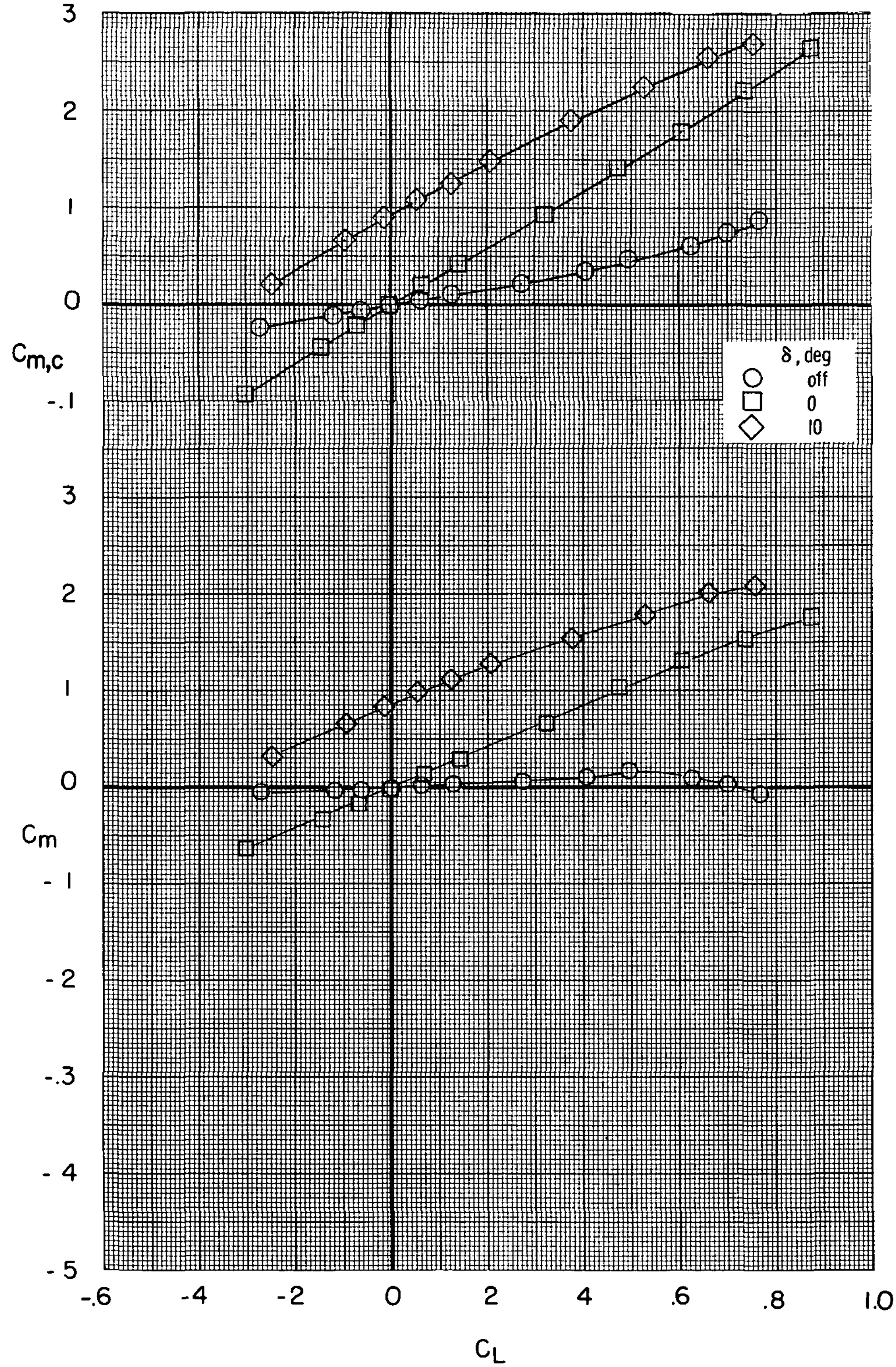

(c) Continued.

Figure 12.- Continued.

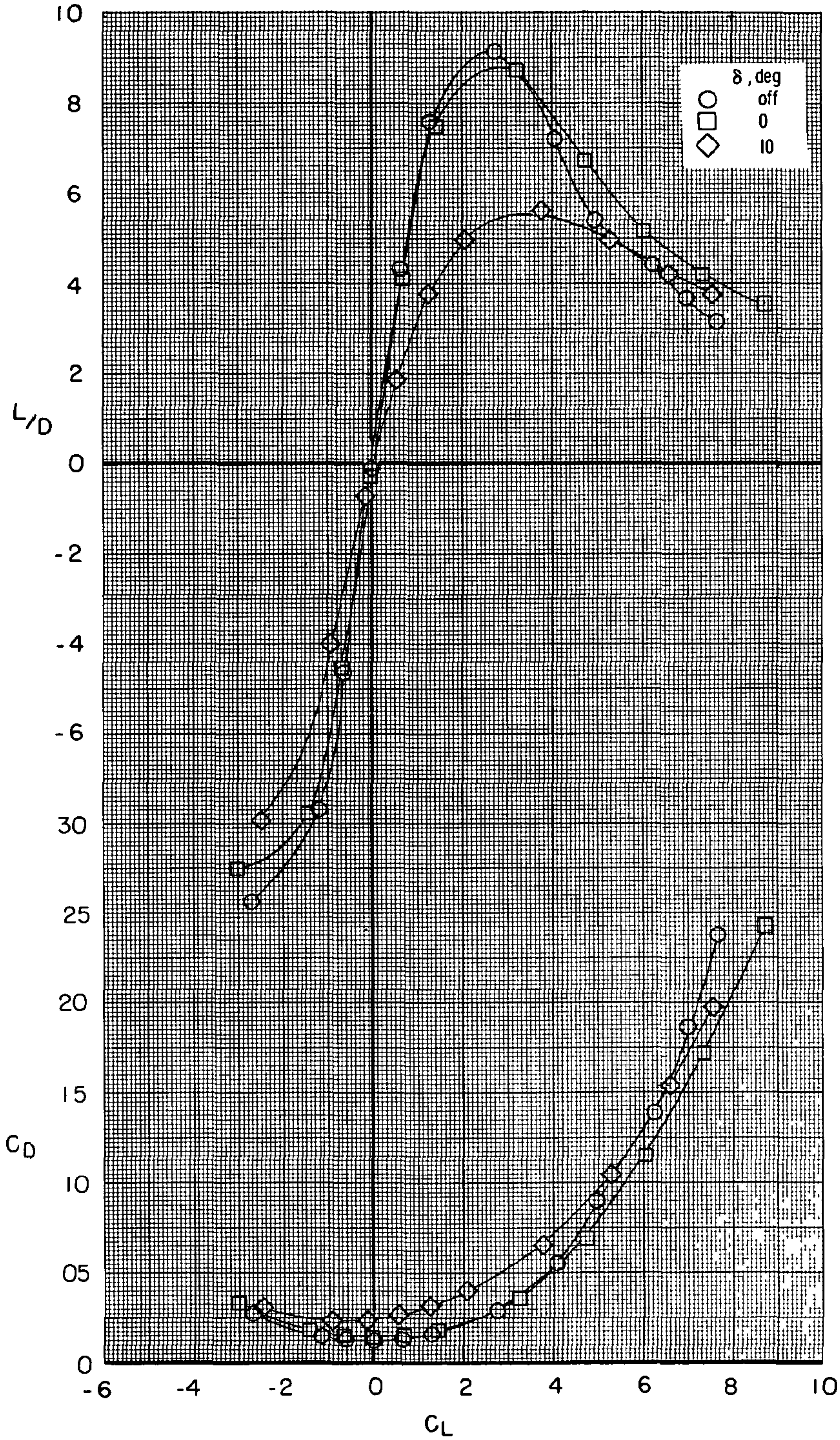

(c) Concluded.

Figure 12.- Concluded.

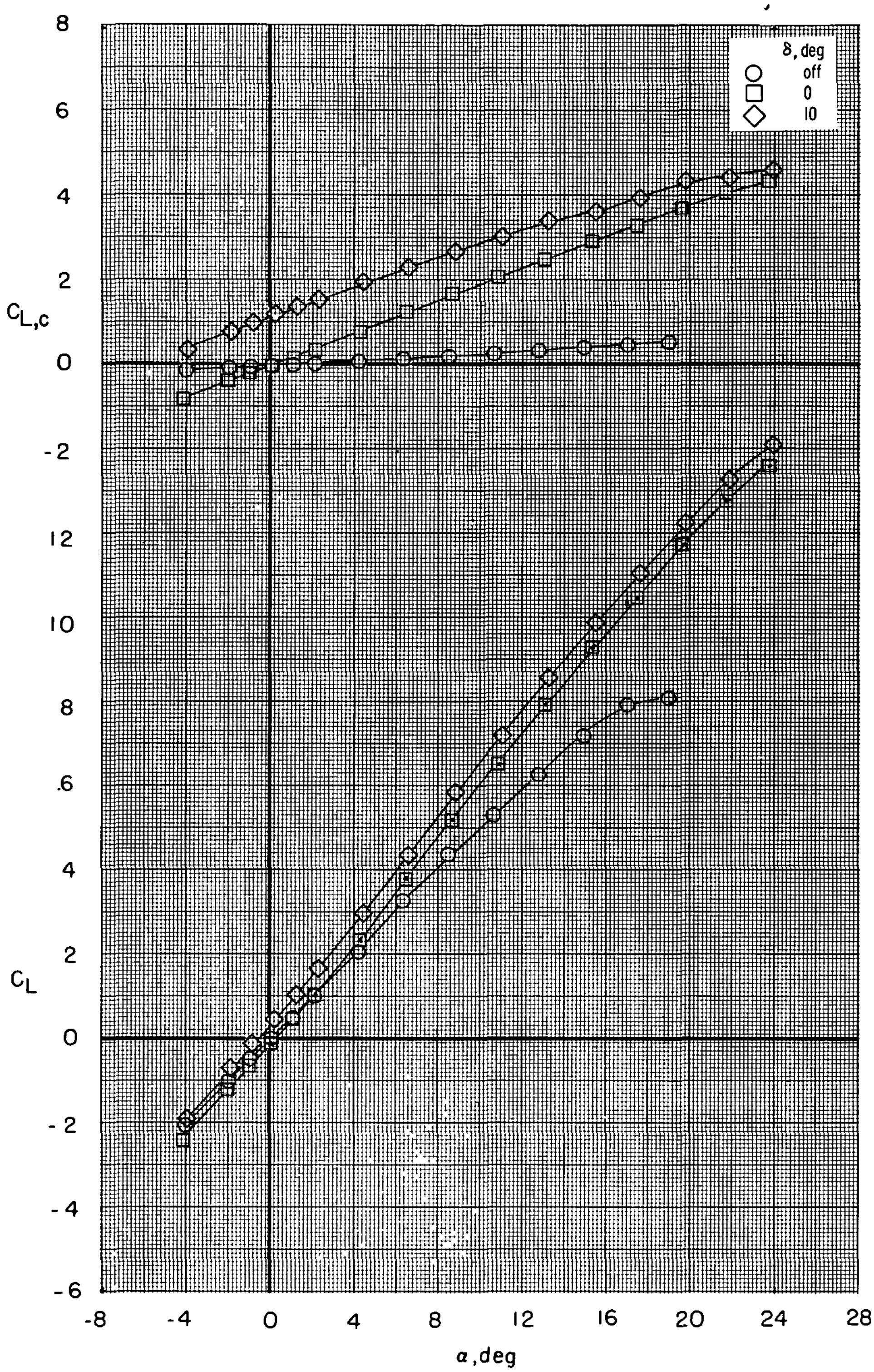

(a) M = 0.40.

Figure 13.- Effect of canard II (S_c/S_W = 0.22) deflection on longitudinal characteristics for wing II (Λ_W = 44°), $z/\bar{c}$ = 0.185.

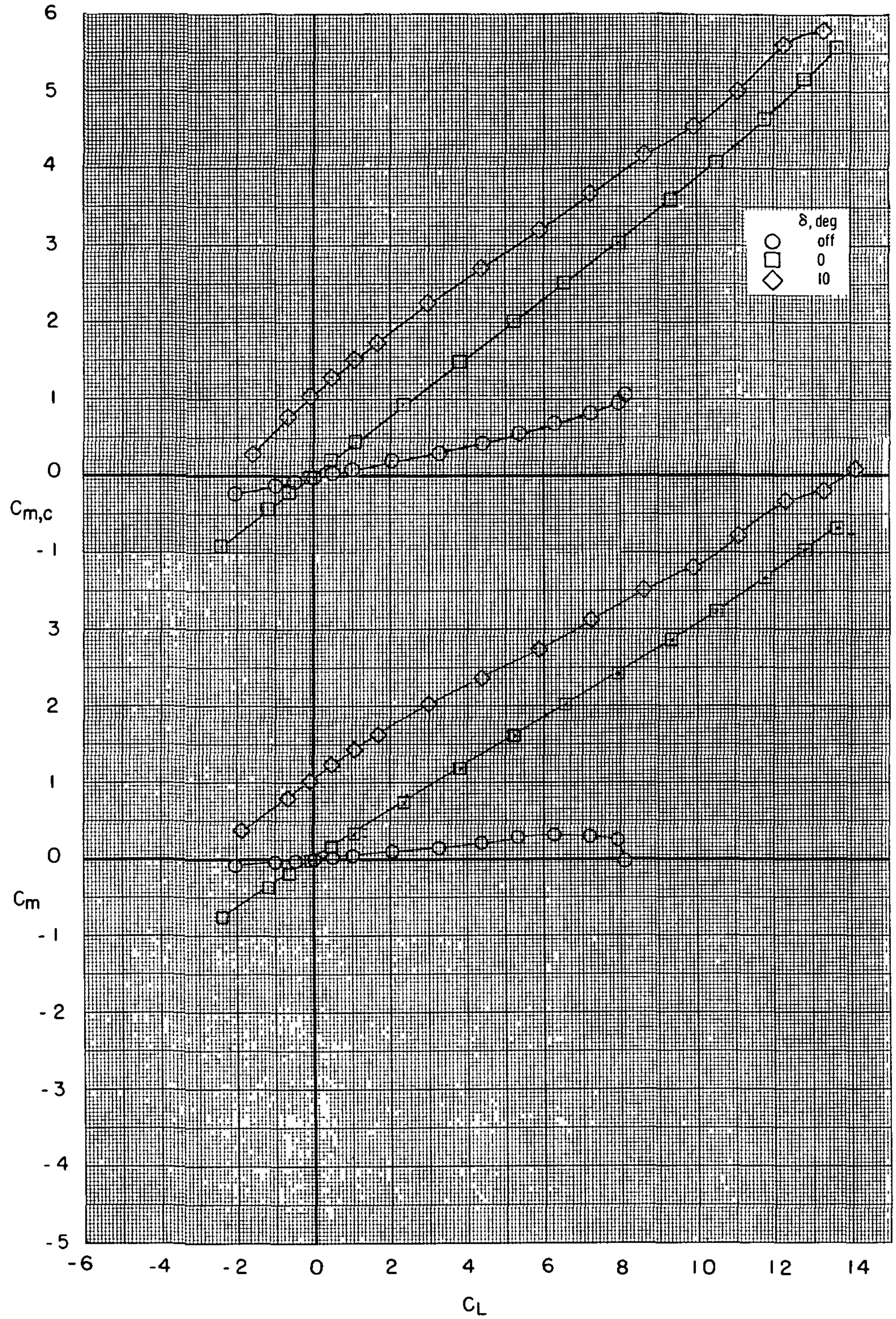

(a) Continued.

Figure 13.- Continued.

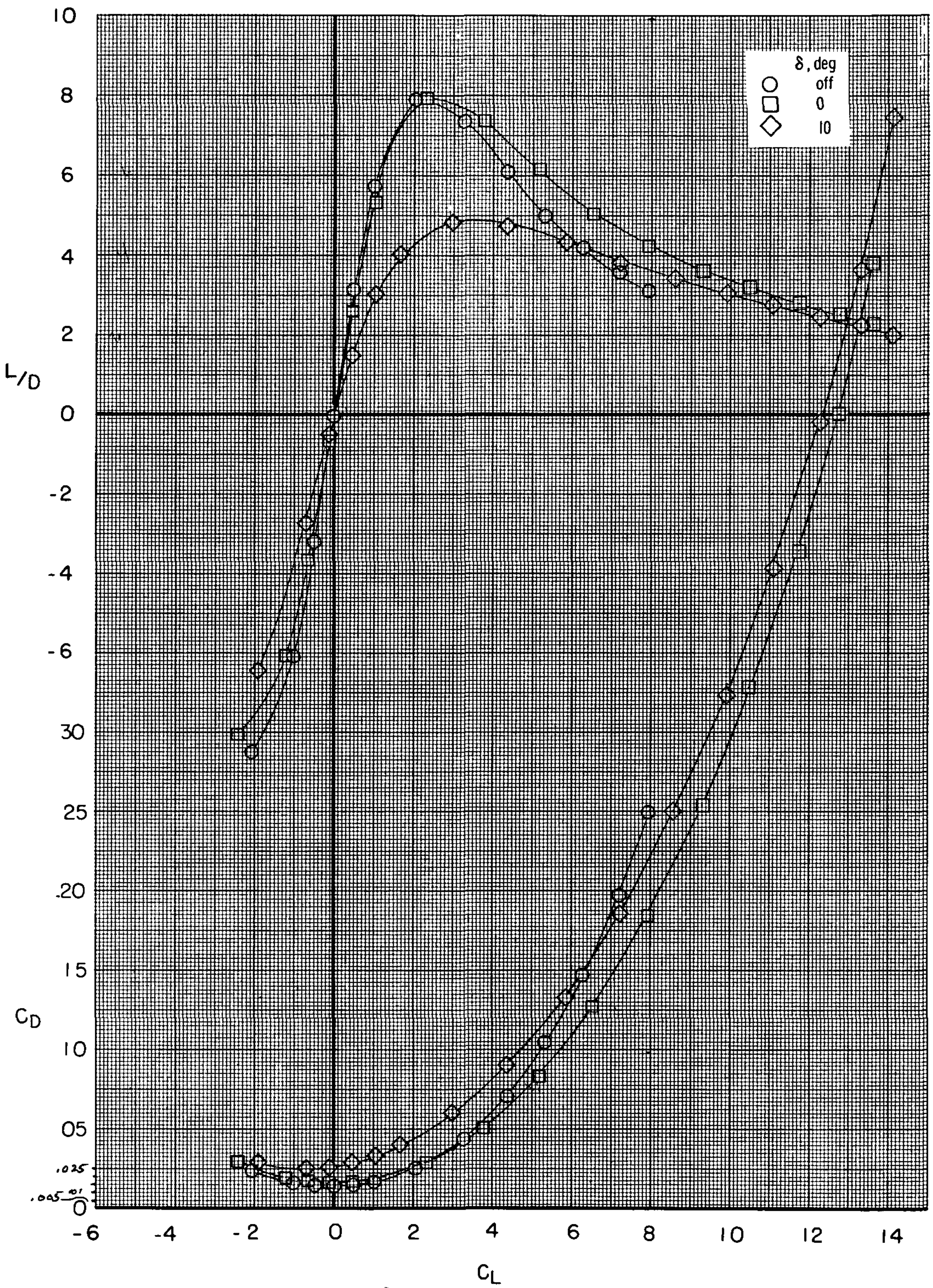

(a) Concluded.

Figure 13.- Continued.

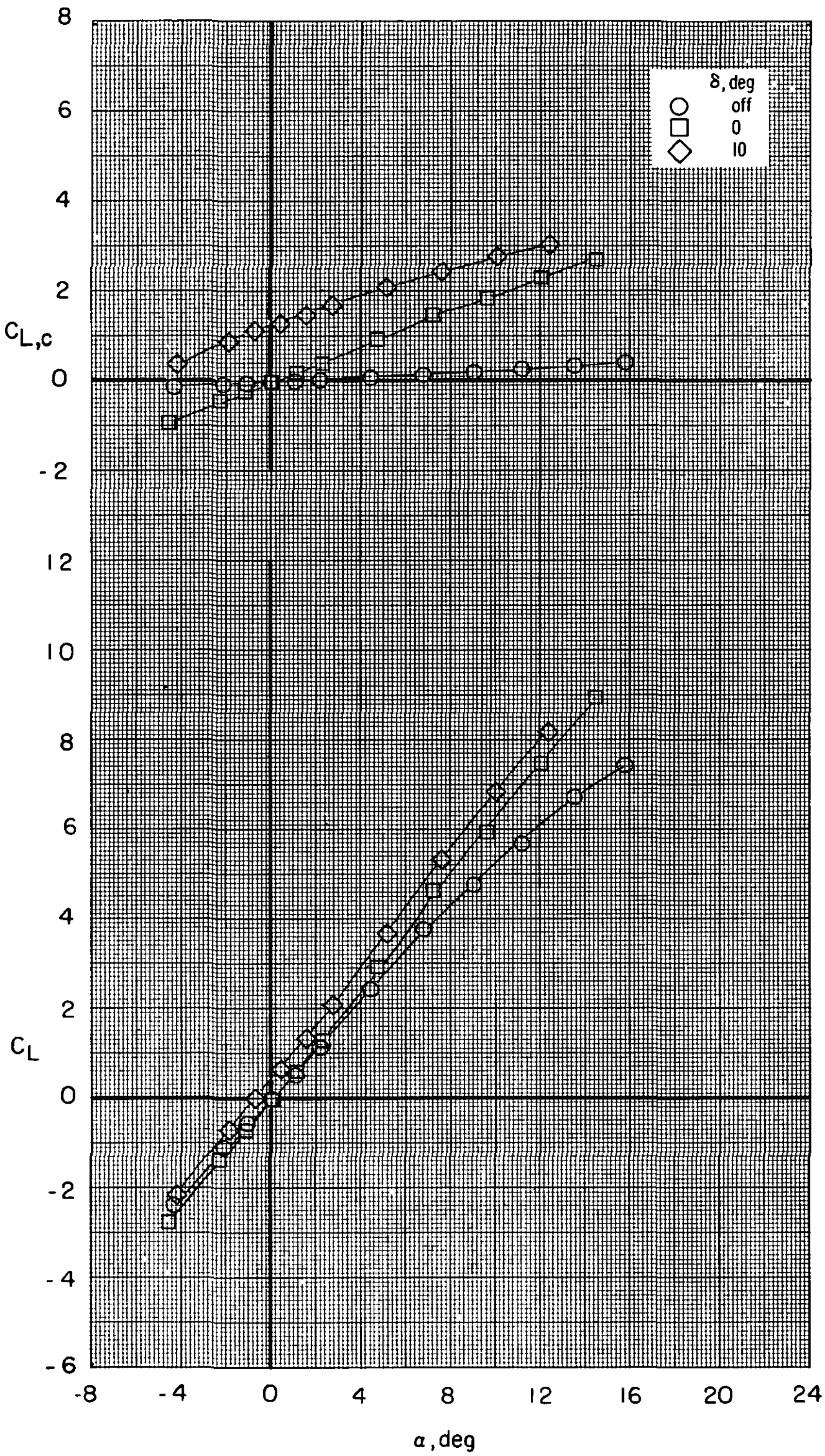

(b) M = 0.70.

Figure 13.- Continued.

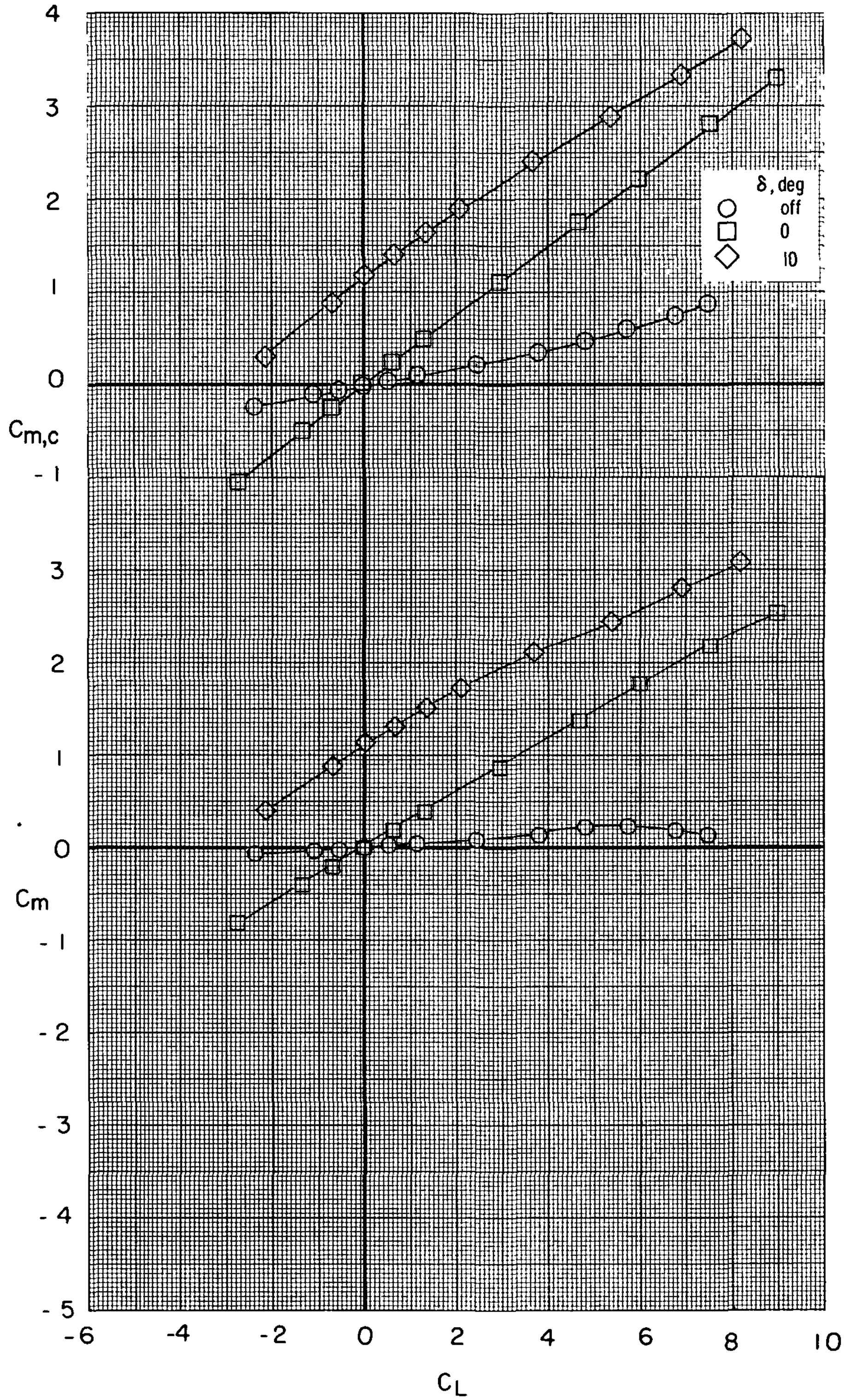

(b) Continued.

Figure 13.- Continued.

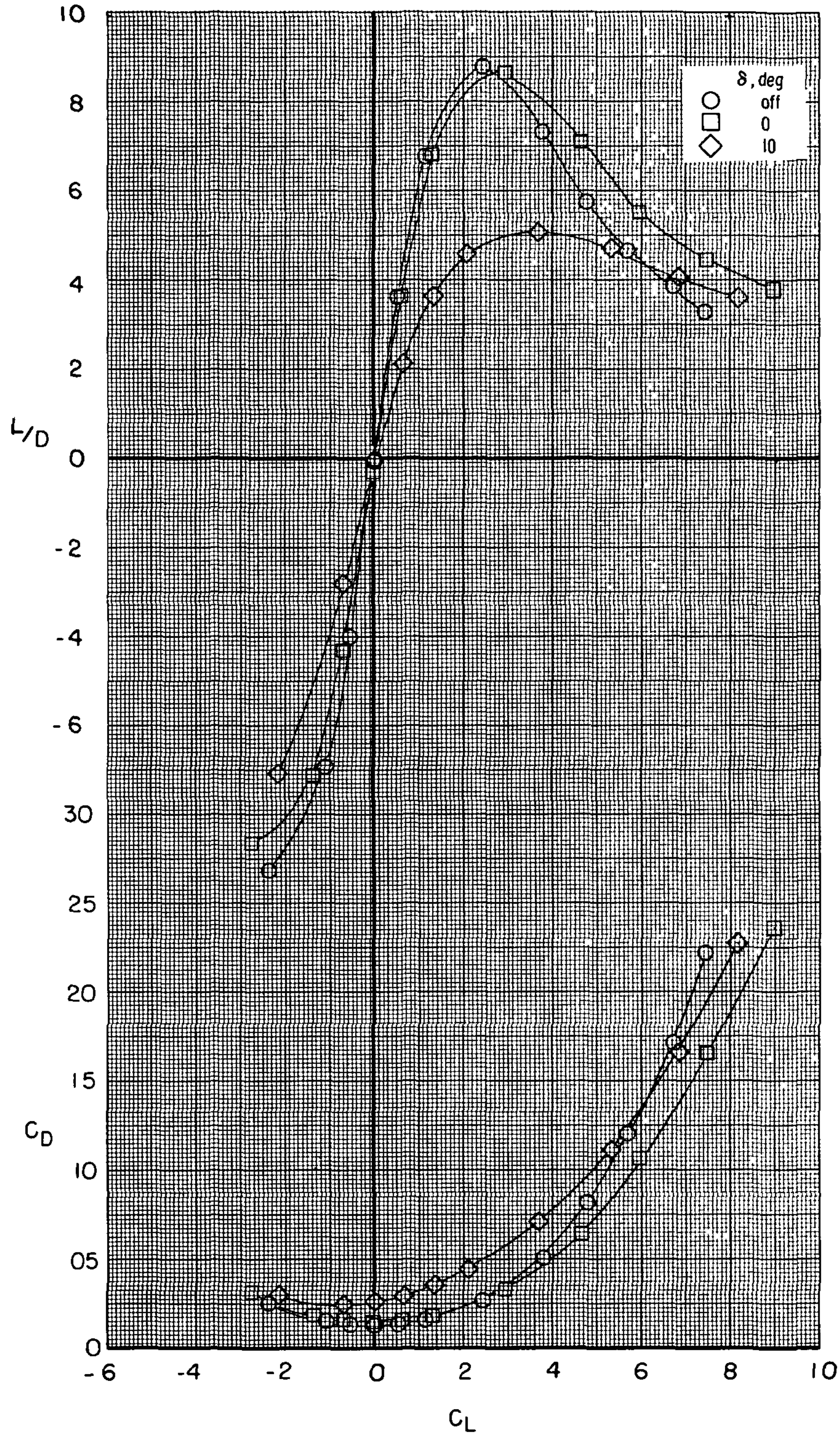

(b) Concluded.

Figure 13.- Continued.

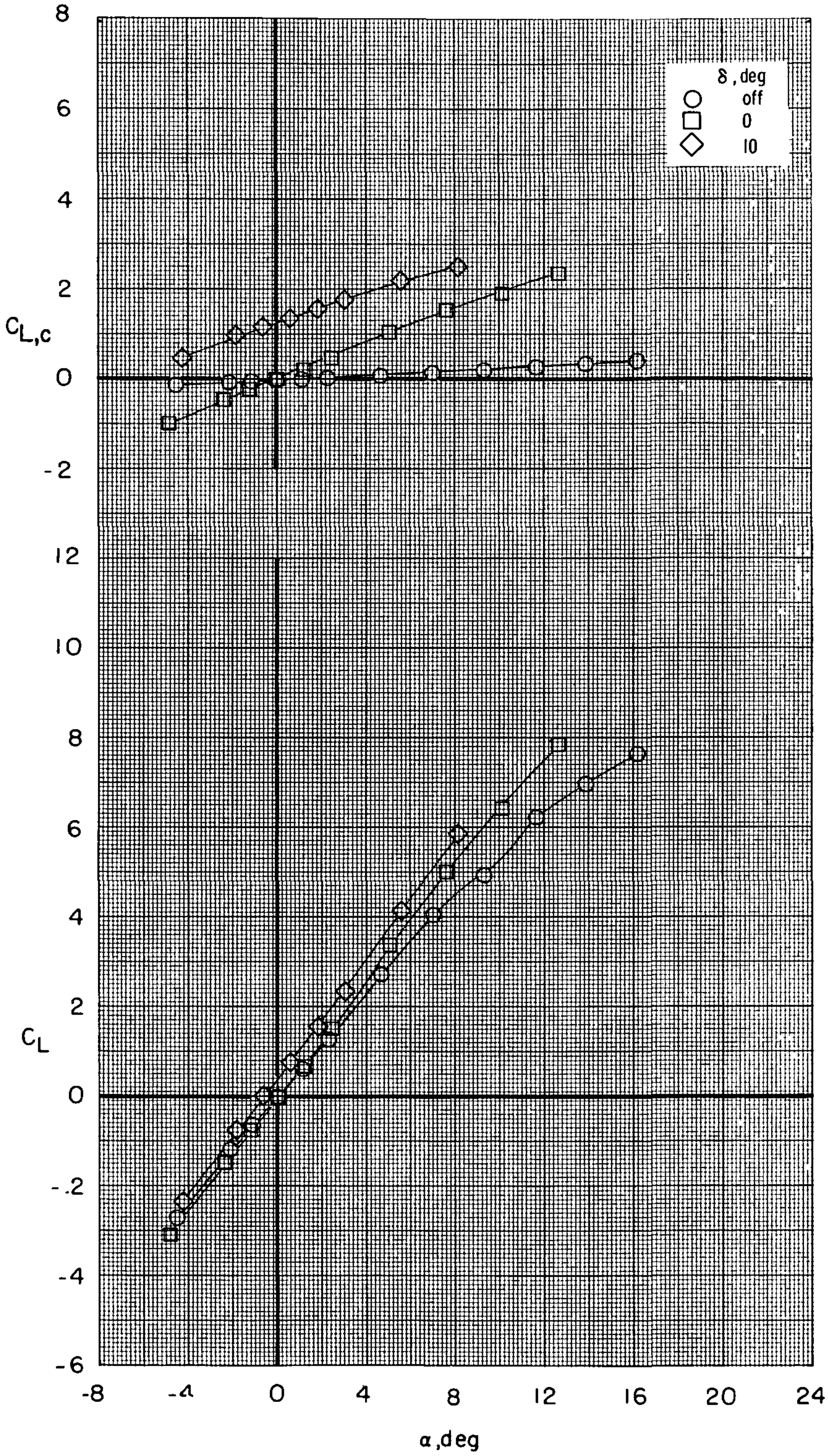

(c) M = 0.85.

Figure 13.- Continued.

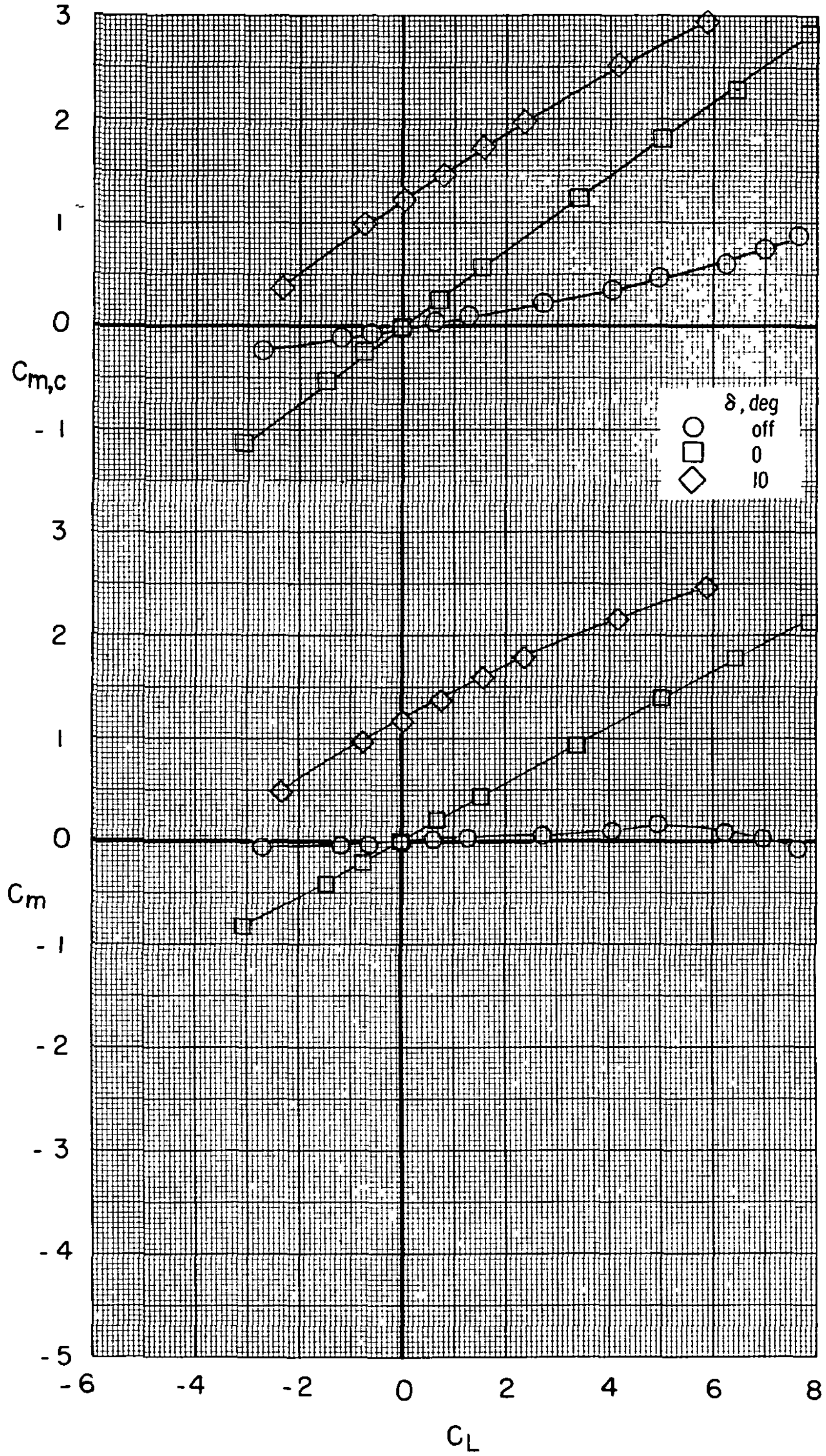

(c) Continued.

Figure 13.- Continued.

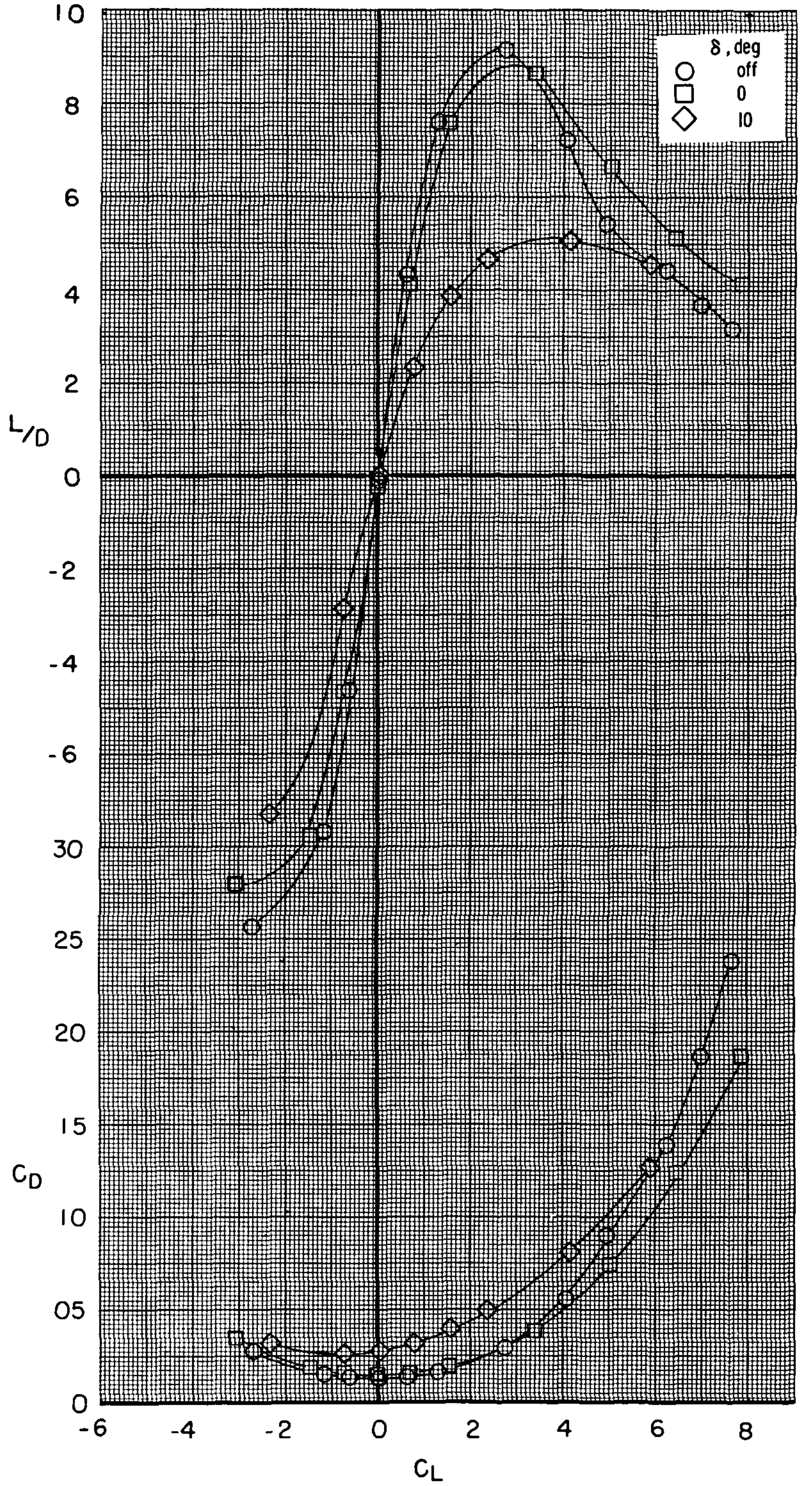

(c) Concluded.

Figure 13.- Concluded.

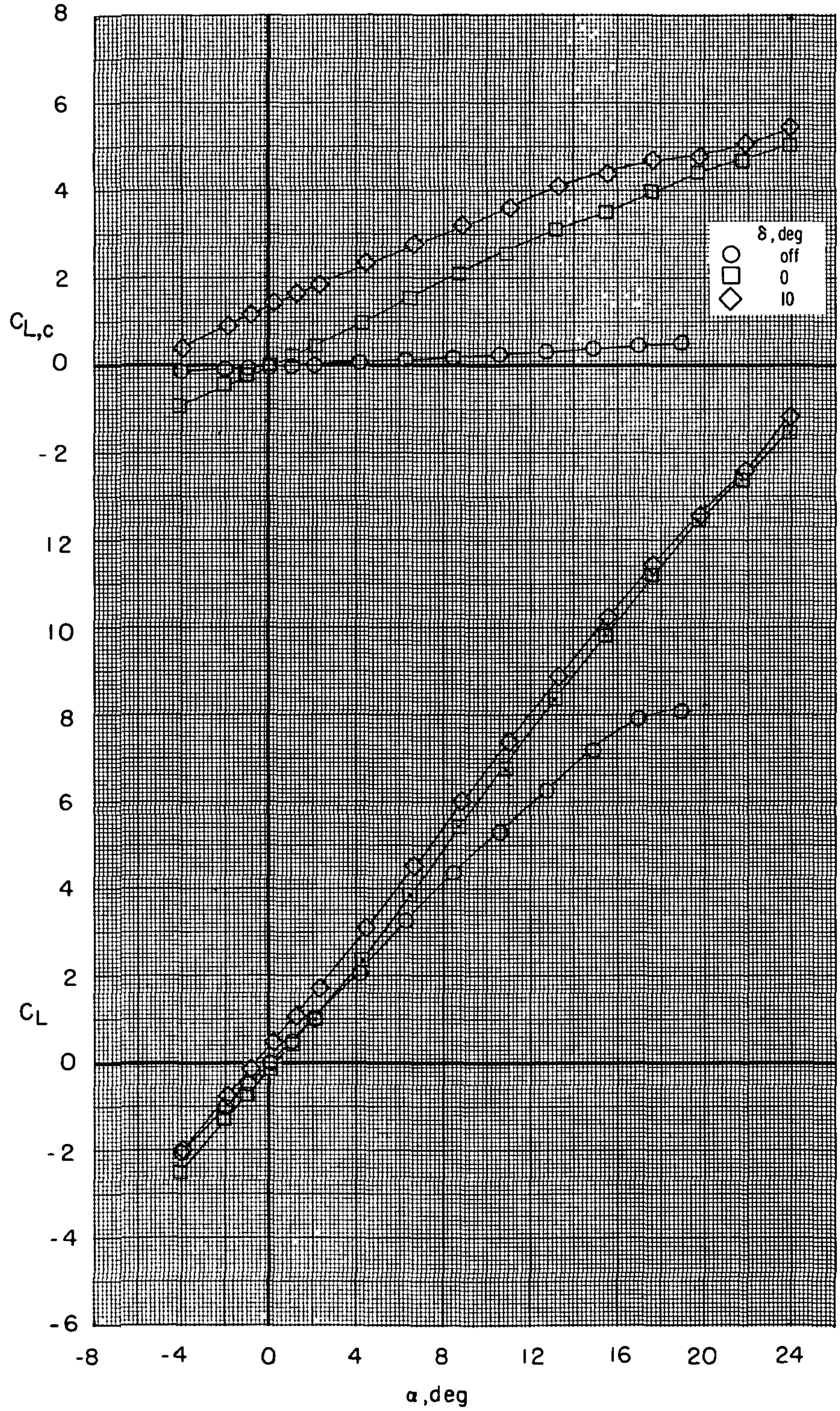

(a) M = 0.40.

Figure 14.- Effect of canard III (S_c/S_w = 0.28) deflection on longitudinal characteristics for wing II (Λ_w = 44°), $z/\bar{c}$ = 0.185.

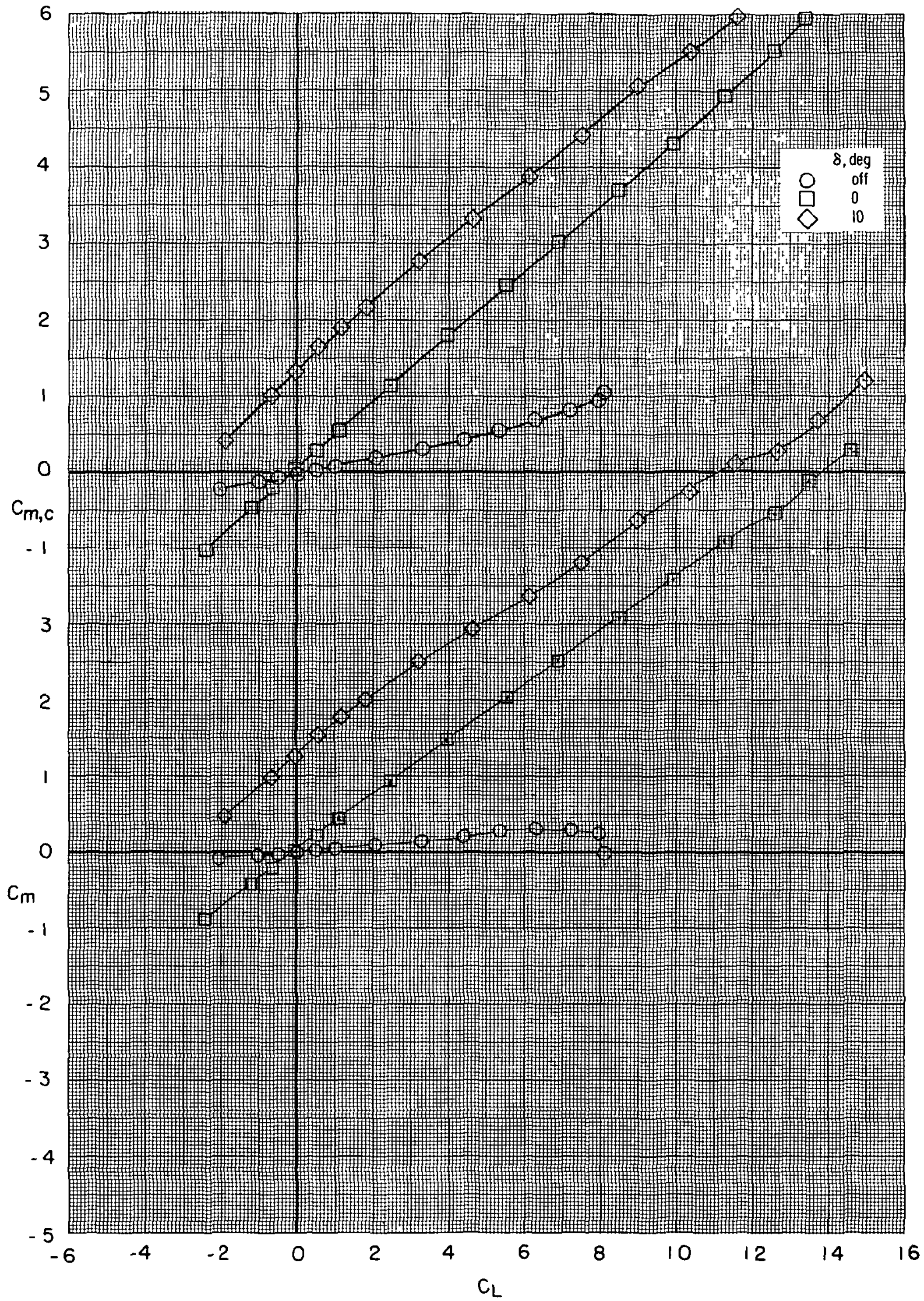

(a) Continued.

Figure 14.- Continued.

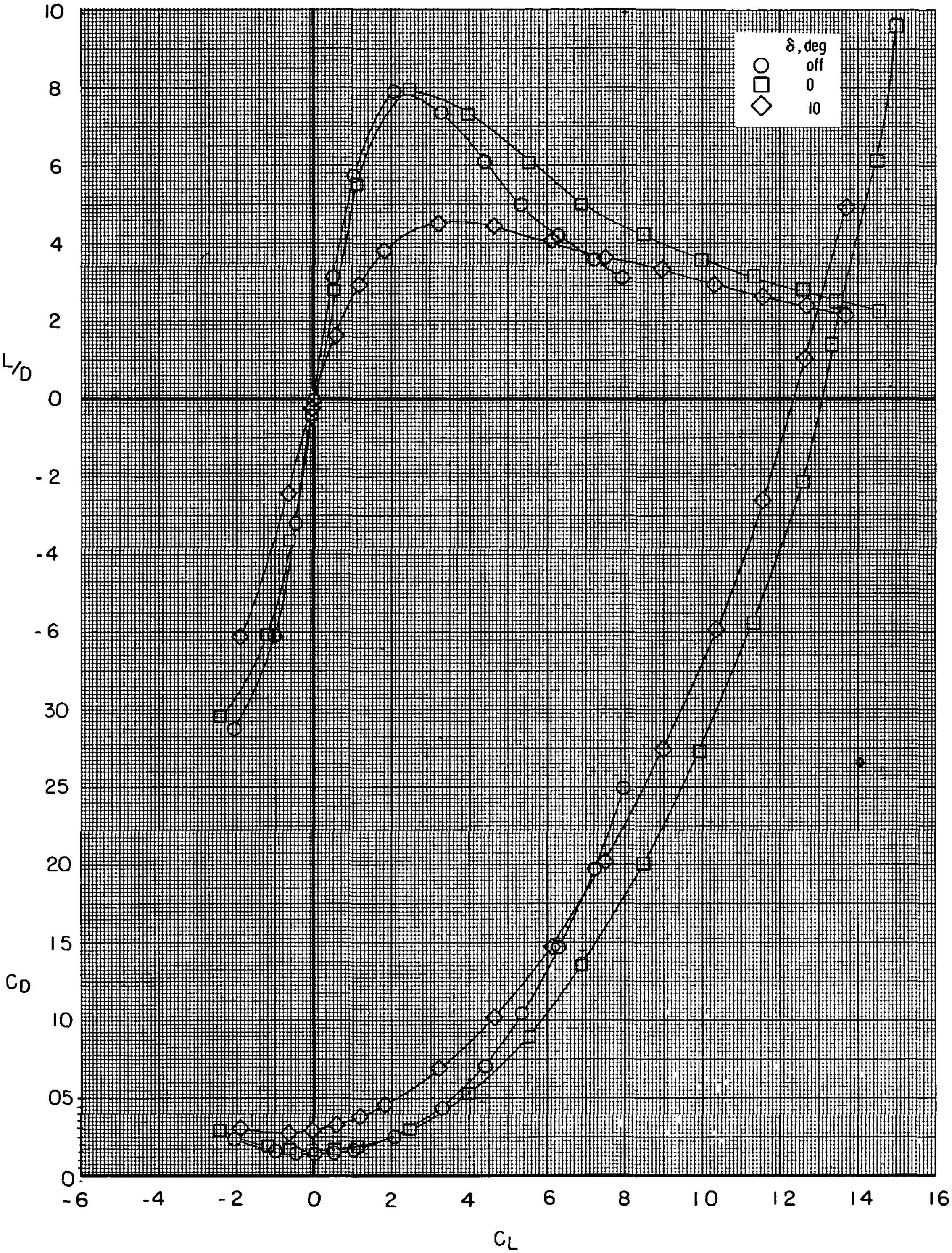

(a) Concluded.

Figure 14.- Continued.

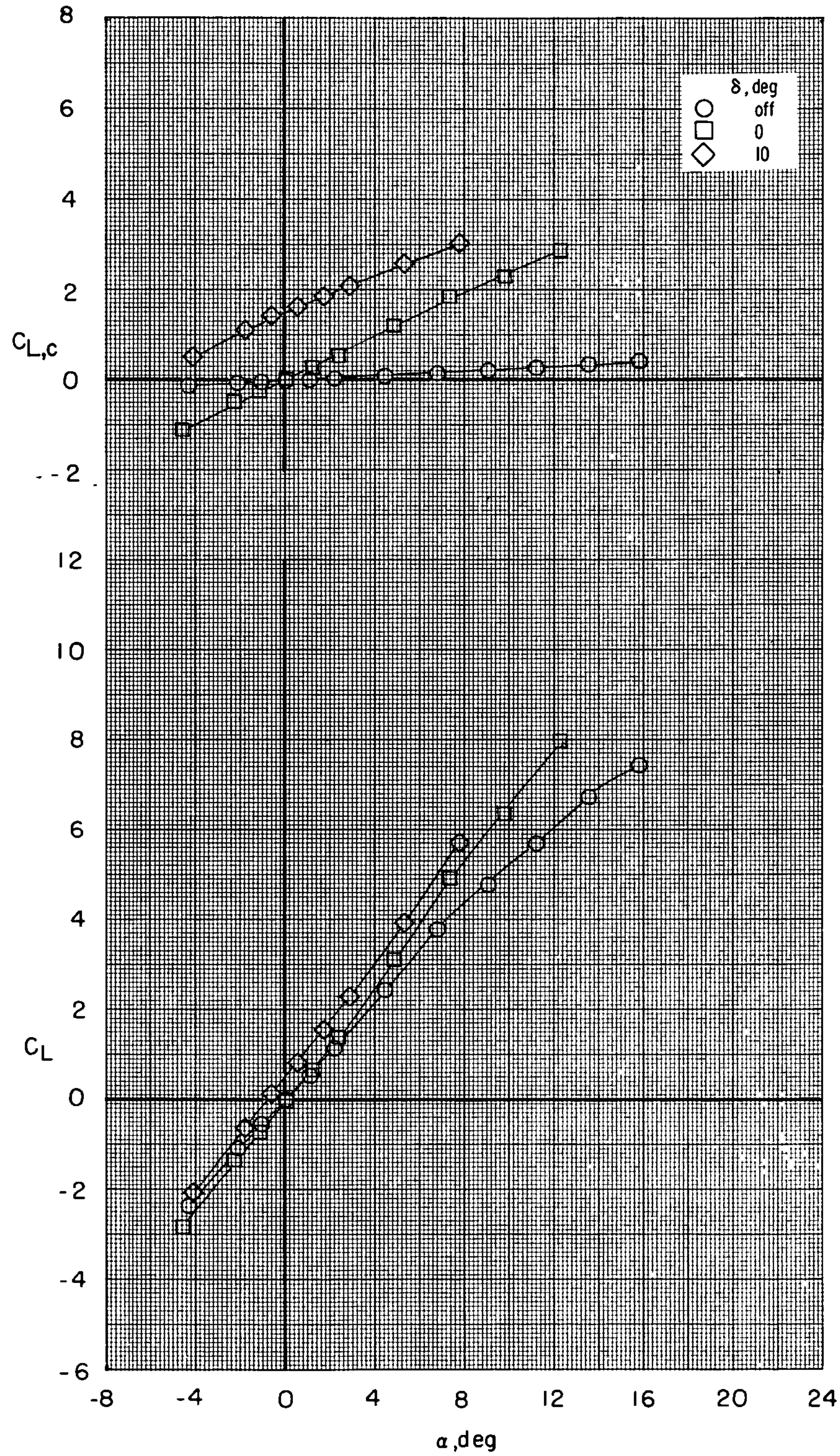

(b) M = 0.70.

Figure 14.- Continued.

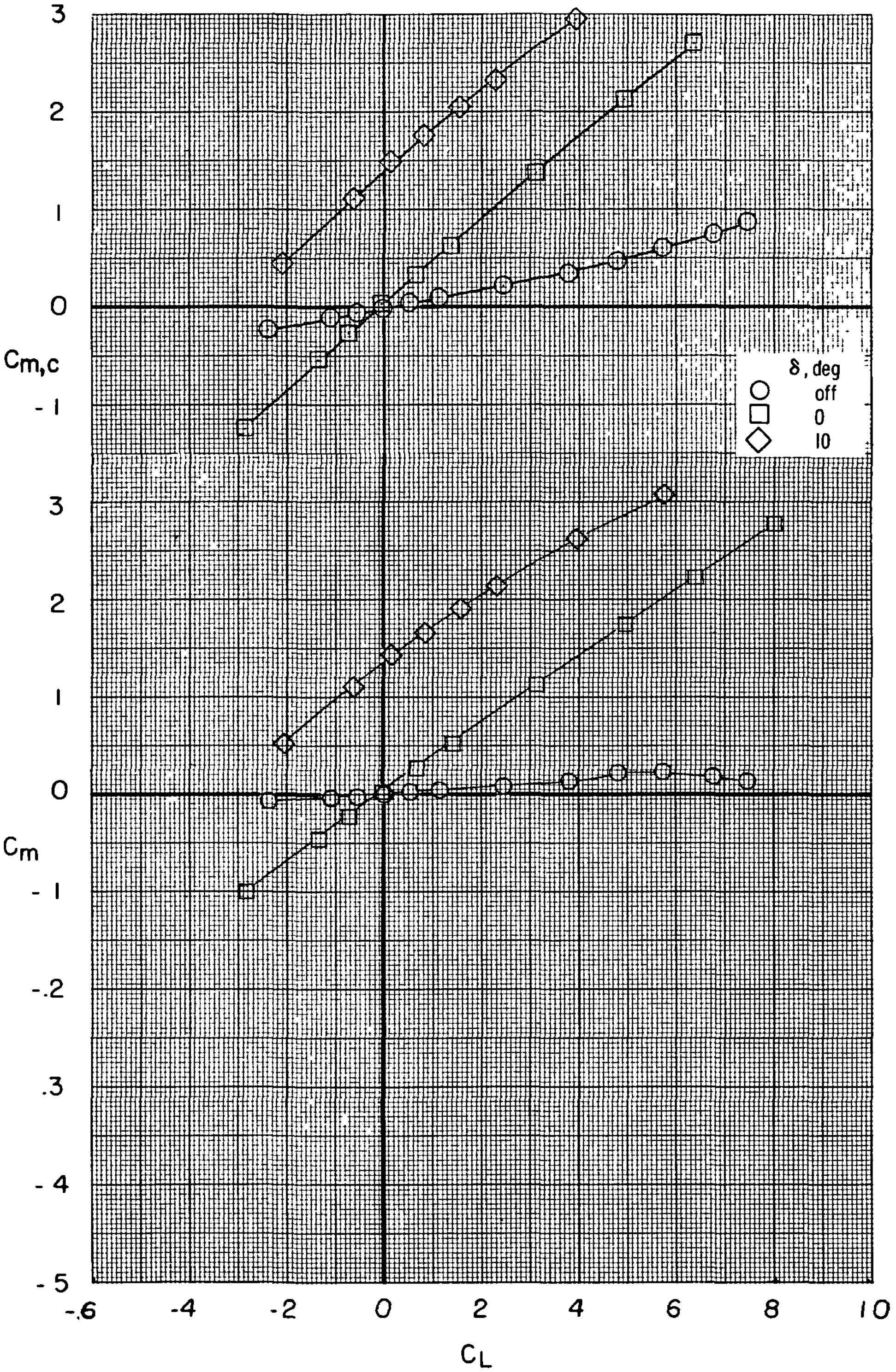

(b) Continued.

Figure 14.- Continued.

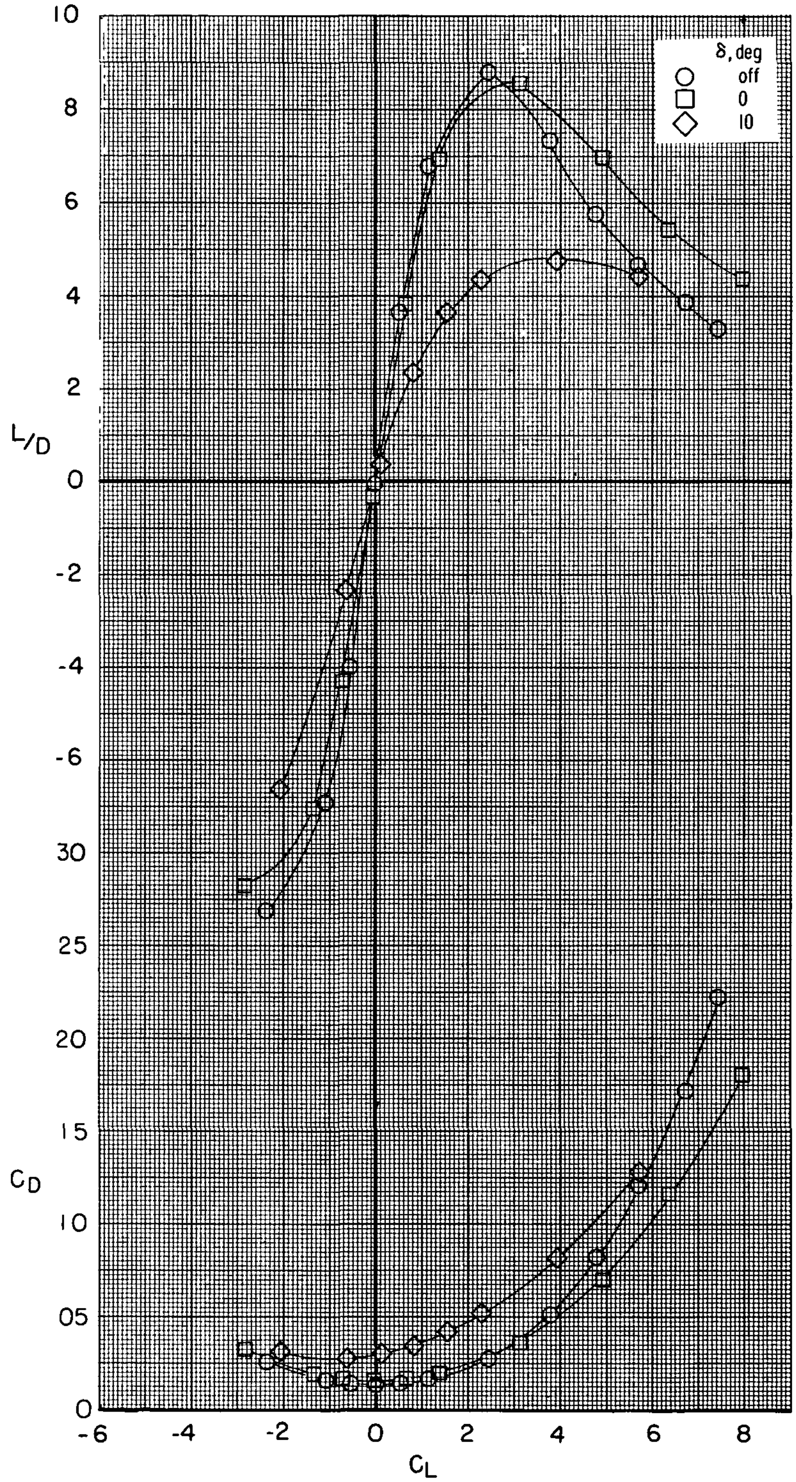

(b) Concluded.

Figure 14.- Continued.

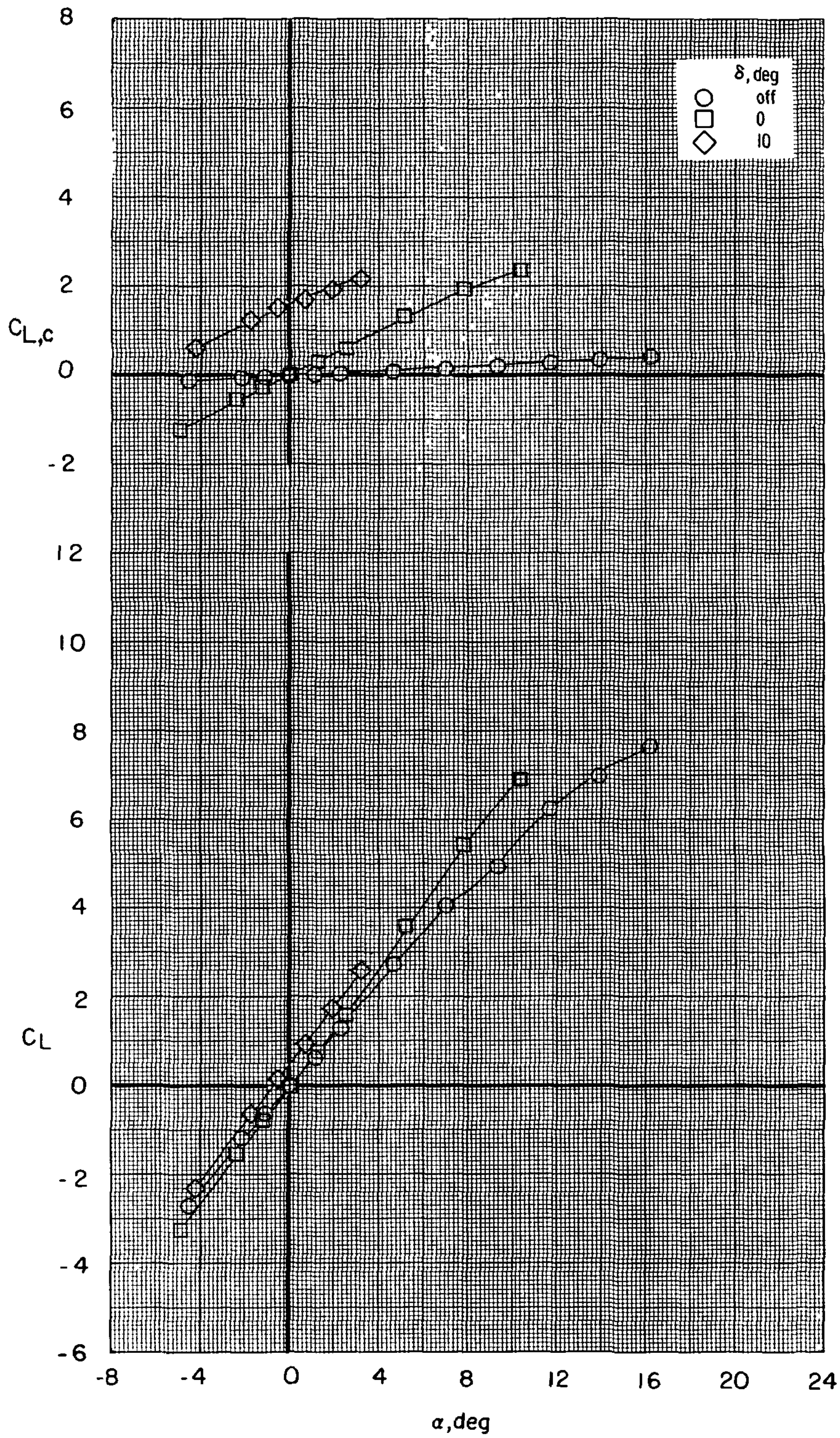

(c) M = 0.85.

Figure 14.- Continued.

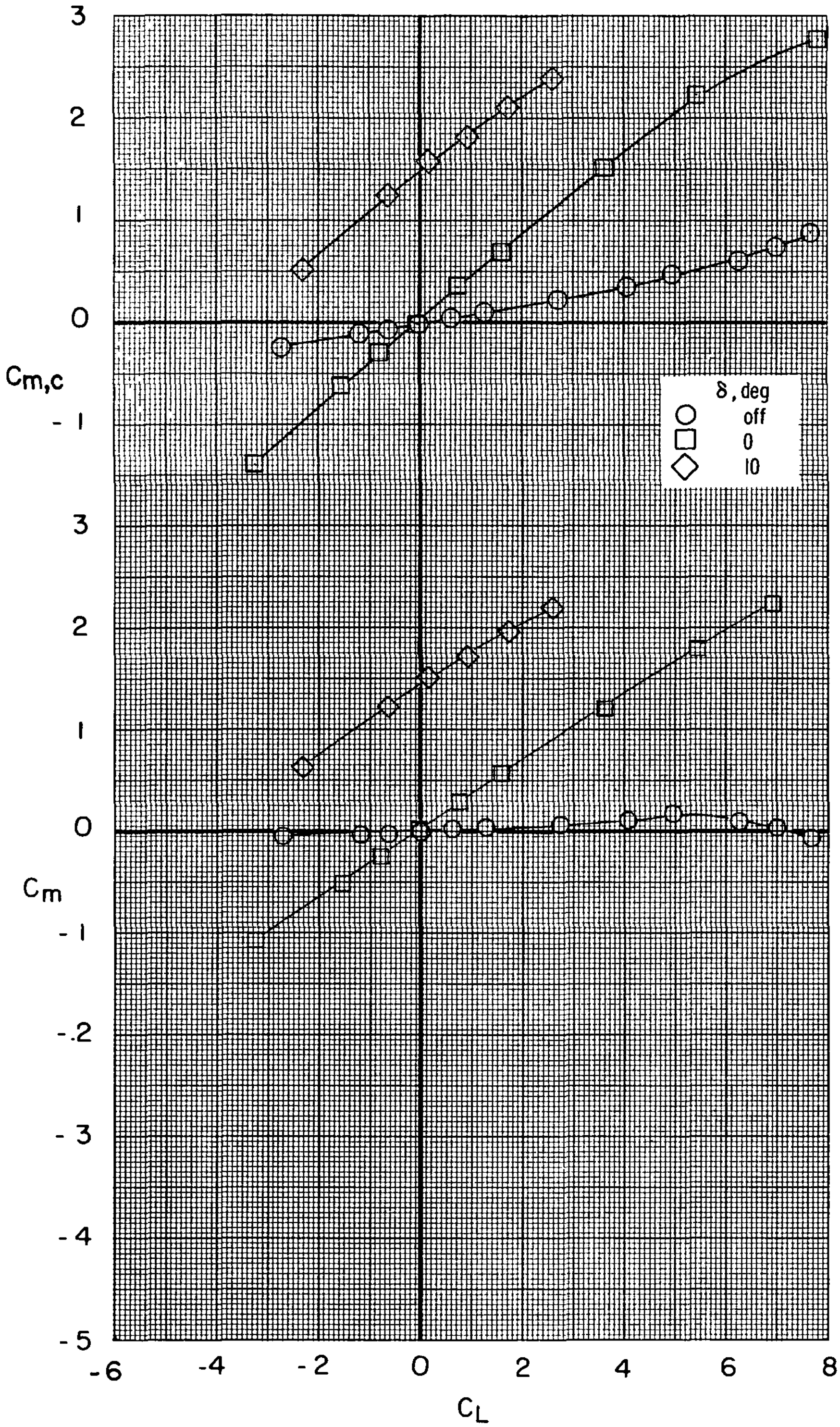

(c) Continued.

Figure 14.- Continued.

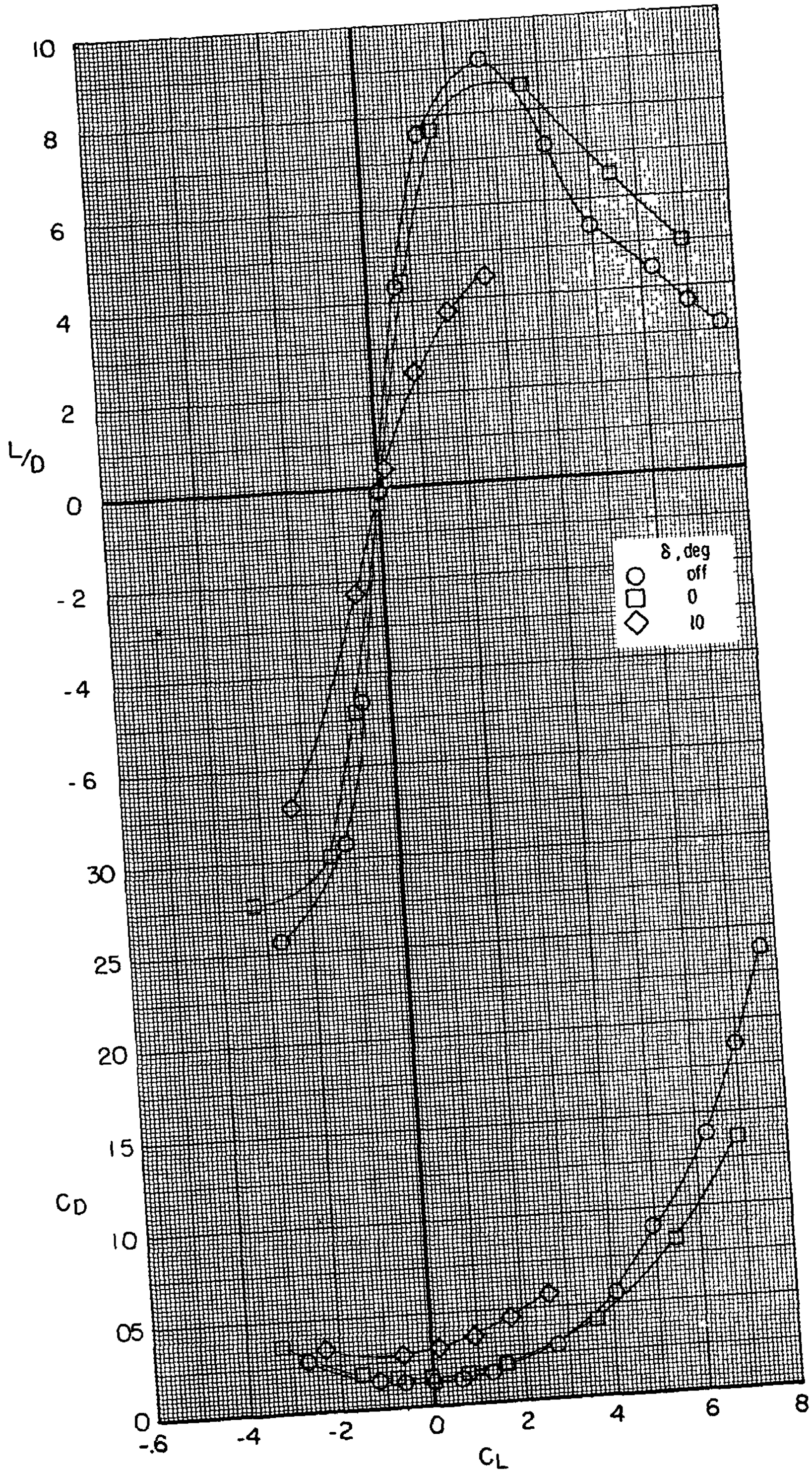

(c) Concluded.

Figure 14.- Concluded.

1 Report No	2 Government Accession No	3 Recipient's Catalog No
NASA TM-78790		

4 Title and Subtitle	5 Report Date
EFFECT OF CANARD VERTICAL LOCATION, SIZE, AND DEFLECTION ON CANARD-WING INTERFERENCE AT SUBSONIC SPEEDS	December 1978
	6 Performing Organization Code
7 Author(s)	8 Performing Organization Report No
Blair B. Gloss, Edward J. Ray, and Karen E. Washburn	L-12523
9 Performing Organization Name and Address	10 Work Unit No
NASA Langley Research Center Hampton, VA 23665	505-11-23-13
	11 Contract or Grant No
12 Sponsoring Agency Name and Address	13 Type of Report and Period Covered
National Aeronautics and Space Administration Washington, DC 20546	Technical Memorandum
	14 Sponsoring Agency Code

15 Supplementary Notes

16 Abstract

A generalized close-coupled canard-wing configuration was tested in the Langley high-speed 7- by 10-foot tunnel at Mach numbers of 0.40, 0.70, and 0.85 over an angle-of-attack range from -4° to 24°. Studies were made to determine the effects of canard vertical location, size, and deflection and wing leading-edge sweep on the longitudinal characteristics of the basic configuration. The two wings tested had thin symmetrical circular-arc airfoil sections with characteristically sharp leading edges swept at 60° and 44°. Two balances which allow separation of the canard-forebody contribution from the total forces and moments were used in this study. The data in this report supplement several earlier publications by the National Aeronautics and Space Administration.

17 Key Words (Suggested by Author(s))	18 Distribution Statement
Canard wing Canard interference Canard deflection	Unclassified - Unlimited Subject Category 02

19 Security Classif (of this report)	20 Security Classif (of this page)	21 No of Pages	22 Price*
Unclassified	Unclassified	117	$6.50

* For sale by the National Technical Information Service, Springfield, Virginia 22161

NASA-Langley, 1978

National Aeronautics and Space Administration

Washington, D.C. 20546

Official Business

Penalty for Private Use, $300

THIRD-CLASS BULK RATE

Postage and Fees Paid
National Aeronautics and Space Administration
NASA-451

U.S.MAIL

11 2 1U,A, 111378 S90844HU
MCDONNELL DOUGLAS CORP
ATTN: PUBLICATIONS GROUP PR 15246-A
P O BOX 516
ST LOUIS MO 63166

NASA

POSTMASTER: If Undeliverable (Section 158 Postal Manual) Do Not Return